HHS Public Access

Author manuscript

Chem Rev. Author manuscript; available in PMC 2015 June 24.

Published in final edited form as:

Chem Rev. 2006 August ; 106(8): 3140–3169. doi:10.1021/cr050308e.

Multidimensional Tunneling, Recrossing, and the Transmission Coefficient for Enzymatic Reactions

Jingzhi Pu, **Jiali Gao***, and **Donald G. Truhlar***

Department of Chemistry and Supercomputer Institute, University of Minnesota, 207 Pleasant Street S.E., Minneapolis, Minnesota 55455-0431

1. Introduction

Although many aspects of enzyme catalysis have been constructively analyzed,[1–52] there are still many aspects that are imperfectly understood. Of particular interest in this regard are the roles that nonstatistical dynamical effects play, as manifested in quantum mechanical nuclear tunneling,[16,25,27,30,31,39,42,44,49,53–163] dynamical recrossing,[24,27,46,97,104,113,115,121,127,131,133,137,138,144,153,163–173] and nonequilibrium effects.[24,27,46] The language of enzyme dynamical effects has also been used in various contexts to refer to protein fluctuations (protein dynamics, protein motion, protein vibrations),[13,33,37,38,49,99,109,174–188] conformational changes,[46,49,189–197] motions of individual vibrational modes,[119,125] ensemble-averaged collective geometry changes along the reaction coordinate,[179,180,198–200] and many more aspects of enzyme kinetics. However, these kinds of effects can often be included in rate calculations by a proper treatment of the free energy of activation, which is a statistical quantity. The separation of effects into statistical and dynamical is not unambiguous since, from the one point of view, the statistical free energy of activation is derived from the dynamical flux through a hypersurface in phase space and, from the other point of view, the dynamical effects of tunneling and recrossing must be statistically averaged. We prefer a division into “quasithermodynamic” and “nonsubstantial” effects, as will be explained below. This too is not unique, but it provides a clear framework for discussion and understanding in terms of generalized transition state theory, which will simply be called transition state theory (TST) in the rest of this article. (The appendix contains a glossary of acronyms and terms with a special usage.)

As a fundamental approach to describing the reaction rate in enzyme-catalyzed reactions, as well as reactions in the gas phase and the solution phase, transition state theory[1,201–203] (TST) provides an important language for interpreting chemically activated processes. In fact, the very existence of a transmission coefficient is tied to TST since the transmission coefficient is defined as the factor that accounts for all effects not included in the TST rate constant. The effects included in the TST rate constant are called quasithermodynamic, because the TST treatment of the transition state, which is not a real molecule, may be expressed in a language analogous to that used by thermodynamics for treating real

*To whom correspondence should be addressed: gao@chem.umn.edu and truhlar@umn.edu.

substances,[204–207] and the effects included in the transmission coefficient may therefore be labeled as nonsubstantial. [We use the word “substance” in the traditional chemical sense of “The Equilibrium of the Heterogeneous Substances”[204] or “Application of the First Law to a Pure Homogeneous Substance”.[206]] Both the quasithermodynamic parameters and the transmission coefficient derive from dynamics, and both quantities must be treated statistically.[205] The ambiguity in partitioning the factors affecting chemical reaction rates into quasithermodynamic and nonsubstrantial, and hence the ambiguity in defining the transmission coefficient, derives from the fact that there is more than one way to apply transition state theory because there is more than one way to define the transition state. When the calculation is well defined though, the concept of a transmission coefficient is very useful. A major objective of the present review is to elaborate on this issue.

To discuss the application of TST to enzyme reactions, we start from the well-known Michaelis–Menten model,[22] in which enzymatic reactions are described by the scheme

$$\mathrm{E+S} \rightarrow \mathrm{ES} \rightarrow \mathrm{E+P} \quad (1)$$

where E, S, and P denote the enzyme, substrate, and product, respectively, and ES is a Michaelis complex. In Michaelis–Menton kinetics, one associates the macroscopic rate constant k_{cat} with the final step of eq 1, where this step represents all the microscopic rate constants from ES to the release of product. A more explicit and widely used generalization of eq 1 is

$$\mathrm{E+S} \rightarrow \mathrm{ES} \rightarrow \mathrm{EP} \rightarrow \mathrm{E+P} \quad (2)$$

We focus on the catalytic step that converts ES to EP, which is associated with a microscopic rate constant to be denoted as k. The actual rate-determining step of the enzymatic reaction may occur at any of the three arrows in eq 2 (or the mechanism may be more complicated, such as involving a ternary complex with a coenzyme or involving one or more additional intermediates), but we assume that the mechanism has been sorted out (e.g., by analyzing intrinsic kinetic isotope effects (KIEs)[158,208–210] or other specially designed experiments) and that k_{cat} is known. In particular, we will be concerned here especially with reactions where k_{cat} has also been simulated.

The fundamental assumption of transition state theory is that there exists a hypersurface in coordinate space or phase space (the space of coordinates and momenta) that divides the reactant region from the product region. This hypersurface is usually called the transition state dividing surface or simply the transition state (TS). Typically, the transition state is chosen as a $(3N - 1)$-dimensional dividing surface in the coordinate space for a system that contains N atoms. (For gas-phase reactions, which are not of interest here, one usually separates out 3 degrees of overall translation and 3 degrees of overall orientation, and $3N - 1$ becomes $3N - 7$.) As in thermodynamics, one key issue in using TST is specifying the “system”. In general, the system can exchange energy with its surroundings, but it is usually convenient for discussing enzyme kinetics to refer to “closed systems”,[206,207] by which we mean that all atoms are definitely assigned to either the system or its surroundings. The

system must contain at least a part of the substrate, and it may contain all or part of the coenzyme(s), the apoenzyme, and the solvent. The partition into a system and its surroundings is very familiar in the theory of molecular solutions where one often uses the language of “solute” and “solvent”. For enzyme kinetics, it is usually more appropriate to refer to a “system/bath” or “system/environment” separation. We also sometimes use the language “primary zone/secondary zone”. The flexibility in how the system is defined is the first example of the fact mentioned above that there is more than one way to apply TST to a given problem.

TST also makes the assumption of local equilibrium, namely that the internal states of the reactant and the transition state are in a Boltzmann distribution. This is also called the quasiequilibrium assumption, and it should be well satisfied for most reactions in solution and most enzyme reactions.[46] As a consequence of local equilibrium, the TST approximation for k_{cat} can be written

$$k^{\mathrm{TST}}=\gamma(T)\frac{k_{\mathrm{B}}T}{h}\exp\left[-\frac{\Delta G^{\ddagger}_{T}}{RT}\right] \quad (3)$$

where $\gamma(T)$ is the transmission coefficient, k_B is Boltzmann’s constant, h is Planck’s constant, T is temperature, R is the gas constant, and $\Delta G^{\ddagger}_{T}$ is the quasithermodynamic molar free energy of activation for the reaction of interest at the given temperature T and is given by

$$\Delta G^{\ddagger}_{T}=G^{\ddagger}_{T}-G^{\mathrm{R}}_{T} \quad (4)$$

In eq 4, G^{R}_{T} is the molar free energy of reactants, and $G^{\ddagger}_{T}$ is a quasithermodynamic quantity used to describe the free energy of the transition state, which is an imaginary species in that one degree of freedom corresponding to the reaction coordinate is missing; thus $G^{\ddagger}_{T}$ and $\Delta G^{\ddagger}_{T}$ are called quasithermodynamic quantities to distinguish them from the quantities such as G^{R}_{T} that correspond to true physical substances.

When comparing eq 3 to experiment, it is important to compare it to the phenomenological expression often used to interpret experimental data, namely

$$k=\frac{k_{\mathrm{B}}T}{h}\exp\left[-\frac{\Delta G^{\mathrm{act}}_{T}}{RT}\right] \quad (5)$$

where $\Delta G^{\mathrm{act}}_{T}$ will be called the phenomenological free energy of activation. Comparing eq 5 to eq 3 yields

$$\Delta G^{\mathrm{act}}_{T}=\Delta G^{\ddagger}_{T}+\Delta G_{\mathrm{extra}}(T) \quad (6)$$

where ΔG_{extra} is the extrathermodynamic contribution to the free energy of activation and is given by

$$\Delta G_{\mathrm{extra}} = -RT\ln\gamma(T) \quad (7)$$

One often sees discussions of "the validity of TST". Since γ may be defined[211] to make eq 3 exact (assuming that a phenomenological rate constant even exists, which is another matter[24,212–214]), TST is always valid. In general though, the meaning of such discussions of the validity of TST is "How accurate is TST with $\gamma = 1$?" or "How accurate is TST with some particular model for γ?" One source of ambiguity is that the model used for γ is not always specified, although it should be.

Precise discussions of the validity of TST are ultimately rooted in classical mechanics because TST can be derived rigorously only in a classical mechanical world. For eq 3 to be valid in classical mechanics with $\gamma(T) = 1$, the transition state dividing surface must provide a dynamical bottleneck for the flux from the reactant to the product region of phase space; that is, once trajectories originating on the reactant side of the transition state dividing surface cross it in the forward direction (i.e., toward the product side), they do not return to the reactant side via recrossing through the dividing surface. Furthermore, all such forward crossing trajectories must have originated on the reactant side. Under this assumption, the one-way forward flux of the reactive trajectories is equivalent to the net flux through the transition state dividing surface that corresponds to the phenomenological reaction rate constants, and TST is exact, at least in classical mechanics.

There would be no recrossing if the reaction coordinate were separable. When the nonrecrossing assumption is not satisfied, a transmission coefficient may be used to account for its breakdown. Equation 3 then provides the basis for partitioning the phenomenological reaction rate into a "substantial" part and a "nonsubstantial" part,[215] where the former involves the use of equilibrium thermodynamic variables such as free energies [e.g., the exponential part in eq 3] for describing the transition state as a substance and the latter involves the transmission coefficient γ. (The "substantial/nonsubstantial" language is based on the description "substances" by thermodynamics, and "nonsubstantial" does *not* mean "unimportant" in this context.)

When hydrogen motion is involved, nuclear quantum effects, in particular quantized vibrations and tunneling, become important. In classical mechanics (and hence in most molecular dynamics simulations that have been carried out on proteins), vibrational energies can take on a continuous distribution of values, and the averaged vibrational energy per mode is often well approximated by the classical harmonic-oscillator value, which is given in molar energy units by *RT*. In quantum mechanics, though, vibrational energies of bound states are limited to a discrete set of values; this is called quantization. The lowest allowed value is called the zero point energy. For a harmonic oscillator, the zero point energy in molar energy units is $^1/_2 N_A hc\bar{\nu}$, where N_A is Avogadro's number, c is the speed of light, and $\bar{\nu}$ is the vibrational frequency of the mode in wavenumbers (cm^{-1}). For a mode with $\bar{\nu} = 3000\ cm^{-1}$ (a typical value for a C–H stretch), the zero point energy is 4.3 kcal/mol, whereas

RT at 300 K is 0.6 kcal/mol. Thus, the quantized energy requirements can be very important. Since the transition state is a metastable state, strictly speaking, it does not have quantized energy levels. However, to a good approximation, one may assume that all the bound modes still have a quantized energy requirement,[216] and this assumption has been used since the early days of transition state theory.[217] It is also well validated by more recent studies employing accurate quantum dynamics.[218,219] In fact, most workers usually discuss the quantized energy levels of the transition state without even mentioning that such quantization is an approximation. Since the transition state has an unbound mode (the reaction coordinate, which corresponds to motion with a barrier potential rather than a Hooke's Law potential), it has a finite lifetime (~5–30 fs), and the quantized energy levels are broadened. Thus, some systems pass through the transition state with less than the quantized energy that would be calculated if the transition state had an infinite lifetime; this is tunneling.[219] Usually, though, tunneling is visualized in a different way (one of the beauties of quantum mechanics, sometimes dizzying to newcomers, is that there is more than one correct way to understand nonclassical phenomena[220–223]); in particular, one uses an effective barrier model. In this kind of model, one identifies a tunneling coordinate (a nuclear-motion coordinate that may be the same as the classical reaction coordinate but need not be and, in multidimensional tunneling models, usually is not). The effective potential along this tunneling coordinate consists of the potential energy surface (which, by the Born–Oppenheimer approximation, ultimately represents the quantized electronic energy requirement plus nuclear repulsion) plus the energy requirement of the quantized vibrations in the other nuclear coordinates, computed as if they are not lifetime broadened. (In multidimensional tunneling models the effective barriers may also contain internal centrifugal terms due to the fact that the tunneling coordinate is curvilinear. In one-dimensional tunneling models, one neglects the variation of the quantized vibrational energies as a function of progress along the tunneling coordinate.) Now one has reduced the tunneling problem to an *effective* one-dimensional problem with an effective potential and effective reduced mass for one-dimensional motion, and tunneling shows up as the ability of a quantum wave packet to pass a barrier even when its average energy is less than the barrier top. Semiclassically speaking (we always use "semiclassical" to refer to approximate ways to carry out quantum mechanical calculations that are based on classical concepts,[224–227] such as the Wentzel–Kramers–Brillouin (WKB) approximation;[228–230] we never use "semiclassical" to mean neglect of tunneling, which is a widespread usage in the isotope effect community[209,231]), tunneling in this picture is passage through a barrier with negative kinetic energy and, hence, imaginary momentum and imaginary action[226] (here we use "action" in the sense in which it occurs in Hamilton's principle in classical mechanics).

The effect of quantizing vibrations is *usually* included in $\Delta G_T^{\ddagger}$ with tunneling contributions included in γ, but there is more than one way to include quantum effects in TST. Independently of how individual effects are partitioned between γ and $\Delta G_T^{\ddagger}$, both quantized vibrational effects and tunneling are included in $\Delta G_T^{\mathrm{act}}$.

The goal of the present article is to provide an overview of all these issues, with a special focus on tunneling and recrossing effects in enzymatic reactions and with recent theoretical developments highlighted. The organization of the article is as follows. Section 2

summarizes the previous reviews covering tunneling and recrossing in enzymes. In section 3, we open our discussion by providing a historical overview of the existing experimental evidence suggesting the importance of quantum tunneling in enzymatic reactions. Conceptual models that have been proposed and widely used to interpret these experimental kinetics data in terms of tunneling are discussed in section 4. Following that, sophisticated quantitative models that are capable of revealing detailed tunneling mechanisms at the atomic level are explained and compared in section 5; section 6 considers recrossing. Section 7 provides a survey of important enzyme systems that have been studied with the most complete theories and summarizes the tunneling and dynamical recrossing effects in these systems. Section 8 gives the concluding remarks.

This review is primarily concerned with tunneling and recrossing. Tunneling is most important for reactions involving the transfer of a proton, hydride ion, hydrogen atom, deuteron, deuterium atom, deuteride ion, triton, tritium atom, or tritide ion. Rather than repeat the litany of charge states and isotopes, we will often just say hydrogen or H nucleus to refer to all nine of these cases. Similarly, when we say kinetic isotope effect (KIE) without specifying the isotopes, it means a deuterium KIE, that is, k_H/k_D, where k is a rate constant.

This review does not consider electron transfer reactions or pressure effects on reaction rates.

2. Previous Reviews

The investigation of quantum mechanical tunneling effects in enzymes and the question of nonstatistical dynamical effects in enzyme reactions have attracted increasing attention during the past 15 years, marked by an intensive interplay between experiment and theory. A number of reviews of enzyme kinetics are available, with emphasis on one or more aspects.[1,7,8,11–14,18,23–42,44,46,48,49,63,84,94,95,124,143,144,179,232–236] In this section, we provide a few remarks about the most relevant previous reviews.

The application of dynamical simulation techniques to enzyme reactions requires quantum mechanical treatment of the potential energy surface (PES) because of the electronic delocalization that accompanies chemical bond rearrangement. Because of the large size of the protein–substrate–cofactor complex and because of the importance of its interaction with solvent, the field has been greatly advanced by the development of new techniques for the efficient and more accurate treatment of such PESs. An earlier review[31] entitled Quantum Mechanical Methods for Enzyme Kinetics overviewed practical methods for incorporating electronic quantum mechanics into PESs for enzyme reactions as well as methods for incorporating nuclear quantum effects that affect enzyme dynamics, with a special emphasis on the combined quantum mechanical and molecular mechanical[237] (QM/MM) approach for PESs, approximate quantal methods for tunneling dynamics, and quantized TST with semiclassical nuclear dynamics. Two other reviews[30,144] focused more specifically on ensemble-averaged variational transition state theory with multidimensional tunneling (EA-VTST/MT) including practical procedures for applying the method to enzyme kinetics, along with summaries of applications of the method to rate constants and KIEs, and a related

review[236] focuses on this kind of treatment for KIEs of both enzymatic and nonenzymatic reactions. Another review[46] provided a discussion of how the catalytic effect of enzymes may be understood in terms of the free energy of activation and modern transition state theory (TST) augmented by inclusions of nuclear quantum effects, dynamical recrossing corrections, and nonequilibrium effects.

Reviews of using KIEs as experimental tools for probing tunneling and dynamical motions in enzymes have been presented by Klinman and Kohen,[35,63,84,94] Cleland,[234,235] Romesberg and Schowen,[143] and Schramm and co-workers.[232,233] Liang and Klinman also summarized the progress on hydrogen tunneling studies from a structural point of view based on three particular enzyme systems, where the temperature dependence of KIEs is also discussed.[44] Hydrogen tunneling effects in general and as elucidated by experiments on flavoproteins and quinoproteins have been reviewed by Scrutton, Sutcliffe, and co-workers.[39,124] The most recent review by Masgrau et al.[39] provides an especially clear and catholic overview of theoretical models and methods and is highly recommended.

Compared to the extensive coverage of hydrogen tunneling in enzymes, the subject of dynamical recrossing in enzymes has been less intensively reviewed, in part because the concept of dynamical recrossing is a theoretical concept closely related to transition state theory, and in part because of the fast time scale (fs) in which recrossing events occur, which has been experimentally intractable. The lack of an experimental procedure to monitor the dynamical recrossing events makes this subject a field in which the interplay of direct experimental observations and theory is missing, and theoretical modeling has played the major role in furthering our understanding. Karplus has reviewed dynamical recrossing in enzymes and, more generally, in proteins, along with other aspects of protein reaction dynamics, such as conformational change and protein folding kinetics, that deviate from the simple behavior experienced in the gas phase and solution phase reactions,[24] and discussions of recrossing are also provided in other reviews.[26,29–31,46,49,144,179,236]

Villa and Warshel have provided a review focused on many vexing questions about dynamical effects in enzyme reactions, including both quantum effects and recrossing; the preorganization of the active site was emphasized as a major contribution to enzyme catalysis.[27] Recently, Hammes-Schiffer[49,179] reviewed hydride tunneling, recrossing, and protein motions in enzyme reactions based on work on three enzyme systems. Another review of enzyme dynamics focusing on coupled-network promoting enzyme motions has been provided by Benkovic and Hammes-Schiffer.[37]

Daniel et al. reviewed the role of dynamics in enzymes from a broader point of view, where various aspects such as protein flexibility, enzyme stability, and solvation effects were discussed as well as hydrogen tunneling in relating enzyme activity with protein dynamics.[33]

3. Experimental Manifestations of Hydrogen Tunneling in Enzymes

KIEs are a powerful tool to elucidate reaction mechanisms, and they provide a means of characterizing the properties of the transition state of any reaction. They have been widely used to probe the degree to which quantum mechanical tunneling contributes to enzymatic

reaction rates; however, uncertainties in such interpretations are often caused by the masking of intrinsic KIEs by the multiple-step nature of reaction mechanisms; this complication has been referred to as kinetic complexity.[75,80,111,178,238] Sophisticated methods have been developed by experimentalists for extracting the intrinsic KIEs that directly reflect the chemical step from the observed KIEs obtained from raw experimental kinetic data.[12,208,210,239,240]

3.1. Kinetic Isotope Effects and Swain–Schaad Exponents

Intrinsic KIEs are frequently used as tunneling indicators.[209,241] One way to use KIEs and related quantities to reveal tunneling is to establish guidelines as to certain ranges of values that signal the presence of tunneling. Such values are usually called semiclassical[231] or quasiclassical tunneling criteria. Simple tunneling criteria include a primary H/D KIE greater than about 7–8[202,242] or 7–10,[243] a secondary H/D KIE greater than 1.15 for reactions involving an $sp^3 \rightarrow sp^2$ change in hybridization,[143,244] or an exalted value of the Swain–Schaad exponent[245] relating H/T and D/T KIEs.

The argument about the maximum quasiclassical primary KIE is as follows:[242] If only the A–X and D–X (A and D are donor and acceptor; X is hydrogen or deuterium) stretches contribute to the KIE, and if the transition state is perfectly symmetric, then the D–X vibration transforms into the A–X–D symmetric stretch. But in that symmetric stretch, X does not move (because it is a symmetric vibration), so the A–X–D frequency is isotope independent. Then the entire isotopic dependence of the D–X stretch energy contributes to the KIE. Putting in a typical D–X frequency gives a factor of 7. This is well-known to be oversimplified because most transition states are not symmetric, and even if they were, there are also isotopically affected bends, rotations or librations, etc., so one needs a full vibrational analysis.

The Swain–Schaad criterion is especially useful for secondary KIEs, as reviewed recently.[209] However, since all of these criteria are based on breaking down nontunneling models, none of them is as reliable as carrying out tunneling calculations, especially full simulations with validated methods for including quantum mechanical effects.

The first experiments revealing the importance of quantum mechanical hydrogen tunneling in enzymatic reactions date back to 1980, in particular the secondary KIEs for reactions catalyzed by glutamate dehydrogenase[246] and formate and alcohol dehydrogenases[247] as interpreted in terms of coupled motion and tunneling by Huskey and Schowen.[59] (A review is available.[143]) A few years later, Cha et al. reported deviations of measured KIEs from “quasiclassical” expectations for the hydride transfer step in the oxidative conversion of benzyl alcohol to benzaldehyde catalyzed by yeast alcohol dehydrogenase (YADH).[16] By “quasiclassical” we mean “in the absence of tunneling”. (As mentioned in section 1, this is sometimes[209,231] called “semiclassical” but we prefer to reserve that adjective for classical-like approximate quantal treatments such as those based on the WKB[226,228–230] approximation.) In particular, Cha et al. found Swain–Schaad exponents (3.58 ± 0.08 for primary KIEs and 10.2 ± 2.4 for secondary KIEs) that exceed approximate quasiclassical limits (3.26[245] or 3.34[248,249] if the reduced mass of the cleaved bond is used). These inflated exponents were interpreted as indicating large tunneling contributions.

It has been pointed out that the secondary exponents measured by Cha et al. in their mixed labeling experiment may display significant deviation from the quasiclassical values that are predicted from single isotope substitution on the primary position, compromising the reliability of this tunneling criterion. The exponents for secondary KIEs measured in mixed-labeling experiments are augmented by potential coupling of the primary and secondary positions and can be derived by combining Swain–Schaad exponents with the rule[250] of geometric mean. Exponents from such mixed-labeling experiments converge to pure Swain–Schaad ones only in the case that isotopic substitution at one position does not affect the KIEs at the other position (no isotope effects on isotope effects). On the basis of analysis and model simulation based on the Bigeleison–Mayer formula[251] plus consideration of kinetic complexity, Kohen and Jensen[252] suggested a larger tunneling criterion of 4.8 for the secondary exponent in a mixed-labeling measurement. Further analysis of KIEs based on Swain–Schaad exponents was carried out for thermophilic alcohol dehydrogenase.[99]

Although the secondary Swain–Schaad exponent has been widely used as an indicator of the degree of tunneling, the reliability of this simple tunneling criterion has recently been questioned,[253] and it has been tested in the absence of tunneling for a large variety of organic reactions based on realistic potential energy surfaces,[254] and subjected to additional generalization.[255] The most serious problem with using Swain–Schaad-type arguments to derive quasiclassical limits for the relationship of H/T to D/T KIEs is that such arguments are based on one-dimensional models of tunneling, but we have known for a long time that the effective potential for tunneling depends on the isotopic composition of the system.[256,257] This and other multidimensional effects on tunneling[57,258–261] invalidate the use of one-dimensional models for reliable work.[236]

3.2. Isotope Effects on Arrhenius Pre-exponential Factors

Sometimes it is useful to analyze the individual Arrhenius parameters A and E_a when the rate constant is fit to

$$k = A\exp(-E_a/RT) \quad (8)$$

Various workers[262,263] proposed that a value of A_H/A_D less than 0.7–1.0 indicates a large extent of quantum mechanical tunneling. Such a tunneling criterion has been questioned and tested recently.[253] More conservative criteria invoke tunneling when $A_H/A_D < 0.5$.[241] Some workers also use a criterion based on activation energy, namely $E_a(D) - E_a(H) > 1.2$[262] or 1.4[243] kcal/mol. The use of such a criterion seems to be based on an implicit assumption that tunneling should be invoked only where there is a phenomenon that cannot be explained otherwise. For hydrogen transfer reactions with barriers of more than a few kilocalories per mole, the opposite operating procedure may be more justifiable; that is, one can assume tunneling is present unless there is a phenomenon that can only be explained in the absence of tunneling. It is still of interest though to ask how much tunneling increases the rate as compared to the hypothetical situation (here called quasiclassical) where there is no tunneling. It may be on the order of a factor of 2, or it may be orders of magnitude.

3.3. Temperature Dependence of KIEs

The temperature dependence of KIEs can be an important source of information about transmission coefficients. This section introduces this subject by giving a partial list of references using the temperature dependence of KIEs.

Banerjee and co-workers[103,264,265] measured the temperature dependence of the primary KIE for the hydrogen atom transfer reaction coupled to the cobalt–carbon bond homolysis catalyzed by methylmalonyl-CoA mutase (MMCM), and three aspects of the results indicate that the reaction is dominated by tunneling, namely the small value (0.08) of the A_H/A_D ratio, the large magnitude (36 at 293 K) of the KIE, and the large value (3.4 kcal/mol) of $E_{a,H} - E_{a,D}$. The KIE increases from 36 at 293 K to 50 at 273 K. TST calculations with multidimensional tunneling contributions[118,162] also show a large T dependence, 20–43%, depending on the size of the model system considered and the PES.

Scrutton and co-workers measured the temperature dependences of the KIEs for oxidation of amines by methylamine dehydrogenase[88,89,95,116,158] (MADH) and C–H bond cleavage catalyzed by a heterotetrameric enzyme sarcosine oxidase.[101,158] In some cases, they suggested a ground-state quantum mechanical tunneling mechanism to explain the KIE data. However, a ground-state mechanism is very unlikely at or near room temperature. Ground-state tunneling reactions have been observed but are expected to be observable only at temperatures below about 15–100 K, depending on the reaction and the medium.[266–269] They also studied the temperature dependence of the KIE in aromatic amine dehydrogenase,[116,158,244] for which the results at 300 K were successfully interpreted using small-curvature tunneling, which is discussed in section 5.1.

Whittaker et al. probed the temperature dependence of the primary KIE for hydrogen atom radical abstraction in the galactose oxidase-catalyzed reaction[85] and found that it decreased from 22.5 at 277 K to 13 at 318 K, with $A_H/A_D = 0.25$ and $E_a(H) - E_a(D) = 2.5$ kcal/mol, all of which are consistent with a reaction dominated by tunneling.

Klinman and co-workers studied the temperature dependences of the KIEs of the oxidations of benzyl alcohol catalyzed by yeast and liver alcohol dehydrogenase (YADH and LADH),[67,72] the bovine plasma amine oxidase (BSAO)-catalyzed oxidation of benzylamine with ring substituted substrates,[67] the oxidation of linoleic acid catalyzed by soybean lipoxygenase (SBL or SLO),[78,92] the oxidation of glucose to gluconolactone catalyzed by glucose oxidase (GO),[80,122] the hydride transfer from Zn-bound alcohol catalyzed by a thermophilic alcohol dehydrogenase (htADH),[99] and H abstraction from glycine in the reaction catalyzed by peptidylglycine α-hydroxylating monooxgenase (PHM).[270]

Fan and Gadda[271] interpreted their KIEs for the C-to-N hydride transfer catalyzed by choline oxidase as environmentally enhanced tunneling based on the temperature dependence of the KIE.

3.4. Survey of Tunneling Systems

In this subsection, we first discuss several systems that display large KIEs unequivocally, indicating a large extent of tunneling simply based on the size of the KIE. Then we briefly

survey experiments that have been analyzed in terms of significant tunneling contributions, based on symptoms that deviate from quasiclassical behavior, which is defined here as the result that would be obtained if all quantum mechanical and dynamical effects are included except that the reaction coordinate is treated as classical rather than quantal.

3.4.1. Soybean Lipoxygenase—Soybean lipoxygenase (SLO), a non-heme iron enzyme, catalyzes the oxidation of the unsaturated fatty acid linoleic acid. The chemical step is a net hydrogen atom transfer. Large primary H/D KIEs (~80) were found at room temperature for the wild-type SLO-catalyzed reaction; in addition, the KIE is only weakly temperature dependent.[73,129,272] The pre-exponential isotope effect was found to be much greater (A_H/A_D = 27 after extrapolation to infinitely high T) than the quasiclassical limit,[78] and the activation energy is very small (ΔE^{act} = 2.1 kcal/mol).[129] The mechanisms involving large magnetic isotope effects[273] or branch reactions[274] have been ruled out. Interestingly, the secondary KIE for the SLO reaction seems to be normal.[73,92,275]

3.4.2. Methylamine Dehydrogenase and Related Enzymes—MADH is a tryptophan tryptophylquinone-dependent enzyme that catalyzes the oxidation of primary amines to aldehyde and ammonia. The MADH reaction displays large primary KIEs (16.8[276] or 17.2[89]), which are almost temperature independent, resulting in a large A_H/A_D of 13.3. When enthanolamine is used as the substrate for MADH, the KIE deflated to 14.7, and it becomes temperature dependent,[116] which was interpreted as a switch to a tunneling mechanism modulated by gating motion.[126] Calculations[113,114,123,139] including multidimensional tunneling contributions are in good agreement with experiment and are discussed further below.

The MADH KIE reported by Scrutton and co-workers[89] has posed a qualitative challenge for theory in that the activation energy and KIE are both high, but the measured KIE is nearly temperature independent. Recently, this group has issued a caution about mechanistic complications that can give rise to observed KIEs and T dependences that do not correspond to the intrinsic KIEs.[39] Siebrand and Smedarchina[149] have suggested that the rate constants and their T dependence reflect the influence of kinetic steps prior to the proton transfer.

3.4.3. Aromatic Amine Dehydrogenase—Aromatic amine dehydrogenase (AADH), like MADH, is an amine oxidase based on tryptophan tryptophylquinone. The chemical step involves proton transfer from an iminoquinone intermediate to an active-site base. Hyun and Davidson[277] found primary KIEs of 8.6–11.7 for AADH-catalyzed reduction of the tryptophilquinone cofactor by dopamine. When tryptamine is used as substrate, the AADH-catalyzed C–H cleavage displays a remarkably large H/D primary KIE of 54.7, which is temperature independent over the temperature range measured.[92] AADH was also studied by Basran et al.,[116,158] who found a KIE of 12.9 for dopamine.

3.4.4. Methylmalonyl-CoA Mutase—MMCM was already discussed in section 3.3. TST calculations including multidimensional tunneling contributions were carried out on model systems[118,162] and yielded primary KIEs at 293 K of 32–94, depending the PES and model system. These are in reasonable agreement with the experimental primary KIE of 36. MCMM is a B_{12}-dependent (i.e., adenosylcobalamin-dependent) isomerase, and glutamate

mutase, a related enzyme in the same family that also involves coupled homolysis of a Co–C bond and atom transfer, also shows a large primary KIE,[112,278] suggesting the importance of hydrogen tunneling in the rate constant. Doll and Finke[134,136] experimentally studied uncatalyzed analogues of reactions catalyzed by B_{12} enzymes and found similar temperature-dependent KIEs to those for the enzyme-catalyzed case. This comparison has been investigated theoretically by Siebrand and Smedarchina.[160]

3.4.5. Dihydrofolate Reductase—Another enzyme for which the temperature dependence of the KIE has been studied is the hydride transfer reaction catalyzed by *E. coli* dihydrofolate reductase (EcDHFR). These experiments and associated computational studies will be discussed in section 7.

3.4.6. Other Systems—Karsten et al. measured the α-secondary tritium KIEs for the oxidation of L-malate catalyzed by nicotinamide adenine dinucleotide–malic enzyme.[91] The results were interpreted in terms of hydrogen tunneling and coupled motion during the enzyme-catalyzed reaction.

Deviations from the quasiclassical expectation of the KIEs have been observed for a number of other systems as well, including, in alphabetical order, the following: BSAO,[67,82,84,91] Δ9 Desaturase,[279] EcDHFR,[146] *E. coli* thymidylate synthase (EcTS),[142] flavoenzyme nitroalkane oxidase,[280] GO,[80,84,94,122] human lipoxygenase,[281] liver alcohol dehydrogenase (LADH)[72,74,83,84,94,102,104,105,111,115–117,119,121,123,130,141,154,155,157,178,209,236,282], methane monooxygenase (MMO),[283–285] methanol dehydrogenase,[39,286] methylmalonyl-CoAmutase(MMCM),[103] monoamine oxidase (MAO),[287] morphinone reductase,[288] PHM,[270] soybean lipoxygenase (SLO),[44,49,73,78,84,92,126,129,140,149,151] thermophilic alcohol dehydrogenase (htADH),[99,105,119,126,185,209] thermophilic dihydrofolate reductase from *Thermotoga maritima* (TmDHFR),[289] thermophilic dihydrofolate reductase from *Bacillus stearothermophilus* (BsDHFR),[150] tyrosine hydroxylase,[290] andyeastalcoholdehydrogenase(YADH).[16,67,74,96] Large KIEs have also been reported for the xylene hydroxylation by cytochrome P-450[291] and dopamine *β*-monooxygenase.[292] It is almost impossible to make a complete list since many, many catalytic reactions have hydrogen transfer as the chemical step, and hydrogen transfer reactions with barriers of a few kilocalories per mole or higher are probably all dominated by tunneling at room temperature in the sense that 50% or more of the reactive events occur by tunneling.

4. Models

As reviewed above, for a number of enzyme-catalyzed reactions, the magnitudes of the measured KIEs and their temperature dependences suggest significant tunneling effects. In one approach to explaining these data, new conceptual models, typically involving the concepts from electron transfer theory[45,57,262,293–310] (especially the formalisms of Marcus and Dogonadze, Levich, and Kuznetsov), have been proposed specifically to interpret these data. Another approach is to see how well they can be explained by using transition state theory, especially with transmission coefficient approximations previously validated for gas-phase reactions. This section (section 4) reviews the electron-transfer-like models that have

been proposed, and section 5 reviews the full quantitative calculations that have been carried out using TST with multidimensional tunneling contributions.

The Marcus formalism is well explained elsewhere, typically in the context of electron transfer,[57,293,295,299,301,303,304,306,309,310] which is beyond the scope of the present review. For electron transfer, Marcus theory is based on using Franck–Condon arguments for the situation of weak overlap of electronically diabatic electronic wave functions.[293] (Some workers prefer the etymologically bi-linguistic double negative "nonadiabatic" (based on Latin *non*- and Greek *a*-) to "diabatic". Others use both words, depending on the context, a practice we will follow here.) Marcus theory has also been extended to proton transfer and other chemical reactions,[57,120,262,303,308,309,311–328] which typically involved stronger coupling, i.e., the adiabatic case.

The original Marcus formalism was classical and dealt mainly with the free energy of activation, which has been studied further by many other workers.[70,308,328–337] The transmission coefficient was introduced into electron transfer theory by Dogonadze and Levich,[294,296,297] who used a quantum mechanical approach based on the golden rule[338] of Fermi. The first-order perturbation theory approach again leads to Franck–Condon factors, and it was also employed by Marcus.[304] This approach was extended to proton transfer;[300,302] it includes solvent modes as well as proton motion in the reaction coordinate, and it takes account of excited vibrational states of the proton. In later work, they introduced gating modes[339] and a combined treatment involving both gating modes and excited proton states.[340] The theory also allows for corner-cutting tunneling[305,341] and for the coupling of high-frequency modes to low-frequency ones.[342,343] The resulting theory, usually in simplified forms leading to approximate analytical expressions, has been widely applied.[305,307]

A difficulty with applying weak-overlap electron transfer theory, based on Franck–Condon arguments, to proton transfers was expressed by Marcus:[57] "In the case of weak electronic interaction between the two channels, the usual Franck–Condon approach could be used, and there is a strong similarity to the usual weak-overlap electron transfer case. However, in the much more likely case, for proton transfers, of strong electronic interaction, the weak-overlap Franck–Condon approach would break down numerically." The original very simple approach is called totally nonadiabatic or fully diabatic to indicate that both electronic and protonic motions are nonadiabatic, which is only valid for weak electronic interaction, which is not the case in hydrogen, proton, and hydride transfer reactions, although it is sometimes valid for electron transfers. A modified Franck–Condon approach for the case of "partially adiabatic" charge transfer, i.e., electronically adiabatic proton transfer with weak overlap of initial and final proton wave functions, has been presented[93,159,344] and also used to describe electron-coupled proton transfer.[345] Warshel and Chu also extended electron transfer theory to treat quantum effects on adiabatic proton transfer.[65]

Kuznetsov and Ulstrup[93] applied this kind of theory to KIEs of condensed-phase proton and hydrogen-atom transfers. Their treatment involves applying some key concepts of electron transfer theory to H^+ and H transfer. In particular, the H^+ or H is assumed to transfer in a Franck–Condon-like process only when other nuclear coordinates happen to be in a

configuration where the light particle can transfer without exchanging energy with other degrees of freedom. In applying the theory to KIEs, Kuznetsov and Ulstrup used a model formulated earlier[300,302,340] to derive a TST-like rate constant (Marcus theory can be derived as a special case of TST[120,295,299]) for achieving the most favorable configuration for tunneling times a distribution function for a gating coordinate, assumed to be the donor–acceptor distance. Both factors affect the KIE.[93] In many respects, this theory is similar to TST with a transmission coefficient based on large-curvature tunneling.[147,236,260–262,346–353] In both cases, the TST rate constant is multiplied by a factor that reflects the "interplay between donor–acceptor configuration and nuclear tunneling". Their general expression for the transition probability takes account of all possible paths averaged over energy[305,307] and in this respect is similar to the large-curvature tunneling coefficient that involves,[260,347,351–354] for each energy, a convolution of the probability of a given nuclear configuration and the tunneling probability at that configuration, followed by a Boltzmann average over energies. Kuznetsov and Ulstrup approximated the more general expression by a ratio of two exponentials. The Franck–Condon picture of the tunneling process leads to a picture of "fluctuational barrier preparation"[354] in which high barriers between tunneling-conducive conformations may "gate" the tunneling process.[93] The TST-plus-large-curvature tunneling process, on the other hand, incorporates the average over fluctuations into the free energy of activation and the convolutional average of the transmission coefficient. In this regard, it is useful to keep in mind a succinct summary of the issues by Warshel:[356] "It has been frequently implied that dynamical effects are important in enzyme catalysis. In exploring this issue, it is important to realize that all reactions involve dynamical fluctuations of the reacting atoms. The chance that the fluctuations will take the system to the transition state, however, is determined solely by the relevant activation free energy." Thus, for example, Bruno and Bialek[68] and Frauenfelder[100] discuss tunneling through "fluctuating barriers", and Grishanin et al.[109] discuss tunneling in a fluctuating potential. Fluctuating barriers correspond to passing (whether by a tunneling or an overbarrier mechanism) through the transition state at different configurations in the $(3N - 1)$-dimensional configuration space dividing surface with a distribution of potential energies; thus, the effect is included in all properly conducted TST calculations. The correct way to account for the probability of reaching the transition state quasiclassically is to calculate a quasiclassical free energy of activation (see section 5). A correct way to account for the extra rate enhancement due to systems that do not reach the transition state quasiclassically but nevertheless react by tunneling through this dividing surface is by performing a Boltzmann average over the distribution of tunneling paths weighted by their tunneling probability, as is done in the more complete approaches[260,305,307,347,351] mentioned above as well as in variational transition state theory with a multidimensional transmission coefficient (section 5).

Knapp, Rickert, and Klinman[126,129,140] have interpreted their recent experiments in terms of the Kuznetsov–Ulstrup formalism, which they call environmentally modulated or environmentally coupled tunneling. They assume that the system reacts exclusively via a tunneling mechanism, where the tunneling event is triggered when the enzyme environment attains certain reactive configurations, which are generated by the thermal fluctuations, as in the theory of electron transfer or TST. The TST-like term involving the reorganization

energy to attain a tunneling configuration is called passive dynamics, and the Franck–Condon factor is called active dynamics. The passive dynamics factor is assumed to be isotope insensitive but strongly dependent on temperature. The Franck–Condon factor contributes the entire KIE, which is modeled in terms of ground-state harmonic-osillator wave function overlap. The temperature enters via a Boltzmann factor associated with the energy cost required to change the distance between the potential wells. The product of the Gaussian overlap and the Boltzmann factor is integrated over a range of the gating coordinate. The average of a tunneling factor depending on the donor–acceptor distance (or, in quantum language, on the population of excited states of a promoting mode), weighted by the probability of the system being at that distance, occurs in more generality in the large-tunneling model;[260,261,347,351–354] both theories involve deuterium tunneling over a shorter distance than protium in thermally averaged systems, as do one-dimensional tunneling models. Although the large-curvature tunneling model does not use the Franck–Condon language (which is more appropriate for spectroscopy and electron transfer, where there is a separation of time scales), a Franck–Condon process may be used as a way to visualize the tunneling event, if desired.[320]

Knapp, Meyer, and Klinman[126,151] applied the Franck–Condon-like nonadiabatic Kuznetsov–Ulstrup model (not the partially adiabatic one) to SLO, and Siebrand and Smedarchina[149] also applied a similar electron-transfer-like model with a Golden Rule treatment of tunneling to SLO.

A very clear summary of the assumptions behind the Kuznetsov–Ulstrup model has been provided by Masgrau et al.,[39] who also summarize the application of this model by their group to MADH and AADH as well as the analytical frameworks used by other groups. Following Knapp et al.,[126,129] they write the tunneling contribution to the rate constant as proportional to two factors: (i) a Marcus-like term controlling the probability that thermally activated protein fluctuations (vibrations) bring the system to “a configuration compatible with tunneling” and (ii) the integral over a modulating coordinate (taken to be a motion of the donor–acceptor distance that modulates or gates the H transfer) of a Franck–Condon factor controlling tunneling along the coordinate corresponding to transfer of the H nucleus and a Boltzmann factor accounting for the energetic cost of modulation. The first factor is assumed to be isotope independent (although that would deny the existence of secondary KIEs) and to contribute most of the activation energy. The Franck–Condon factor is isotope dependent and has variable temperature dependence, including the possibility—in most cases they treat—of being temperature independent. Temperature dependence of the primary KIEs can arise in two ways: from the Franck–Condon factor itself (due to the population of excited reactant vibrational levels) or from the effect of the temperature-dependent Boltzmann average.

The Franck–Condon factor is assumed to be independent of temperature if only the lowest vibrational state of the nuclear wave function of the H is occupied in the reactant. Since hydrogen stretching frequencies are high (~3000–3600 cm^{-1}), this seems on first analysis to be a reasonable assumption. However, there are three questionable features. First, the Fermi golden rule treatment, with an appropriate choice of the perturbation operator, may be valid when the tunneling probability is small,[294,296,297,305,342] but the Boltzmann average also

involves (and is sometimes dominated by) situations where the tunneling probability is too large to treat by perturbation theory. Second, the analysis is based on a simplified version of the theory that assumes that, with the possible exception of a modulating mode, the hydrogen stretch motion is separable enough from other modes that the probability of barrier passage is solely a function of the energy in the stretch mode. There are a myriad of other vibrational states between the ground state and the first fundamental excitation of the stretch. As the system moves toward the transition state, it is very likely that many of these low-frequency modes and their combinations contain a nonzero component of the reaction coordinate and/or couple to it, and on average the reaction probability should be an increasing function of the energy in these modes and hence an increasing function of temperature. Even the higher-frequency modes may couple to some extent to the reaction coordinate, due to reaction-path curvature and to the dependence of the transverse force constants (and hence frequencies) on the reaction coordinate.[357] Third, even if the hydrogen vibration were nearly separable, and even if the hydrogen vibration were the same as the reaction coordinate (so all other vibrations were orthogonal to the reaction coordinate), and even if the hydrogen vibration were separable so that other degrees of freedom do not couple to the reaction coordinate (or only one modulating mode so couples), the model treatments are cast entirely in terms of unperturbed reactant states. This corresponds to a diabatic or sudden picture of hydrogen dynamics, whereas detailed chemical dynamics studies of non-biochemical hydrogen transfer dynamics show that it is much better characterized by a vibrationally adiabatic or partly adiabatic multidimensional model[218,219,358–365] than by a fully diabatic or sudden one- or two-dimensional model; it is not clear why enzymes should be different from gas-phase dynamics in this respect, and in fact they probably are not.

Schwartz and co-workers[82,119,125,154,366–374] have elaborated the model of thermally activated vibrational modes that promote reaction. They first identify the donor–acceptor distance as a gating (promoting) mode, because the height and width of the barrier depend on the donor–acceptor distance. The width of the barrier is singled out because of its effect on tunneling. They identify residues important in creating a protein promoting vibration by examining the correlation of the motion of various residues with the donor–acceptor vibration in classical molecular dynamics simulations.[369,373]

Antoniou and Schwartz[25] have reviewed the nonadiabatic Levich–Dogonadze–Kuznetsov–Marcus proton transfer theory[294,302] in the context of recent work; they make an analogy between “fast flip” tunneling (i.e., the sudden or Franck–Condon-like nonadiabatic tunneling with bath frozen) and “large-curvature”[260,261] tunneling. (“Corner-cutting” tunneling, which they also mention, is more general and includes both small-curvature tunneling and large-curvature tunneling, which are discussed in section 5.1.) They contrast “fast flip/large-curvature” tunneling to a more adiabatic case where tunneling occurs near the saddle point (this would be better described as almost-adiabatic).[259] This contrast was apparently first made by Marcus,[57] who also presented seminal discussions[57,258,358,359] of corner-cutting tunneling. The small-curvature tunneling[259,351,354,375] (SCT) and large-curvature tunneling[260,347,351–354] (LCT) approximations are formalisms for calculating corner-cutting tunneling in general polyatomic systems with full atomic detail and without separate assumptions as to which mode or modes are promoting modes. The formalism determines this from the potential energy surfaces so that all transverse modes are coupled to the

tunneling path (i.e., to the reaction path for tunneling), with the coupling strength depending on the potential energy surface, in particular on the changes in frequency and vibrational eigenvectors (generalized normal modes) as one proceeds along the reaction path and by reaction-path curvature. (The reaction-path curvature is a $(3N - 1)$-dimensional vector, [377] defined such that each component tells how much the minimum-energy path (MEP) is curving into a particular instantaneous generalized normal mode transverse to it.) A key element in the small-curvature case is the emergence, for each energy, of a dominant semiclassical tunneling path.[259] (Failure to include this feature made earlier models[377] based on reaction-path curvature inaccurate.[259]) A key element in the LCT approximation is that it allows a distribution of tunneling paths even at a given energy;[260,347,351] usually the most important aspect of this is tunneling over a range of donor–acceptor distances, as illustrated in Figure 1. This coupling between the tunneling coordinate and the donor–acceptor distance appears also in some models discussed above[65,305,344] and also in related work by Borgis and Hynes.[378] The incorporation of the hydrogen transfer coordinate into the electron-transfer-like theories was also discussed by Schenter et al.,[120] who emphasized that one must be cautious not to assume instantaneous uncoupled hydrogen transfer because the ratio of time scales for the different kinds of motion is finite.

Hammes-Schiffer and co-workers developed a general Marcus theory of coupled electron–proton transfer,[155,379,380] and they applied it to a model of the SLO reaction.[49,155,381] They showed that although the reaction catalyzed by SLO is formally a hydrogen atom transfer, their coupled electron–proton model explains the data quite well, especially the large KIEs with weak temperature dependence. The model indicates that the reaction is electronically adiabatic (as is typical of hydrogen atom transfers) but vibrationally nonadiabatic. The reactant and product states are weakly coupled so that use of the golden rule may be valid. The calculation also elucidated the role of the donor–acceptor distance. Siebrand and Smedarchina also treated SLO by an electron-transfer-like theory. Another calculation[145,148] on the SLO reaction is discussed in section 5.3.

Kiefer and Hynes[156,326,382,383] have also employed the extension of electron transfer theory to proton transfer. They consider that the reaction is driven by configurational changes in the medium surrounding the proton. Kiefer and Hynes,[156] as in other studies mentioned above,[65,93,159,297,298,344] distinguish two regimes for modeling hydrogen transfer reactions —an adiabatic one where the electronic resonance integral between the reactant and product valence bond electronic wave functions is large, and hydrogen motion is over the barrier, and a nonadiabatic regime where the electronic resonance integral is small, and the hydrogen transfer proceeds entirely by tunneling. Kuznetsov and Ulstrup and co-workers[93,159,340] and Chu and Warshel[65] also emphasize a third (intermediate) regime called “partially adiabatic” in which the electronic resonance integral is not small so the usual description in terms of a single Born–Oppenhiemer potential energy surface applies, but the reaction still occurs mainly by tunneling. In fact, this may be the most common regime for hydrogen transfer reactions (as also noted, see above, by Marcus[57] and as assumed in our own work), although the nuclear tunneling need not be totally diabatic.

Kuznetsov and Ulstrup also remark,[159] and we agree,[120] that the totally diabatic picture (nonadiabatic picture) “may have a heuristic character” in that “proton transfer processes

mainly belong to the adiabatic limit" and may only "approach" the diabatic limit. It is a strength of the full simulation methods discussed in section 5 that one does not need to specify a regime beforehand; these simulation methods automatically include all three regimes as well as borderline cases.

Recently, an approximate instanton method[384,385] (AIM) has been implemented[386] and applied to enzymatic reactions and biologically interesting systems to incorporate nuclear quantum effects.[87,135] This method is more closely related to (but more approximate than) the methods discussed in the next section than to electron transfer theory.

5. Quantitative Computational Methods

Although sometimes the conceptual models can provide qualitative interpretations of the kinetics of enzymatic reactions, they do not describe the detailed mechanism of tunneling processes at the atomic level. For example, methods to identify and separate specific gating-mode motions and thus to verify the assumptions on which the environmentally coupled tunneling or rate-promoting-vibration model is based are only starting to be developed.[373] It is also unclear how to calculate secondary KIEs with the models reviewed in section 4. Moreover, the generality of these models is sacrificed by introducing a number of assumptions and hypotheses. Recently, progress has been made in developing full computational models for simulating enzyme dynamics, employing advances in techniques for calculating potential energy surfaces for treating large and macromolecular systems, and using quasiclassical and semi-classical (WKB-like) multidimensional dynamical methods for incorporating quantum effects into simulations. At the present time, all-atom simulations must partner with X-ray crystallography to get a starting structure for the enzyme. When these methodologies are also combined with experiments on rate constants, KIEs, and the effects of mutations, they can yield a remarkably complete atomic-level description of enzyme-catalyzed reactions.

In what follows, we will review state-of-the-art computational models that have been developed and applied to elucidating the role of quantum mechanical tunneling and recrossing in enzyme catalysis.

5.1. Ensemble-Averaged Variational Transition State Theory with Multidimensional Tunneling (EA-VTST/MT)

The unimolecular rate constant k (with dimensions of s^{-1}) for the catalytic step is the elementary rate constant for ES → E + P in eq 1 or ES → EP in eq 2. This rate constant is approximated by transition state theory, as eq 3 is more sensitive to $\Delta G_T^{\ddagger}$, which occurs in an exponent, than to γ-(T), which does not. The accuracy of the calculated rate constants depends on both the quality of the potential energy surface and the dynamical method used to calculate the rate constant from the potential energy surface. The present review is primarily concerned with the latter. The computational approach for calculating reaction rate constants for enzymatic reactions that is considered in this section is called ensemble-averaged variational transition state theory with multidimensional tunneling (EA-VTST/MT).[121,137,138,144] This theory incorporates nonclassical nuclear quantum effects, in particular, zero point energy, tunneling, and dynamical recrossing corrections that take

account of zero point requirements in a systematic fashion. We will review this theory in detail for two reasons. First, it was used for many of the tunneling and recrossing calculations reviewed in this article. Second, it provides a conceptual framework that is also used for discussing tunneling and recrossing more broadly.

The concept of potential of mean force[98,167,205,387–401] (PMF) plays an important role in condensed-phase TST. The PMF is usually computed by classical mechanics as a function of a single coordinate, called the distinguished coordinate and here denoted z. (An example of z will be given below.) The PMF computed this way is denoted by $W_C(z)$, which is sometimes called the free energy profile. This quantity corresponds to a statistical average like true free energy except that it is limited to configurations with a given value of the reaction coordinate z.

The EA-VTST/MT approach has been divided into three stages, corresponding to various degrees of completeness of the dynamical model, although in practice it may often be as accurate or more accurate to stop after stage 2 than to include stage 3. Stage 1 has 2 steps. In step 1 of stage 1, the classical mechanical PMF, $W_C(z)$, is obtained from umbrella sampling[387,402,403] molecular dynamics (or any other suitable method) along a predefined reaction coordinate z; as will be discussed in more detail below, this provides an approximation to the free energy of activation profile for generalized transition states (i.e., transition state dividing surfaces) orthogonal to this reaction coordinate.[161,400] Various types of reaction coordinates can be used in this stage, for example, a geometry-based reaction coordinate, such as a distinguished reaction coordinate (DRC) described by the difference of the breaking and forming bond distances,[30,97,144,170,171,404] or a collective reaction coordinate,[27,120,131,161,168,265,295,299,405–407] defined in terms of the energy gap[406] between the valence bond states corresponding to the reactant and product states.[512–514] Alternatively, for H transfer, when the donor and acceptor experience changes of the hybridization states, recent studies emphasized the usefulness of employing the change of one or both hybridization states as the DRC.[408] Any combination of bond distances, bond angles, or torsion angles is called a valence coordinate, whereas quantities based on diabatic potentials or electrostatic fields that depend on solvent or bath coordinates are often called collective solvent coordinates. Valence coordinates are also called geometrical coordinates.

In this review, we limit our detailed discussion of EA-VTST/MT to cases where a DRC (denoted z) is used in stage one. In the rest of this section, we assume for illustrative purposes that we are considering a hydrogen transfer, and z is defined as

$$z = r_1 - r_2 \quad (9)$$

where r_1 and r_2 refer to the distances of the bonds being broken and formed, respectively. If one is uncertain which bonds to include in eq 9 or which direction to take in combining two or more bond distances for the DRC, one can first carry out an exploratory two-dimensional PMF study of the free energy landscape.[138,409] (For example, different reaction coordinates might be appropriate in the cases of concerted and nonconcerted bond rearrangements. We will return to the subject of more general reaction coordinates in the paragraph below eq 14 and then more fully in section 5.2.)

The free energy profile mapped along the reaction coordinate z is the PMF; in the classical mechanical simulation, it is called $W_C(z)$, where the subscript denotes classical. Rare event sampling techniques such as umbrella sampling,[387] combined with either molecular dynamics or Monte Carlo methods, can be adopted to overcome the sampling difficulty of computing $W_C(z)$ in the vicinity of a reactive energy barrier. As pointed out by Bennett,[410] this involves "a synthesis of molecular dynamics (and Monte Carlo) methods with transition state theory that combines the former's freedom from questionable approximations with the latter's ability to predict arbitrarily infrequent events, events that would be prohibitively expensive to simulate directly". We should note that, in principle, the global variable z against which the PMF is computed is locally equal to the coordinate removed from the system to define a transition-state dividing surface; thus, both variables are usually called the reaction coordinate. If we want to emphasize the distinction, the former may be called the progress coordinate or progress variable.

Once the classical PMF is obtained, the difference between the PMF at its maximum and at the reactants can be computed:

$$\Delta W^{\ddagger}_{\mathrm{C}} = W^{\ddagger}_{\mathrm{C}}(T, z=z^*) - W^{\ddagger}_{\mathrm{C}}(T, z=z_{\mathrm{R}}) \quad (10)$$

This quantity is closely related to the free energy of activation (see below) and may be called the PMF of activation. The subscript C in eq 10 and below denotes "classical". The PMF accounts for free energy contributions associated with all degrees of freedom that are orthogonal to the reaction coordinate. Thus, the free energy associated with the reaction coordinate is missing in the PMF. At the transition state, as discussed in the Introduction, the reaction coordinate is unbounded (like a translational coordinate) and hence it has no zero point energy. (At the transition state, the reaction coordinate does not contribute to the quantized energy requirement, but the vibrational coordinates orthogonal to the reaction coordinate (that is, all vibrations except the reaction coordinate) do contribute.) At the reactant, the reaction coordinate for the unimolecular reaction ES $\rightarrow$ EP or E + P is a bound vibration. Furthermore, unlike the transition state, the reactant is not missing a degree of freedom. Thus, the reaction coordinate of the reactant contributes to the system's total vibrational free energy and must be included. To obtain the classical free energy of activation, this contribution has to be considered along with the PMF of activation. For a Cartesian reaction coordinate (i.e., a reaction coordinate that can be obtained by an orthogonal transformation from atomic Cartesians; this is also called a rectilinear coordinate), one obtains

$$\Delta G^{\ddagger}_{T,\mathrm{C}} = \Delta W^{\ddagger}_{\mathrm{C}}(T) - G^{\mathrm{R}}_{\mathrm{C,F}}(T) \quad (11)$$

where

$$G^{\mathrm{R}}_{\mathrm{C,F}} \equiv G_{\mathrm{C,F}}(T, z=z_{\mathrm{R}}) \quad (12)$$

where $G_{C,F}$ is the classical free energy contribution of the reaction coordinate and z_R is the value of the reaction coordinate corresponding to the reactant state. (Enzymologists often call the reactant state the ground state, but "ground state" has a different meaning in quantum mechanics, so this usage should be abjured.) The magnitude of $G^{R}_{C,F}$ can be estimated by calculating the free energy difference without and with this coordinate by, respectively, projecting and not projecting the reaction coordinate from the Hessian matrix. If a Hessian matrix with the reaction coordinate projected out is used, one obtains $3N - 1$ nonzero normal-mode frequencies, denoted ω_m (m = 1 to $3N - 1$, where N is the number of atoms explicitly treated as quantized nuclear coordinates); for the case where a Hessian matrix without projection is used, $3N$ nonzero normal-mode frequencies are obtained, denoted $\omega^{U}_{m}(m=1\text{ to }3N)$. In the gas phase, $3N - 1$ and $3N$ would be replaced by $3N - 7$ and $3N - 6$, respectively, and there would be six zero-frequency normal modes corresponding to three rotations and three translations. However, those modes are replaced by low-frequency vibrations when the system is surrounded by a nonisotropic, nontranslationally invariant environment like a solvent or a protein.

In step 2 of stage 1, quantization effects on the vibrational free energies are included in $\Delta G^{\ddagger}_{T}$.[121,411] In principle, this should be done for all $3N - 1$ modes at the transition state; however, we make two simplifications. First, we quantize only an N_1-atom primary subsystem, where $N_1 \approx 20$–80 (as compared to $N = O(10^4)$). Second, we note that at least the six lowest frequency modes of the $3N_1 - 1$ modes are expected to be so small that the classical approximation should be valid, and in practice (for technical, practical reasons), we quantize only $3N_1 - 7$ modes at the transition state and $3N_1 - 6$ modes of the reactant. In the language introduced in section 1, this yields a quasiclassical approach to the free energy of activation profile. It is given by

$$\Delta G^{\mathrm{SRC}}_{T,\mathrm{QC}} = \Delta G^{\ddagger}_{T,C} + W_{\mathrm{corr}}(T) \quad (13)$$

where

$$\begin{aligned} W_{\mathrm{corr}} = & -RT\ln\prod_{m=1}^{3N-7}\frac{e^{-(1/2)\hbar\omega_m/k_{\mathrm{B}}T}}{1-e^{-\hbar\omega_m/k_{\mathrm{B}}T}} \\ & -\left(-RT\ln\prod_{m=1}^{3N-7}\frac{k_{\mathrm{B}}T}{\hbar\omega_m}\right) \\ & -\left[-RT\ln\prod_{m=1}^{3N-6}\frac{e^{-(1/2)\hbar\omega^{\mathrm{U}}_{m}/k_{\mathrm{B}}T}}{1-e^{-\hbar\omega^{\mathrm{U}}_{m}/k_{\mathrm{B}}T}}-\left(-RT\ln\prod_{m=1}^{3N-6}\frac{k_{\mathrm{B}}T}{\hbar\omega^{\mathrm{U}}_{m}}\right)\right]_{Z=Z_{\mathrm{R}}} \end{aligned} \quad (14)$$

which corresponds to replacing the classical harmonic vibrational partition functions by the quantal ones. Although the correction is nominally harmonic, the frequencies are averaged over an ensemble of states for each value of z, and this is an approximate way to include anharmonicity. (Technically the average could be obtained by free energy perturbation

theory,[138] and such refinements could be included, but averaging the frequencies is convenient in practice and yielded similar results.[138])

Equation 11 is for Cartesian reaction coordinates, in which case the transition state dividing surfaces are hyperplanes in a Cartesian coordinate system. For more general reaction coordinates, an additional Jacobian term contributes.[400] This is small for the choice of z in eq 9 and may be neglected,[400,412] but it can be significant for more general reaction coordinates, such as an energy gap coordinate.[161,400] Schenter et al.[400] formulated the contribution in a way that makes it clear that it is part of the substantial free energy of activation. This contribution was neglected in all papers employing energy gap reaction coordinates until the recent study of Watney et al.,[161] who reformulated the TST rate constant including this contribution and used it for a full calculation. However, the way that they reformulated it does not allow the rate constant to be separated into substantial and nonsubstantial factors.

The calculated VTST rate constant with quantized vibrations is

$$k^{(1)}=\frac{k_{\mathrm{B}}T}{h}\exp[-\Delta G^{\mathrm{SRC}}_{T,\mathrm{QC}}/RT] \quad (15)$$

where $\Delta G^{\mathrm{SRC}}_{T,\mathrm{QC}}$ is the single-reaction-coordinate quasiclassical free energy of activation, at temperature T, which is calculated according to eq 13, and where the "(1)" denotes that this is the stage-1 rate constant. Note that $\Delta G^{\mathrm{SRC}}_{T,\mathrm{QC}}$ is evaluated at the maximum of the sum of the PMF and the quantized vibration correction; the ensemble of geometries corresponding to this maximum is called the variational transition state or the dynamical bottleneck. This is the final result of stage 1.

Coupling the system's reaction coordinate z to $3N_1 - 1$ other degrees of freedom for each member of the transition state ensemble allows one to obtain more highly optimized reaction paths (and hence more accurate reaction coordinates) for the system[30,104,121,413] and, based on calculations employing these more highly optimized reaction coordinates, to estimate an ensemble-averaged recrossing correction:

$$\Gamma=\frac{1}{M}\sum_{i=1}^{M}\Gamma_i \quad (16)$$

where Γ_i is the recrossing transmission coefficient for ensemble member i of the quasiclassical transition state ensemble,[121,144] and M is the number of ensemble members in the average. This leads to an improved rate constant $k^{(i)}_{\mathrm{QC}}$ for ensemble member i that corrects for dynamic recrossing events based on a different reaction coordinate for each member of the transition state ensemble:

$$k^{(i)}_{\mathrm{QC}}=\Gamma_i k^{(1)} \quad (17)$$

Then

$$k_{\mathrm{QC}}=\Gamma k^{(1)} \quad (18)$$

where k_{QC} denotes the ensemble-averaged quasiclassical rate constant. Figure 2 illustrates how choosing a dividing surface at an optimum point along an optimized reaction coordinate may minimize recrossing.

Finally, we calculate a transmission coefficient k_i for quantum effects (tunneling and nonclassical reflection) based on the optimized reaction coordinate of each member of the quasiclassical transition state ensemble, and a stage-2 estimate of the rate constant is given by

$$k^{\mathrm{EA-VTST/MT}}=\gamma k^{(1)} \quad (19)$$

where

$$\gamma=\frac{1}{M}\sum_{i=1}^{M}\Gamma_i\kappa_i \quad (20)$$

Although it is not needed for the rate calculations, it is sometimes interesting for interpretative purposes to compute a tunneling transmission coefficient, which is given by

$$\kappa=\frac{1}{M}\sum_{i=1}^{M}\kappa_i \quad (21)$$

If all ensemble members had the same transmission coefficients, then γ would equal Γ times k. However, this is only approximately true for real systems.

Although the EA-VTST method can in principle be used with arbitrarily accurate approximations for the transmission coefficient, calculations carried out so far[30,104,113,121,127,133,137,138,144,153,163,408] have involved calculating the individual k_i values by optimizing the tunneling paths between small-curvature tunneling[351,375] (SCT) paths and large-curvature tunneling[260,347,351–354] (LCT) paths. When this optimization is carried out as a function of the system's energy, the result is called microcanonically optimized multidimensional tunneling[352] (μOMT). Both the SCT and LCT methods include reaction-path curvature, which leads to corner-cutting tunneling. (Again see Figure 1.) The μOMT method may be considered to be an approximation to a more complete optimization,[372] called the least action approximation because it minimizes the imaginary action along a set of trial tunneling paths. The μOMT and least-action methods give similar quality results in validation tests.[414] Furthermore, the results are often only (but not always) slightly smaller or the same if one limits the calculation to small-curvature tunneling paths, and sometimes this is done to simplify the calculations; neglecting reaction-path curvature completely, though, is usually a serious approximation.[414] Another simplification

occasionally made in LCT calculations, but only when testing shows it is reliable, is to limit the final diabatic vibrational state along the tunneling coordinate to only the ground diabatic vibrational state; this is called[415] LCT(0). Neglecting reaction path curvature is denoted zero-curvature tunneling (ZCT). In this case tunneling proceeds along the minimum energy path (that is, for each ensemble member, along its minimum-energy path); this is still a multidimensional tunneling path because the isotope-dependent effective potential for tunneling includes the vibrationally adiabatic energy release (or energy uptake) of modes transverse to the path.[257,416]

The effective potential for tunneling in the ZCT and SCT calculations may be called $V_i^{\mathrm{G},0}(s^{(i)})$ where $s^{(i)}$ is the reaction coordinate (arc length along the isoinertial MEP of the $3N_1$-dimensional primary subsystem) for ensemble member *i*. The potential curve $V_i^{\mathrm{G},0}(s^{(i)})$ is obtained using the ground-state-transmission-coefficient approximation[416,417] for the $3N_1 - 1$ primary-subsystem modes transverse to the reaction path and using the zero-order canonical-mean-shape approximation[394] for the other modes. In the LCT approximation, the effective potential for tunneling is given by $V_i^{G,0}(s^{(i)})$ in adiabatic regions of coordinate space and by a state-specific diabatic extension[351,353,354,418] elsewhere.

Although there is not a one-to-one correspondence between SCT/LCT and adiabatic/diabatic or adiabatic/partially adiabatic (i.e., the language used in section 4), there is an approximate correspondence. In both SCT and LCT, we treat the electronic state adiabatically; in SCT we treat the nuclear motion as almost adiabatic,[259] and in LCT we treat it as partly diabatic.[260,347,351] In particiular, LCT uses the vibrationally adiabatic approximation when the system is in a classically allowed region *and* the natural collision coordinates[377,419] are single-valued, but it uses a diabatic treatment in the part of the reaction swath that corresponds to extreme corner cutting. Thus, SCT may be called an adiabatic-like treatment, and LCT is electronically adiabatic, partly nuclearly adiabatic, and partly nuclearly diabatic.

Multidimensional tunneling can sometimes exhibit features that are counterintuitive to those used when thinking in terms of one-dimensional tunneling. For example, D can tunnel more than H.[97,128,363,420–423] This would be impossible if both isotopes tunnel along the same path with the same effective potential, but in multidimensional tunneling both the tunneling paths and the effective potentials depend on all the masses in the system. The fact that the tunneling transmission coefficient for D can be larger than that for H can be understood by considering a limiting case. Consider therefore a reaction with a small barrier in which the zero point energy at the dynamical bottleneck is smaller than that of reactants. Because the zero point energy of activation is negative, energy is released into the reaction coordinate, and this energy release should be greater in magnitude for the H case than the D one because of their relative masses. It is possible then that the energy release would be great enough to cancel the barrier for H but not for D. Thus, there would be no effective barrier (and hence no tunneling) for the H case whereas a finite effective barrier and a finite tunneling effect would remain for D. In real cases, this inversion of expectations could occur because the effective barriers have different shapes even when both effective barriers are present and both systems exhibit tunneling. The real cases are also complicated by the isotope dependence of reaction path curvature.

Temperature dependence is folded naturally into the formulation of the multidimensional tunneling (MT) model in that the transmission coefficient accounting for tunneling and nonclassical reflection is written as the ratio of the Boltzmann-weighted quantum mechanical or semiclassical transmission probability P_i^{Q} integrated over all energies (E) to the same integral computed quasiclassically:

$$\kappa_i = I_{\mathrm{Q}}^{(i)} / I_{\mathrm{C}}^{(i)} \quad (22)$$

where

$$I_{\mathrm{Q}}^{(i)} = \int_{E_0^{\mathrm{RG}}}^{\infty} P_i^{\mathrm{Q}}(E) \exp(-E/k_{\mathrm{B}}T)\, \mathrm{d}E \quad (23)$$

and

$$I_{\mathrm{C}}^{(i)} = \int_{E_0^{\mathrm{RG}}}^{\infty} P_i^{\mathrm{QC}}(E) \exp(-E/k_{\mathrm{B}}T)\, \mathrm{d}E \quad (24)$$

where E_0^{RG} is the ground-state energy of the reactants and P_i^{QC} is the transmission probability implicit in the quasi-classical VTST calculation for ensemble member i:

$$P_i^{\mathrm{QC}} = \begin{cases} 1 & E > V_i^{\mathrm{G},0}(s_*^{(i)}) \\ 0 & E < V_i^{\mathrm{G},0}(s_*^{(i)}) \end{cases} \quad (25)$$

where $s_*^{(i)}$ is the location of the variational transition state along $s^{(i)}$. It is important that the quasiclassical transmission probability in the denominator be consistent with the rate constant (see eq 19) that is being corrected.[394,416,417] Therefore, $P^{\mathrm{QC}}(E)$ is a Heaviside function that discontinuously steps from zero to unity at the reaction threshold V_i^{QC} implied by the quasiclassical calculation for ensemble member i. Unlike the analytical limiting expressions of Kuznetsov–Ulstrup[93] theory, TST smoothly blends the tunneling and overbarrier contributions, and it can accommodate reaction coordinates of either the valence or the collective type. Another advantage is that the formulas are derived from a nonperturbative underlying atomic model, and the factors in the theory have been evaluated from full molecular dynamics simulations based on a potential energy surface, rather than being treated as model parameters.

Equations 22–24 bring out another important issue that is worth a comment, namely the meaning of “more tunneling”. The transmission coefficient may be partitioned into a tunneling contribution k_{T} and an overbarrier contribution k_{OB}:

$$\kappa_i = \kappa_{\mathrm{T}}^{(i)} + \kappa_{\mathrm{OB}}^{(i)} \quad (26)$$

The overbarrier contribution may be further partitioned into the classical part k_{C} minus the nonclassical-reflection part k_{NCR}:

$$\kappa_{\mathrm{OB}}^{(i)}=\kappa_{\mathrm{C}}^{(i)}-\kappa_{\mathrm{NCR}}^{(i)} \quad (27)$$

In these equations

$$\kappa_{\mathrm{T}}^{(i)}=\frac{\int_{E_0^{\mathrm{RG}}}^{V_i^{\mathrm{Q}}} P_i^{\mathrm{Q}}(E)\exp(-E/k_{\mathrm{B}}T)\,\mathrm{d}E}{I_{\mathrm{C}}^{(\mathrm{i})}} \quad (28)$$

$$\kappa_{\mathrm{OB}}^{(i)}=\frac{\int_{V_i^{\mathrm{Q}}}^{\infty} P_i^{\mathrm{Q}}(E)\exp(-E/k_{\mathrm{B}}T)\,\mathrm{d}E}{I_{\mathrm{C}}^{(\mathrm{i})}} \quad (29)$$

$$\kappa_{\mathrm{C}}^{(\mathrm{i})}=\frac{\int_{V_i^{\mathrm{Q}}}^{\infty} \exp(-E/k_{\mathrm{B}}T)\,\mathrm{d}E}{I_{\mathrm{C}}^{(\mathrm{i})}} \quad (30)$$

$$\kappa_{\mathrm{NCR}}^{(i)}=\frac{\int_{V_i^{\mathrm{Q}}}^{\infty} (1-P_i^{\mathrm{Q}})\exp(-E/k_{\mathrm{B}}T)\,\mathrm{d}E}{I_{\mathrm{C}}^{(\mathrm{i})}} \quad (31)$$

where V_i^{Q} is the effective quantum mechanical threshold for ensemble member *i*. Note that

$$V_i^{\mathrm{Q}}=\max_{s^{(i)}} V_i^{\mathrm{G},0}(s^{(i)}) \quad (32)$$

so that

$$V_i^{\mathrm{Q}} \geq V_i^{\mathrm{G},0}(s_*^{(i)}) \quad (33)$$

The tunneling portion of the rate constant is then given by

$$k_{\mathrm{T}}=\frac{1}{M}\sum_{i=1}^{M}(\kappa_{\mathrm{T}}^{(i)}\Gamma_i)k^{(i)} \quad (34)$$

and literally an “increase in tunneling” would refer to an increase in this quantity. However, the intended meaning of “increase in tunneling” is almost always “increase in tunneling transmission coefficient”, that is, increase in

$$\kappa_{\mathrm{T}}=\frac{1}{M}\sum_{i=1}^{M}\kappa_{\mathrm{T}}^{(i)} \quad (35)$$

In the large curvature tunneling (LCT) model and subsequent microcanonically optimized multidimensional tunneling (OMT) model, the optimal tunneling path includes the possibility of tunneling to or from the vibrationally excited states, providing alternative avenues to achieve enhanced tunneling at temperatures where the excited vibrational states are energetically accessible.

Note that step 2 of stage 1 converts the classical TST result into a quasiclassical result, which includes quantum effects in all bound vibrational coordinates but not in the reaction coordinate at the transition state. Stage 2 includes quantum effects in the reaction coordinate at the transition state. During stage 2, the system evolves in a fixed field of its surroundings. This is a reasonable approximation in many cases.[424] If it is not, one can either increase the size of the system or carry out a third stage[121,138,144] that allows the surroundings to vary as a function of the improved reaction coordinates of stage 2. The stage-3 recrossing transmission coefficients can account for the breakdown of the frozen bath assumption when nonequilibrium solvation effects are large.

An important advantage of the EA-VTST/MT approach is that the methods have been well validated against quantum mechanics for small-molecule reactions in the gas phase.[363,414,425–428]

In principle, as mentioned in section 1, in addition to recrossing (in Γ) and tunneling (in k), there is another contribution to the breakdown of TST, namely the violation of the quasiequilibrium assumption. So far, there is no evidence that this is a significant effect, at least in cases where a phenomenological rate constant exists. We will not discuss this issue any further in this review.

The potential energy surfaces (PESs) required in EA-VTST/MT are usually obtained from combined quantum mechanical and molecular mechanical (QM/MM) methods; this approach allows the entire solvated enzyme system to be treated at the atomic level.[31,124,237,429–432] In particular, QM is used to provide an appropriate description of the chemical bond rearrangement of the substrate, cofactor, nearby catalytic residues, and/or any key solvent molecules at the enzyme active centers, and MM is used to treat a large fraction (or all) of the protein environment and the bulk solvent along with any part of the cofactor and substrate that were not treated by QM. The QM/MM interaction accounts for the polarization of the wave function of the reaction center by the environment.[433] The choice for the QM method is typically a semiempirical electronic structure method, such as Austin model 1 (AM1)[434] or parametrized model 3 (PM3),[435] which are popular choices because of their efficiency and reasonable accuracy. Specific reaction parameters[113,404,436–438] (SRPs), semiempirical valence bond (SEVB) corrections,[104] simple valence bond (SVB) corrections,[127,439] or interpolated corrections[404,412,440,441] can be used to improve the quality of the potential energy surface in order to achieve quantitatively accurate results for dynamics. In our applications so far, the generalized hybrid orbital (GHO)[31,113,169,442–447] method is adopted to provide an electrostatically stable and smooth connection between the QM and MM regions; however, other QM/MM methodologies[448] can also be used. In fact, the choice of potential energy surface method is totally separate from the choice of dynamics methods; one could, for example, use empirical valence bond model[18,329] (EVB),

linear-scaling molecular orbital model,[449] or density functional theory[450] instead of GHO. In any case, the method uses the ground-electronic-state Born–Oppenheimer potential energy surface (as opposed to sometimes-incompletely-defined diabatic electronic surfaces) and, therefore, it is systematically improvable.

The computer codes for carrying out reaction rate calculations with EA-VTST/MT have been incorporated in a software package called CHARMMRATE,[451] which is a module of the CHARMM program[452] and which is available via the Internet. This package provides an interface of the versatile program CHARMM for simulating macromolecular systems with the POLYRATE program[453] for variational transition state theory calculations including multidimensional tunneling.

The original reference for EA-VTST/MT is ref 121, and further details of how the calculations are performed were given by Garcia-Viloca et al.[137] (for stages 1 and 2) and Poulsen et al.[138] (for stage 3). An introductory overview was given by Truhlar et al.,[30] and a more mathematical review of EA-VTST/MT has also been presented.[144]

5.2. Mixed Quantum/Classical Molecular Dynamics

To include nuclear quantum effects, Hammes-Schiffer's group has developed a mixed quantum/classical molecular dynamics (MQCMD), where the atom being transferred is represented by a three-dimensional vibrational wave packet and all other degrees of freedom are classical.[117] The Fourier–grid–Hamiltonian multiconfigurational self-consistent-field[107] method is employed to compute the hydrogen vibrational wave packet on a three-dimensional grid in the space. The MQCMD calculation is used to compute a PMF and an approximate TST rate constant. Dynamical recrossing effects are incorporated into a transmission coefficient.[115] In these calculations, the potential energy functions have usually been described by an empirical valence bond (EVB) model,[18,115,117,329] although the use of combined QM/MM potentials based on electronic structure methods has also been developed.[454] The energy gap (elaborated further below) between two diabatic electronic states is employed as the reaction coordinate to include solvent degrees of freedom.[120] This method has been applied to LADH[115,117] and DH-FR.[131,161]

Comparison of MQCMD to EA-VTST/MT brings up another ambiguity in the meaning of transmission coefficients. In EA-VTST/MT, the TST rate constant is quasi-classical. Thus, the transmission coefficient includes recrossing and quantum effects on the reaction coordinate. Because the tunneling dynamics is treated multidimensionally, the transmission coefficient also includes corrections for the nonseparability of the reaction coordinate in the tunneling dynamics. (As pointed out in section 1, the recrossing correction is also a correction for nonseparability of the reaction coordinate.) In MQCMD, the TST rate constant already includes quantum effects on the transferring hydrogen, and other quantum effects are neglected. The transmission coefficient is a correction for recrossing. Thus, the division into substantial and nonsubstantial contributions is different. For interpretative purposes, the EA-VTST rate constant can be evaluated with $k_i = 1$ to sort out the effect of tunneling (this has also been very useful for gas-phase reactions[455]). If an MQCMD calculation is compared to classical molecular dynamics calculations, the difference is due not only to tunneling but also to quantization effects on two other degrees of freedom (or

five if two atoms are quantized). In EA-VTST, the stage-1 rate constant includes the quantum effects of these modes as well as of all the rest of the $(3N_1 - 1)$ other modes in the primary system that are orthogonal to the reaction coordinate.

An accompanying paper[52] in this issue contains further comparison of the two kinds of choices for the reaction coordinate—geometrical reaction coordinates and collective solvent reaction coordinates. The use of a diabatic energy gap as the reaction coordinate dates back to the Marcus theory[293,295,299] of electron transfer. As mentioned in section 5.1, this kind of reaction coordinate is more general (a recent version is available[120]); for example it has heen widely employed for simulating electron transfer and more general reactions in enzymes and solutions by Warshel and coworkers.[27,29,165,168,311,456,457] For simulations of enzymatic reactions and well-defined processes in solutions where direct comparison of PMFs based on these two types of reaction coordinates has been possible, the PMFs of activation are in generally good agreement. There are two reactions that have been treated by both EA-VTST/MT with a geometrical reaction coordinate and MQCMD with a collective solvent coordinate, namely LADH[104,115,117,121] and DH-FR.[131,133,153,161,180,408] The main features of the results are similar, despite the entirely different natures of the reaction coordinates that were used. Protein motions and donor–acceptor modes that correlate with one reaction coordinate are also found to correlate with the other.[133] This provides a demonstration that one can obtain reasonable results with either type of reaction coordinate. It also signals a caution against a literal acceptance of the language used in many electron transfer models (for example, “the reaction is driven by configurational changes in the surrounding polar environment”[156]). The fluctuations of the collective energy gap coordinate do not “drive” the dynamics; rather the solvent coordinate can be used to define a transition state dividing surface through which the equilibrium one-way local flux provides a good approximation to the net global reactive flux, just as the reaction coordinate of eq 9 can be used for this purpose.[512–514] Even when a valence coordinate is a good reaction coordinate, solvent molecules may participate in the reaction and respond to the change of electronic properties of the system.[458]

The variational transition state, which is the dividing surface with the smallest calculated rate constant, depends on the choice of reaction coordinate z since it is defined by a hypersurface of constant z. In principle, one could use a very bad reaction coordinate and correct for it in the transmission coefficient. In practice, though, it seems much safer to use a good reaction coordinate, which is defined as one that has a small recrossing correction at the variational transition state.

5.3. Quantized Classical Path Method

The path integral[222,397,459–470,515] method represents another way to incorporate nuclear quantum mechanical effects in enzyme simulations.[65,66,70,71,79,98,106,157] Enzyme applications have been based on Warshel’s quantized classical path (QCP) algorithm.[66] This is similar in many respects to MQCMD, but it is easier to quantize more than one atom. For example, recent applications quantized three atoms.[106,152,471]

Olsson et al.[145,148] applied the QCP method to SLO. To date, their calculation is the only calculation on this system that includes the dynamics of the explicit protein environment.

The calculation reproduced the observed free energies of activation for both H and D transfer within 1 kcal/mol from 270 to 333 K, which is quite an achievement. However, the calculated KIE is very sensitive to these free energies of activation, and the large temperature dependence of their calculated primary H/D KIE, which decreases from 380 at 270 K to 60 at 333 K, disagrees with experiment. It is very hard to predict the temperature dependence of enzyme-catalyzed rate constants without adjusting parameters to do so. (In fact, very few calculations have even attempted this.) The QCP method has never been used to separate the KIE into factors due to tunneling and those due to other quantum effects, and so this separation is not available from the calculations, but such large effects must be dominated by tunneling.

5.4. Methods Based on a Single Reaction Path

Some tunneling calculations have been based on a single minimum energy path (MEP) connecting a set of stationary points that have been characterized on the potential energy surface as a saddle point or an energy minimum.[32,97,114,123,128,130,139,141] In general, it should be more reliable to use a method that incorporates protein fluctuations and free energy simulations, such as sampling ensemble members from a transition state ensemble identified by a maximum in a PMF profile.

6. Recrossing

Two types of all-atom methods have been used to estimate recrossing transmission coefficients for enzymatic reactions. The first approach is EA-VTST.[144] The second is the reactive flux method[472–474] and its variations.[27,115,117] A third way to estimate recrossing is by model theories such as Grote–Hynes[475] theory. Next, we will describe the major aspects of these three methods and their applications to enzyme systems.

6.1. EA-VTST Recrossing Transmission Coefficients

EA-VTST, as described in section 5.1, provides a systematic approach to estimating recrossing transmission coefficients. The recrossing depends on the choice of the transition state dividing surface. Ideally, if an optimal dividing surface is adopted in the full phase space, the recrossing correction can be eliminated and transition state theory will be classically exact. It should be noted that the choice of dividing surface is equivalent to the choice of reaction coordinate, provided that the transition state is a hypersurface perpendicular to the reaction coordinate. In gas-phase VTST calculations, a multidimensional reaction coordinate is usually adopted by following the minimum energy path (MEP) that connects the transition state to the reactant and product states, and the dynamical bottleneck is identified as a quasiclassical free energy maximum by varying the position of the dividing surface (which is orthogonal to the reaction coordinate) along the reaction coordinate. Note that “quasiclassical” is used here since the vibrations of the degrees of freedom that are orthogonal to the reaction coordinate are quantized in the free energy calculations. The use of a multidimensional reaction coordinate involving all atoms in the system, together with the variationally optimized dividing surface, minimizes recrossing well enough that the recrossing transmission coefficient is usually close to unity for this kind of reaction coordinate at room temperature, and it is omitted.

In the condensed phase, the identification of a single dominant MEP becomes impossible because the potential energy surface for such systems contains numerous energy minima and saddle points, resulting in an ensemble of possible reaction paths. For example, a partial PES of alanine tetrapeptide contains 139 energy minima and 502 transition states.[476,477] Since a tetrapeptide contains only four residues, whereas a typical enzyme contains several hundred amino acid residues plus thousands of solvent molecules, the single-MEP method is certainly unable to provide a complete picture of the dynamics; therefore, an ensemble of reaction paths and transition states is necessary to simulate the dynamics realistically.

The recrossing transmission coefficients of EA-VTST or EA-VTST/MT are corrections for trajectories passing through predefined transition state dividing surfaces more than once. In classical mechanics, the recrossing correction is the full correction for the deviation of TST from the exact classical equilibrium reaction rate constant. In EA-VTST, the stage-1 reaction coordinate is usually a valence coordinate. Such a simple reaction coordinate is not sufficient because the realistic reaction coordinate is multidimensional. This has been systematically corrected in EA-VTST by using optimized multidimensional reaction coordinates. The transmission coefficients that account for recrossing or nonequilibrium solvation are a “fix” to make up for the incomplete optimization of the reaction coordinate and, hence, of the dividing surface.

6.2. Reactive Flux Method

Another approach to calculating the recrossing transmission coefficients is called the reactive flux or activated dynamics method.[213,478] The reactive flux approach is based on trajectories that are initiated at the transition state.[472,473] Starting with an ensemble of transition state configurations, one propagates trajectories starting from the transition state configurations and monitors the transition state recrossing events as a function of time. The recrossing transmission coefficients can be computed from the plateau value of a time correlation function computed from these trajectories.[49,117,213,474,478–480] A disadvantage of this method, as compared to EA-VTST, is that the recrossing correction is determined without quantizing modes transverse to the reaction coordinate whereas the EA-VTST recrossing correction is quasiclassical and fully includes quantization in modes orthogonal to the reaction coordinate.

Hwang et al.[29,165] have used a linear-response approximation to cast the problem of recrossing in terms of the autocorrelation of the diabatic energy gap in order to compare the recrossing effect in enzymes to that in solution.[168]

6.3. Model Theories

Grote–Hynes theory[475] and its variants[424] present another approach to estimating the breakdown of TST due to recrossing. In these theories, the solvent is modeled by a collective solvent coordinate. The Grote–Hynes Γ may be approximated as k^{VTST}/k^{TST}, where k^{TST} is the rate constant calculated with the reaction coordinate defined entirely in terms of system coordinates, and k^{VTST} is the rate constant calculated when the transition state is variationally optimized by allowing it also to be a function of the collective solvent coordinate.[481] This is sometimes called friction.[167] In particular, although it is not a general

rule, recrossing tends to be called friction in phenomenological models with collective treatments of the solvent or when full dynamical simulations are analyzed in terms of concepts from generalized Langevin dynamics,[167,482,483] whereas it tends to be called recrossing when the same effect is calculated with full atomic detail.

The kind of friction we have just discussed may also be called nonequilibrium solvation,[236,484] but it should not be confused with a nonequilibrium distribution of reactants; it is a recrossing effect. When the reaction coordinate is improved by variationally optimizing the transition state dividing surface, the calculated rate constant goes down. When the optimization consists of letting solvent degrees of freedom participate in the reaction coordinate (and, hence, in the definition of the transition state dividing surface, which is normal to the reaction coordinate), the effect is called nonequilibrium solvation.[236]

6.4. Survey

Table 1 gives a survey of calculated recrossing coefficients. It is of particular interest to compare the magnitudes of transmission coefficients determined with a geometrical reaction coordinate (valence coordinate) to those obtained when one uses a collective reaction coordinate (such as an energy gap reaction coordinate) since the meaning of a recrossing transmission coefficient depends on the transition state that is being recrossed. One can argue that a large fraction of the recrossing revealed by a small recrossing transmission coefficient is caused by using an oversimplified reaction coordinate. Since transmission coefficient calculations have not been carried out by the reactive flux method for any enzyme system with a collective reaction coordinate, one cannot directly compare the magnitudes of the recrossing transmission coefficients obtained by the same method for the two types of reaction coordinate. However, if a geometrical reaction coordinate were incapable of effectively capturing solvent and enzyme dynamics along the reaction coordinate, one would expect that the transmission coefficient would be significantly less than unity. The fact that all transmission coefficients calculated to date for enzyme-catalyzed reactions are 0.36 or higher provides evidence that the use of a geometrical reaction coordinate is reasonable.

A number of authors have defined a reference reaction in order to dissect various factors contributing to catalysis. Many comparisons (for example, by Warshel and coworkers[168]) have been made between the free energy of activation for the reaction in an enzyme and for an uncatalyzed reference reaction in water,[52] but quantitative comparison of recrossing transmission coefficients between catalyzed and uncatalyzed reactions has only been made for two enzymes.[169,171–173] Following the same spirit, such comparisons of the tunneling contribution will provide further insight into the role that tunneling plays in enzyme catalysis.[66,70,79] Unfortunately, experiments for quantifying the amount of tunneling for uncatalyzed analogues of enzyme reactions in water have been carried out in only a few cases,[134,280] owing to the difficulty of finding either appropriate models or slow reaction rates for the corresponding solution-phase reaction. However, molecular simulation, by characterizing the tunneling behavior in both catalyzed and uncatalyzed reactions, can provide valuable information about whether the enhancement of quantum mechanical tunneling enhances catalysis. Since the QCP methods and wave packet method cannot

decouple the tunneling contribution from other quantum effects such as zero point energy and the thermal contribution of the quantized vibrational free energies, these methods are limited for identification of tunneling per se. In contrast, since the quantization of the reaction coordinate and degrees of freedom that are orthogonal to the reaction coordinate are carried out separately, the VTST/MT approach, with or without ensemble averaging, is very suitable for extracting useful knowledge of tunneling factors from the overall increase of the rate constant or reduction of the free energy of activation.[144,455] More applications of this approach are expected.

7. Applications

A few applications have been selected here for detailed discussion to illustrate the application of TST. This discussion complements the discussion of selected systems that was already presented in sections 3.1, 3.3, 3.4, and 4.

7.1. Yeast Enolase

The proton transfer catalyzed by yeast enolase (YE) is a very interesting case because the correct primary KIE (as judged by comparison to experiment[485]) can be obtained only by including recrossing, which is greater for H than for D.[97] Furthermore, the tunneling transmission coefficient is larger for H than for D.[97]

7.2. Triosephosphate Isomerase

The activated dynamics technique was first applied to an enzymatic reaction in calculations carried out by Neria and Karplus in 1997; the dynamical recrossing contribution to the reaction rate constants for the proton transfer step in the triosephosphate isomerase (TIM)-catalyzed reaction was evaluated.[474] The reaction involves a C-to-O proton transfer, and the masses of all atoms (including hydrogens) were set to 10 amu to allow a larger time step. (As far as we know, all other simulations discussed in this review were carried out with the correct masses.) The reaction coordinate was defined in a way that reduces to eq 9 for the case considered. The recrossing transmission coefficient was calculated to be 0.43 ± 0.08.[474] The authors tested the validity of a “frozen bath” approximation and compared their results to Grote–Hynes theory.[475] More recently, Wang et al.[170] applied the reactive flux method to calculate the recrossing transmission coefficients for the TIM-catalyzed proton transfer with a different potential energy surface. The same definition of the reaction coordinate was adopted, and a transmission coefficient of 0.47 was obtained,[170] in good agreement with the earlier study. Cui and Karplus[32] calculated the recrossing transmission coefficient by VTST. In particular, as explained in section 5.1, comparing the VTST rate constant for a transition state normal to a distinguished (i.e., arbitrary) reaction coordinate to that for a transition state normal to an optimized reaction coordinate provides an estimate of the amount of recrossing of the former. Using a mass-weighted version of eq 9 as the DRC, they calculated $\Gamma = 0.69$, in qualitative agreement with the activated dynamics estimate. Activated dynamics can overestimate the amount of recrossing (underestimate Γ) because it does not enforce zero point energy requirements when a trajectory returns to the dynamical bottleneck (or even when it leaves it).

Cui and Karplus[32,128] calculated the tunneling transmission coefficient for the proton transfer reaction catalyzed by T1M with an AM1-SRP potential energy surface and the SCT multidimensional tunneling approximation. They found that k = 9.7, with a standard deviation of 4.2 (over the configurations sampled), whereas neglecting reaction path curvature dropped k to 2.1. They also analyzed[32,132] in great detail the coupling of many vibrational modes to the reaction coordinate, showing clearly that it is not realistic to assume that a separable or nearly separable reactant hydrogen stretch is the tunneling coordinate, as in the simplified Kuznetsov–Ulstrup model that has been applied by various workers to enzyme kinetics. The applicability of the VTST/SCT method that they employed was validated by comparing secondary KIEs to experiment. They obtained 1.15[128] (or 1.14[32]) in comparison to an experimental value[76] of 1.12. Taken as a whole, the TIM studies of Cui and Karplus provide an example of the remarkably thorough understanding of an enzyme reaction that can be achieved by modern molecular dynamics simulations.[32]

7.3. Methylamine Dehydrogenase

The MADH system has been studied with multidimensional tunneling employing both the single-reaction-coordinate VTST/MT method[114,123,139] and the multiple-reaction-coordinate EA-VTST/MT method.[113] In both cases, the reaction paths correspond to the motion of a primary system (with 25[113] or 31[114] atoms from the substrate, part of the cofactor, and part of the enzyme) in the presence of a fixed larger secondary system containing all the rest of the atoms. To make a connection with general theoretical concepts, this secondary system (containing most of the enzyme and cofactor and all of the water) may called the “solvent”. The EA-VTST/MT calculations include an average over six solvent configurations. Not only does the averaging more fully represent the statistical mixture of reaction paths present in the real system, where the “solvation” by the secondary subsystem depends on its configuration, but by allowing the reaction path to depend on the enzyme configuration, one also allows the enzyme coordinates to participate in the reaction coordinate, which, as discussed above, is the essence of what is usually called nonequilibrium solvation.[236]

Table 2 shows the tunneling transmission coefficients from the EA-VTST calculation.[113] In addition to the ensemble-averaged values, the table shows the standard deviation computed from the ensemble of reaction paths. This provides a quantitative measure of the diversity of reaction paths that contribute to the process. Table 1 also shows the large effect of reaction path curvature, which increases k from 34.6 to 83.6 for CH_3NH_2 substrate. There is also recrossing in this system with Γ = 0.76 for CH_3NH_2 substrate and Γ = 0.81 for CD_3NH_2 substrate. The calculated isotope effect including recrossing and tunneling with reaction-path curvature is 18.3, in good agreement with the experimental values of 16.8–17.2.

7.4. Alcohol Dehydrogenase

Hwang et al.[486] suggested that the computationally demanding reactive flux calculation can be avoided by recognizing the close relationship between the recrossing transmission coefficient and the energy gap reaction coordinate autocorrelation functions. They carried out simulations of the alcohol dehydrogenase-catalyzed reaction for the enzyme case and for the uncatalyzed reaction in solution and concluded, by inspecting the shapes of the trajectory distributions of the two systems, that no significant difference exists for the two cases. Their

conclusion is largely not altered by applying the approach to a mutant compared to wild-type enzyme.[487] (More recently, Warshel and coworkers have made this argument based on the autocorrelation function of the energy gaps for the catalytic reaction of subtilisin and the corresponding reaction in water.[168])

The quantum tunneling effects in ADH have been very challenging for theory. In particular, using one-dimensional tunneling models, it was never possible to simultaneously get agreement of a theoretical model with the primary and secondary KIEs with a reasonable force field. However, multidimensional tunneling calculations explain the primary and secondary KIEs extremely well, as discussed elsewhere.[104,121] As discussed there, the isotopic dependences of the effective potentials for tunneling, of the reaction-path curvature, and of the relative alignment of the positions of maximum reaction-path curvature with the maxima of the effective potentials all play important roles in these KIEs. Transmission coefficients[121] are given in Table 3. Basran et al.[116] and Tresadern et al.[123] compared the effective potentials for tunneling in ADH, MADH, and AADH, and SLO.

7.5. Thermophilic Alcohol Dehydrogenase

Kohen et al.[99,105] studied the thermophilic BsDHFR and concluded from the shapes of Arrhenius-like plots of KIEs that the relative importance of tunneling increases with increasing temperature. A perhaps even more striking aspect of their results than the Arrhenius-like plots of the KIEs are the Arrhenius plots of the rate constants themselves, which are convex. As pointed out elsewhere,[488] convex Arrhenius plots are rather rare, but their interpretation is that the average energy of molecules that react increases less rapidly with temperature than does the average energy of all possible reactants. (This has been used to directly fit thermophilic alcohol dehydrogenase data.[489]) Various explanations are possible for the average energy of molecules that react increasing less rapidly than the average energy of all possible reactants; for example, there could be a pool of especially reactive states that does not broaden as temperature increases. Antoniou and Schwartz[119] have postulated that convex Arrhenius plots could arise from tunneling strongly coupled to a promoting vibration. It is not clear if this stimulating suggestion is the correct explanation in this case, but it raises the issue that it is dangerous to interpret the temperature dependence of Arrhenius plots of ratios of rate constants when one does not understand the temperature dependences of the individual rate constants. Therefore, the arguments that the relative importance of tunneling increases with temperature are unconvincing.

7.6. Haloalkane Dehalogenase

Further insights into understanding of the role that protein dynamics play in enzyme catalysis are provided by comparing the recrossing transmission coefficients for an enzyme-catalyzed reaction and the uncatalyzed one in aqueous solution. This comparative approach is highlighted by the recent studies of haloalkane dehalogenases (DHase) reported from several groups.[169,171,490–492] DHases involve nucleophilic displacement by a catalytic Asp residue in the active site to catalyze the conversion of chlorinated hydrocarbons into alcohols and chloride ion. Nam et al. studied the recrossing events both in DHase and in water with activated dynamics calculations based on a QM/MM potential energy surface.[169] The recrossing transmission coefficients they obtained are 0.53 and 0.26 in enzyme and in

water, respectively. They demonstrated that the reaction rate is enhanced in the enzyme by reducing the dynamical recrossing by a factor of 2 compared to the uncatalyzed reaction in water; hence, dynamical recrossing contributes to the enzyme catalysis, although it is not the most dominant factor. Importantly, analysis of the friction kernels at the transition state for both the catalyzed and uncatalyzed reactions demonstrated that the origins of the dynamical effects are very different, despite the similarity in the computed Γ values. In solution, the forces acting on the reaction coordinate are dominated by electrostatic interactions with aqueous solvent, whereas, in the enzyme, they are dominated by the symmetric stretch vibrational mode of the nucleophilic O on the Asp and the substrate C that undergoes attack. This change is consistent with a picture that desolvation in the active site plays a critical role in lowering $\Delta G_T^{\ddagger}$. In a subsequent calculation, Soriano et al. performed a similar comparison for the same reaction in enzyme and in aqueous solution;[171] although somewhat larger transmission coefficients of 0.77 and 0.57 were obtained in enzyme and in water, respectively, the quantitative conclusion of Nam et al. was not altered, although the interpretation of the role of the enzyme was quite different.

The intrinsic chlorine primary KIE for the dehalogenation reaction of dichloroethane by haloalkane dehalogenase has been determined by Devi-Kesavan and Gao using the EA-VTST/MT method.[492] The calculated value of 0.31% is in reasonable agreement with the experimental result of 0.66% for a 1-chlorobutane substrate.[516] The slight discrepancy may be due to the use of different substrates. It also reflects a small structural difference between the semiempirical QM/MM potential and high-level G2 and DFT methods. The semiempirical model yielded a tighter transition state that has a shorter distance for the forming C–O bond by about 0.06 Å than that of the optimized structure using G2 theory. Similar findings were obtained by Paneth and coworkers from a separate investigation.[516]

7.7. Dihydrofolate Reductase from *E. Coli*

DHFR catalyzes the reductive conversion of 7,8-dihydrofolate to 5,6,7,8-tetrahydrofolate with the key chemical step being a hydride transfer reaction from the nicotineamide ring of the reduced form of nicotineamide adenine dinucleotide phosphate coenzyme.[38] DHFR offers a target for anticancer and antibacteria drugs because of the important role of tetrahydrofolate in the biosynthesis of several amino acids and nucleotides.[493] Asa paradigmatic system, DHFR also has been subject to numerous experimental and theoretical investigations.[37,38,49,131,133,146,153,161,172,180–182,186,188,195–197,289,408,433,494–499]

Agarwal et al. employed the MQCMD approach to study the reaction mechanism and KIEs in the hydride transfer reaction catalyzed by EcDHFR; recrossing transmission coefficients of 0.80 ± 0.03 and 0.85 ± 0.01 were obtained for reactions transferring a hydride and deuteride, respectively, at 300 K.[131] The same system was investigated by Garcia-Viloca et al. with the EA-VTST/MT approach.[133] Their transmission coefficients are in Table 4, along with the standard deviations. Although a qualitatively different approach was adopted, transmission coefficients of 0.75 ± 0.26 and 0.82 ± 0.21 were obtained for H and D reaction, respectively,[133] similar to the results of Agarwal and co-workers.

The temperature dependence of the primary KIEs has been measured from 278 to 318 K by Sikorski et al., and they found that the H/D and H/T primary KIEs are almost temperature independent over the temperature range of the measurement.[146] The authors interpreted their results as environmentally coupled tunneling and vibrationally enhanced ground-state tunneling, where the modulation of the tunneling amplitude by a gated motion varies with temperature.[146] We, in collaboration with Ma,[153] carried out free energy simulations and computed KIEs as a function of temperature by using EA-VTST/MT based on a combined QM/MM potential. Interestingly, our calculations (see Tables 5 and 6) reproduced the trend of weak temperature-dependent KIEs of the DHFR-catalyzed H transfer within experimental errors. Furthermore, two features that might be used to explain this small *T* dependence were identified from these calculations.

The first interesting feature is the sliding along the reaction coordinate of the variational transition state location as temperature is varied; this introduces different amounts of quantized vibrational contribution to the KIE at 278 and 318 K. This temperature-dependent shift of the transition state toward the product side can be seen even in the classical PMF profile, which is consistent in trend with the Hammond postulate;[500] that is, the transition state resembles the reactant less in terms of free energy when temperature rises, resulting in a more symmetric barrier location at the higher temperature. As is often the case, the more symmetric barrier is also thinner. (This effect is not directly related to tunneling because the tunneling calculations are based on the barrier top of the quasiclassical PMF around the variational transition state, but it is suggestive.) The response of the KIE to a variation of the transition state location is an old subject in KIE theory, and it was discussed in a very early paper[242] where Westheimer proposed that larger KIEs would be observed for a reaction that has a symmetric transition state than for one that has a transition state resembling reactant or product; this is also known as the “Westheimer effect” in the literature. The Westheimer effect used to be applied at the saddle point, but we now understand that it must be interpreted in light of dynamical bottlenecks discovered by VTST.

The second interesting feature is an unusual temperature dependence of tunneling transmission coefficients; this was analyzed by tunneling calculations for a hypothetical situation in which the effective barrier ensemble determined at one temperature is used for calculate tunneling at another temperature. This computer experiment offers an opportunity to separate the intrinsic temperature dependence of tunneling from the observed *T* dependence that includes a contribution from the environmental change. The effective barrier ensemble at the higher *T* turns out to be more symmetric and thinner, hence facilitating tunneling at the higher *T*, providing a balance effect to cancel part of the “normal” or “intrinsic” temperature dependence of tunneling. The rigid barrier combined with a fixed transition state position predicts a change of 12% in H/D KIEs from 278 to 318 K, compared to the smaller KIE change of 6.5% in the consistent calculation, in which the system tunnels through a consistent effective barrier sampled at the consistent temperature. The temperature dependence of KIEs has also been compared with a gas-phase reaction, with similar amplitude of the KIEs. It was found that the gas-phase reaction has a much stronger temperature dependence of the KIE over the same temperature range at which the enzyme system was studied.

As an example of the broad distribution of enzyme configurations included in the calculations, Table 6 shows the transmission coefficients for all 20 of the ensemble members at each temperature. The averages and standard deviations are shown in Table 5. Table 6 shows that the distribution is broader at 278 K, primarily because of five ensemble members with κ values greater than 5.

7.8. Hyperthermophilic DHFR from *Thermotoga Maritima*

Primary H/D KIEs have also been measured for the hydride transfer step catalyzed by the hyperthermophilic TmDHFR,[289] where the enzyme reaches its optimal activity at about 353 K, which is approximately 40 degrees higher than the physiological temperature of its mesophilic homologue in *E. coli*.[501] The extraordinary resistance of this hyperthermophilic enzyme to heat denaturation seems to be optimized by nature in a way that sacrifices some of DHFR's catalytic power since TmDHFR is a "slower" enzyme than EcDHFR, when each is considered at its own optimal temperature.[497] From the structural perspective, one distinguishing feature of TmDHFR is that it exists as a homodimer, which is believed to contribute primarily to its enhanced thermostability at elevated temperatures.[497]

The temperature dependence of KIEs has been suggested to be an indicator of coupling between the chemical bond rearrangement and the enzyme environment. In particular, for the DHFR reaction, the energy barrier for the hydride ion to tunnel may be modulated to different extents by the vibrational motions of the protein at different temperatures. Evidence from NMR relaxation experiments[494] and crystal structures reveals that several flexible regions, especially the so-called M20 loop, undergo significant conformational change during the DHFR catalytic cycle.[495] If the weak dependence of KIEs on temperature in DHFR is correlated to particular protein dynamical features, as suggested by a number of recent studies, a correlation of the dynamics of these loop regions with the unusual KIEs may be established to offer a better understanding of these kinetic data at a molecular level. However, such a hypothesis has not been examined with simulations that include full atomic details.

The TmDHFR system provides a unique case to test the hypothesis of environmentally coupled tunneling because of the following two reasons. First, it was found that the flexible loop, which adopts a "closed" conformation to protect the ligand from being accessed by bulk solvent in EcDHFR,[495] is locked into the dimer interface in TmDHFR and therefore adopts an "open" conformation that cannot form a hydrophobic binding pocket as well as its mesophilic homologue.[497] Second, both the crystal structure and kinetic measurement of the TmDHFR-catalyzed hydrogen transfer KIEs are available, making the system a good test case. The enhanced thermostability allows TmDHFR to retain significant catalytic activity over a wider range of temperature. The Arrhenius plot of the primary H/D KIEs for TmDHFR-catalyzed hydrogen transfer, measured from 279 to 338 K, displays a characteristic biphasic shape with a maximum magnitude of its curvature at 298 K; the KIE is strongly temperature dependent below 298 K, and the KIE becomes weakly *T*-dependent when temperature is increased above 298 K.

In collaboration with Pang and Allemann,[163] we have carried out EA-VTST/MT studies for the TmDHFR system based on the combined QM/MM potential that was developed

previously for simulating[133,153,433] the EcDHFR system. Since DHFR and TmDHFR catalyze the same reaction, calculations employing the same parametrization of the quantum mechanical electronic structure model are expected to faithfully reflect the structural and dynamical differences in these two enzymes. The PMF profiles have been computed[163] at 278, 298, and 338 K for the TmDHFR-catalyzed reaction, where the wild-type enzyme forms a homodimer. In order to shed light on the effect of the dimerization on the enzyme activity, we also carried out a control simulation at 298 K where only the protein monomer is included in the modeling. The calculations[163] give classical PMFs of activation of 23 and 21 kcal/mol for the TmDHFR-catalyzed H transfer at 298 and 338 K, respectively, which are about 6 kcal/mol higher than that of the EcDHFR reaction at 338 K. The quasiclassical free energy of activation, including nuclear quantum effects such as zero point energy, is lower than the classical one by 2–3 kcal/mol, similar to the EcDHFR case.[133] Interestingly, the control simulation in which only one monomer of TmDHFR is included gives a classical free energy of activation as high as 26 kcal/mol, indicating that the monomeric enzyme loses its activity significantly, which suggests that the dimerization contributes to enzyme catalysis in TmDHFR. The EA-VTST/MT calculations yield H/D primary KIEs of 3.0, 2.9, and 2.2, at 279, 298, and 338 K, respectively, for the TmDHFR-catalyzed H transfer, as shown in Table 7, compared to 6.7, 4.0, and 3.7 measured experimentally at these temperatures. The tunneling transmission coefficients averaged over 14 configurations increase monotonically when temperature is decreased, which is in accord with the conventional picture that tunneling becomes more important at low temperatures. Significant changes in the free energy barrier shape and shift of the locations of variational transition states are also observed at different temperatures, which have been suggested to explain the weakly *T*-dependent KIE in EcDHFR.[153] Another finding in our calculation is that the standard deviations of the tunneling, recrossing, and overall transmission coefficients are smaller at high temperature than at low temperature. Interestingly, similar temperature-dependent behavior of the transmission coefficients has also been observed in the EcDHFR system.[153] If these standard deviations can be viewed as a reflection of fluctuations of the dynamical barrier, these data seem to suggest that the system climbs over and tunnels through more rigid barriers at high temperatures, which fluctuate less significantly than those at low temperatures.

7.9. Xylose Isomerase

Xylose isomerase (XyI) catalyzes the interconversion of D-xylose and D-xylulose in bacteria. In an EA-VTST/MT study of xylose isomerase carried out by Garcia-Viloca et al.,[127,137] the recrossing transmission coefficients have been reported as 0.95 ± 0.04 for H and 0.95 ± 0.02 for D, respectively.[137] In this study, a valence coordinate is used as the reaction coordinate and the potential energy surface is obtained by using QM/MM/SVB based on the PM3 method. See Table 8 for transmission coefficients.

7.10. Short-Chain Acyl-CoA Dehydrogenase

In an EA-VTST/MT study of short-chain acyl-CoA dehydrogenase (SCAD) carried out by Poulson et al., the recrossing transmission coefficients calculated in stage 2, that is, with the static-secondary-zone approximation, are 0.36 ± 0.3 for H and 0.40 ± 0.3 for D, respectively.[138] See Table 9. The significant amount of recrossing in the small transmission

coefficients was attributed to the necessity of including solvent response in the second-stage reaction coordinate which can also be understood as the breakdown of the static-secondary-zone approximation. Allowing the secondary zone to relax along the minimum energy path, which is realized by introducing additional free energy perturbation calculations in stage 3, inflated the recrossing transmission coefficients to 0.86 ± 0.04 and 0.82 ± 0.01 for H and D, respectively.[138]

7.11. Catechol O-Methyltransferase

Activated dynamics simulations have been performed by Roca et al. for the methyl transfer reaction catalyzed by catechol *O*-methyltransferase (COMT) and a corresponding model reaction in water.[172,173,503] The reaction coordinate was like eq 9 but was suitably modified for C transfer, as opposed to H transfer. A larger degree of recrosssing is observed for the aqueous solution-phase reaction with a computed recrossing transmission coefficient of 0.62 ± 0.04, compared to a recrossing transmission coefficient of 0.83 ± 0.03 in the enzyme.[172] The observation of a reduced extent of recrossing in the enzyme compared to that in the uncatalyzed reaction is consistent with the studies on DHase.[136,139] Grote–Hynes theory[475] gave excellent agreement with full dynamics for both aqueous solution and the enzyme, yielding 0.58 and 0.89, respectively, which agrees with full dynamics within the combined statistical uncertainties of the two calculations.[173]

7.12. Glyoxalase I

Glyoxalase I catalyzes the conversion of a hemiacetal intermediate to *S*-D-lactoylglutathione by abstraction of a proton from a nonacidic carbon atom of a substrate by a glutamate residue.[471] Feierberg et al.[106] simulated this reaction using a diabatic energy gap reaction corodinate and the QCP method to include quantum effects. They found an H/D primary KIE of 5 ± 1 in the enzyme and 4 ± 1 in aqueous solution. The experimental KIE for the enzyme reaction is ~3.[502]

8. Further Discussion of Ensembles

A very interesting recent paper[190] has the questioning title “Transition State Ensemble in Enzyme Catalysis: Possibility, Reality, or Necessity?” The authors conclude that indeed this concept is real and needed. We agree. The transition state is an ensemble of phase points even for the gas-phase H + HD $\rightarrow$ H_2 + D reaction,[144] where the ensemble is centered on a single reaction path, but for enzymes there is also an ensemble of reaction paths. To sample only one reaction path is very dangerous, as the distributions of transition states shown in this review have demonstrated.

In recent years, the introduction of single-molecule enzymology has provided a new set of opportunities for understanding the dynamic disorder of enzymes.[504–511] This method, at least in principle, offers the opportunity to directly study the distribution of protein fluctuations that participate in catalysis. Ensemble-averaged TST includes these fluctuations, and comparison of full dynamical simulations to the results of single-molecule experiments should prove interesting in the future.

9. Concluding Remarks

Transmission coefficients are sometimes viewed as corrections to transition state theory, but in modern formulations, the transmission coefficient is an important part of the calculation and is fully integrated into the theory, not treated as an afterthought or correction. A rate calculation may be carried out in two stages. The first stage calculates the probability of producing the transition state ensemble. This may be based on various kinds of reaction coordinates, including a valence coordinate such as a function of the interatomic distances of breaking and forming bonds or a collective coordinate such as one that measures the reorganization of the protein and the solvent. Each reaction coordinate produces its own transition state ensemble and a corresponding quasithermodynamic free energy of activation. In a second stage (or second and third stages, depending partly on nomenclature and partly on the complexity of the calculation), one calculates a transmission coefficient that accounts for recrossing (the fraction of members of the transition state ensemble moving toward products that originated as reactants and will proceed to products without returning to the transition state) and quantum effects on the reaction coordinate. The latter includes nonclassical reflection as well as tunneling (which is nonclassical transmission) but is usually dominated by tunneling and so is often called the tunneling transmission coefficient. Since a reliable tunneling calculation is multidimensional (i.e., not based on a single separable tunneling coordinate), the tunneling transmission coefficient also includes dynamical quantum effects on coordinates coupled to the reaction coordinate. Stage 2 is usually based on atoms in the active site and may include a refinement of the reaction coordinate or an ensemble of reaction coordinates and hence a refinement of the transition state ensemble. The best way to define the transition state ensemble for a given progress coordinate is variational transition state theory, which corresponds to maximizing the quasithermodynamic free energy of activation. In conventional notation, the result of stage 1 is written with the quasithermodynamic free energy of activation in an exponent and the transmission coefficient as a pre-exponential factor. Although pre-exponential factors such as the transmission coefficient have a much smaller effect (~ <1–2 orders of magnitude at room temperature) on rate constants than do catalytic effects on quasithermodynamic free energies of activation, transmission coefficients are often very sensitive to the detailed nature of the reactive motion and can have large effects on KIEs and their temperature dependences, which are key experimental observables for probing the details of reaction-coordinate motion.

The two main contributions to the transmission coefficients for enzyme reactions—recrossing and tunneling—should both be calculated with vibrations transverse to the reaction coordinate quantized. Furthermore, the method should be validated against accurate quantum dynamics for simpler systems where accurate dynamics calculations are feasible. Accurate transmission coefficients to account for tunneling should be multidimensional because one-dimensional models of reactive tunneling have been found to be unreliable. Finally, for reactions in liquid-phase solutions and enzymes, the transmission coefficient should properly reflect the diversity of reaction paths that contribute to a typical condensed-phase reaction. A formalism, namely EA-VTST/MT, satisfying all these requirements has now been developed and is reviewed here along with other procedures that have been

applied for estimating transmission coefficients of reactions catalyzed by enzymes. Full dynamical simulations are now available for many enzyme-catalyzed reactions, and they allow a detailed picture of motion along representative reaction coordinates and tunneling paths. They can also be used to test more approximate simplified analytical expressions that, if valid, can be used to illustrate qualitative features, and they provide quantitative estimates of the magnitudes of transmission coefficients for realistic models of enzyme-catalyzed reactions with reasonable choices of reaction coordinates.

The recrossing factor for enzyme-catalyzed reactions seems to be between 0.3 and 1.0 in most cases with practically usable definitions of the transition state. This means that transition state theory provides a good starting point for qualitative and quantitative modeling of enzyme kinetics.

Quantum mechanical tunneling plays a significant role in enzyme-catalyzed reactions. It has been known for a long time[363,425] that gas-phase hydrogen atom transfer reactions with barriers of 5–10 kcal/mol or higher are dominated by tunneling at room temperature, even when the primary KIE is <7. There was no reason to expect that proton, hydrogen-atom, or hydride transfer reactions catalyzed by enzymes should be different, and indeed, it is now clear that they are not. When faced with a reaction of this type, it is no longer reasonable to search for evidence of tunneling. If a surprising discovery were to be made, it would require searching for the absence of tunneling. It is also clear now that one-dimensional models of tunneling and models that neglect reaction-path curvature are inadequate to explain either the magnitude of the tunneling contribution or the qualitative nature of KIEs.

Acknowledgments

The authors are grateful to Ruedi Allemann, Sudeep Bhattacharyay, Agnieszka Defratyka, Mireia Garcia-Viloca, Shuhua Ma, Dan Major, Kwangho Nam, Piotr Paneth, Jiayun Pang, Michael Rostkowski, Javier Ruiz-Pernía, and Iñaki Tuñon for assistance and collaboration on related projects and to Sharon Hammes-Schiffer, Amnon Kohen, Alexander M. Kuznetsov, Vicente Moliner, Michael Sutcliffe, Iñaki Tuñón, and Arieh Warshel for helpful comments on the original manuscript. This work has been supported in part by Grant CHE03-40122 (P.I.: D.G.T.) from the National Science Foundation and Grant GM46736 (P.I.: J.G.) from the National Institutes of Health.

References

1. Eyring H, Stearn AE. Chem Rev. 1939; 24:253.
2. Pauling L. Chem Eng News. 1946; 24:1375.
3. Pauling L. Nature. 1948; 161:707. [PubMed: 18860270]
4. McElroy, WD.; Glass, B., editors. Mechanism of Enzyme Action. Johns Hopkins Press; Baltimore, MD: 1956.
5. Koshland DE Jr. Proc Natl Acad Sci, USA. 1958; 44:98. [PubMed: 16590179]
6. Storm DR, Koshland DE Jr. J Am Chem Soc. 1972; 94:5805.
7. Jencks W. Adv Enzymol. 1975; 43:219. [PubMed: 892]
8. Knowles JR, Albery WJ. Acc Chem Res. 1977; 10:105.
9. Warshel A. Proc Natl Acad Sci. 1978; 75:5250. [PubMed: 281676]
10. Walsh, CT. Enzymatic Reaction Mechanism. Freeman; New York: 1979.
11. Warshel A. Acc Chem Res. 1981; 14:284.
12. Northrop DB. Annu Rev Biochem. 1981; 50:103. [PubMed: 7023356]
13. Karplus M, McCammon AJ. Annu Rev Biochem. 1983; 52:263. [PubMed: 6351724]

14. Kraut J. Science. 1988; 242:533. [PubMed: 3051385]
15. Cooper, A.; Houben, JL.; Chien, LC., editors. The Enzyme Catalytic Process: Energetics, Mechanism, and Dynamics. Plenum; New York: 1989.
16. Cha Y, Murray CJ, Klinman JP. Science. 1989; 243:1325. [PubMed: 2646716]
17. Suckling, CJ., editor. Enzyme Chemistry: Impact and Applications. 2. Chapman and Hall; London: 1990.
18. Åqvist J, Warshel A. Chem Rev. 1993; 93:2523.
19. Cleland WW, Kreevoy MM. Science. 1994; 264:1887. [PubMed: 8009219]
20. Warshel A. J Biol Chem. 1998; 273:27035. [PubMed: 9765214]
21. Eustace SJ, McCann GM, More O'Ferrall RA, Murphy MG, Murray BA, Walsh SM. J Phys Org Chem. 1998; 11:519.
22. Fersht, A. Structure and Mechanism in Protein Science: A Guide to Enzyme Catalysis and Protein Folding. Freeman; New York: 1999.
23. Bruice TC, Benkovic SJ. Biochemistry. 2000; 39:6267. [PubMed: 10828939]
24. Karplus M. J Phys Chem B. 2000; 104:11.
25. Antoniou, D.; Schwartz, SD. Theoretical Methods in Condensed Phase Chemistry. Schwartz, SD., editor. Kluwer; Dordrecht: 2000. p. 69Progress in Theoretical Chemistry and Physics Series 5
26. Wolfenden R, Snider MJ. Acc Chem Res. 2001; 34:938. [PubMed: 11747411]
27. Villa J, Warshel A. J Phys Chem B. 2001; 105:7887.
28. Bugg TDH. Nat Prod Rep. 2001; 18:465. [PubMed: 11699881]
29. Warshel A, Parson WW. Quantum Rev Biophys. 2001; 34:563.
30. Truhlar DG, Gao J, Alhambra C, Garcia-Viloca M, Corchado J, Sanchez ML, Villa J. Acc Chem Res. 2002; 35:341. [PubMed: 12069618]
31. Gao J, Truhlar DG. Annu Rev Phys Chem. 2002; 53:467. [PubMed: 11972016]
32. Cui Q, Karplus M. Adv Protein Chem. 2003; 66:315. [PubMed: 14631822]
33. Daniel RM, Dunn RV, Finney JL, Smith JC. Annu Rev Biophys Biomol Struct. 2003; 32:69. [PubMed: 12471064]
34. Dudev T, Lim C. Chem Rev. 2003; 103:733. [PubMed: 12630851]
35. Kohen A. Prog React Kinet Mech. 2003; 28:119.
36. Himo F, Siegbahn PEM. Chem Rev. 2003; 103:2421. [PubMed: 12797836]
37. Benkovic SJ, Hammes-Schiffer S. Science. 2003; 301:1196. [PubMed: 12947189]
38. Schnell JR, Dyson HJ, Wright PE. Annu Rev Biophys Biomol Struct. 2004; 33:119. [PubMed: 15139807]
39. Masgrau L, Basran J, Hothi P, Sutcliffe MJ, Scrutton NS. Arch Biochem Biophys. 2004; 428:41. [PubMed: 15234268]
40. Noodleman L, Lovell T, Han WG, Li J, Himo F. Chem Rev. 2004; 104:459. [PubMed: 14871132]
41. Meunier B, deVisser SP, Shaik S. Chem Rev. 2004; 104:3947. [PubMed: 15352783]
42. Marti S, Roca M, Andres J, Moliner V, Silla E, Tuñón I, Bertrán J. Chem Soc Rev. 2004; 33:98. [PubMed: 14767505]
43. Tousignant A, Pelletier JN. Chem Biol. 2004; 11:1037. [PubMed: 15324804]
44. Liang ZX, Klinman JP. Curr Opin Struct Biol. 2004; 14:648. [PubMed: 15582387]
45. Grieg IR, Kirby AJ. J Phys Org Chem. 2004; 17:498.
46. Garcia-Viloca M, Gao J, Karplus M, Truhlar DG. Science. 2004; 303:186. [PubMed: 14716003]
47. Deeth RJ. Struct Bonding. 2004; 113:37.
48. Zhang X, Houk KN. Acc Chem Res. 2005; 38:379. [PubMed: 15895975]
49. Hammes-Schiffer S. Acc Chem Res. 2006; 39:93. [PubMed: 16489728]
50. Schramm VL. Arch Biochem Biophys. 2005; 433:13. [PubMed: 15581562]
51. Shaik S, Kumar D, deVisser SP, Altun A, Thiel W. Chem Rev. 2005; 105:2279. [PubMed: 15941215]

52. Gao J, Ma S, Major DT, Nam K, Pu J, Truhlar DG. Chem Rev. 2006; 106:3188–3209. http://dx.doi.org/10.1021/cr050293k. [PubMed: 16895324]
53. Gold HJ. Int J Quantum Chem Symp. 1971; 4:353.
54. Alberding N, Austin RH, Beeson KW, Chan SS, Eisenstein L, Frauenfelder H, Nordlund TM. Science. 1976; 192:1002. [PubMed: 1273579]
55. Khoshtariya DE. Bioorg Khim. 1978; 4:1673.
56. Gol'danski. Chem Scr. 1979; 13:1.
57. Marcus, RA. Tunneling in Biological Systems. DeVault, DC.; Frauenfelder, H.; Marcus, RA.; Schrieffer, JR.; Sutin, N., editors. Academic; New York: 1979. p. 109
58. Banacky P. Biophys Chem. 1981; 13:39. [PubMed: 7260327]
59. Huskey WP, Schowen RL. J Am Chem Soc. 1983; 105:5704.
60. Hermes JD, Cleland WW. J Am Chem Soc. 1984; 106:7263.
61. Verhoeven JW, Koomen GJ, Van der Keck SM. Recl Trav Chim Pays-Bas. 1986; 105:343.
62. Bibbs JA, Demuth HU, Huskey WP, Mordy CW, Schowen RL. J Mol Catal. 1988; 47:187.
63. Klinman JP. Trends Biochem Sci. 1989; 14:368. [PubMed: 2688201]
64. Xue L, Talalay P, Mildvan AS. Biochemistry. 1990; 29:7491. [PubMed: 2223781]
65. Warshel A, Chu ZT. J Chem Phys. 1990; 93:4003.
66. Hwang JK, Chu ZT, Yadav A, Warshel A. J Phys Chem. 1991; 95:8445.
67. Rucker J, Cha Y, Jonsson T, Grant KL, Klinman JP. Biochemistry. 1992; 31:11489. [PubMed: 1445883]
68. Bruno WJ, Bialek W. Biophys J. 1992; 63:689. [PubMed: 1420907]
69. Anderson VE. Curr Opin Struct Biol. 1992; 2:757.
70. Warshel A, Hwang JK. Faraday Discuss. 1992; 93:225. [PubMed: 1337846]
71. Warshel, A. Molecular Aspects of Biotechnology: Computational Models and Theories. Bertrán, J., editor. Kluwer; Dordrecht: 1992. p. 175
72. Bahnson BJ, Park DH, Kim K, Plapp BV, Klinman JP. Biochemistry. 1993; 32:5503. [PubMed: 8504071]
73. Glickman MH, Wiseman JS, Klinman JP. J Am Chem Soc. 1994; 116:793.
74. Bahnson BJ, Klinman JP. Methods Enzymol. 1995; 249:373. [PubMed: 7791619]
75. Klinman JP. Spec Publ R Soc Chem. 1995; 148:38.
76. Alston WC II, Kanska M, Murray CJ. Biochemistry. 1996; 35:12873. [PubMed: 8841131]
77. Berendsen HJC, Mavri J. Int J Quantum Chem. 1996; 57:975.
78. Jonsson T, Glickman MH, Sun S, Klinman JP. J Am Chem Soc. 1996; 118:10319.
79. Hwang JK, Warshel A. J Am Chem Soc. 1996; 118:11745.
80. Kohen A, Jonsson T, Klinman JP. Biochemistry. 1997; 36:2603. [PubMed: 9054567]
81. Moiseyev N, Rucker J, Glickman MH. J Am Chem Soc. 1997; 119:3853.
82. Antoniou D, Schwartz SD. Proc Natl Acad Sci USA. 1997; 94:12360. [PubMed: 9356454]
83. Bahnson BJ, Colby TD, Chin JK, Goldstein BM, Klinman JP. Proc Natl Acad Sci, USA. 1997; 94:12797. [PubMed: 9371755]
84. Kohen A, Klinman JP. Acc Chem Res. 1998; 31:397.
85. Whittaker MM, Ballou DP, Whittaker JW. Biochemistry. 1998; 37:8426. [PubMed: 9622494]
86. Colby TD, Bahnson BJ, Chin JK, Klinman JP, Goldstein BM. Biochemistry. 1998; 37:9295. [PubMed: 9649310]
87. Smedarchina Z, Zgierski MZ, Siebrand W, Kozlowski PM. J Chem Phys. 1998; 109:1014.
88. Scrutton NS. Biochem Soc Trans. 1999; 27:767. [PubMed: 10830100]
89. Basran J, Sutcliffe MJ, Scrutton NS. Biochemistry. 1999; 38:3218. [PubMed: 10074378]
90. Grant KL, Klinman JP. Biochemistry. 1989; 28:6597. [PubMed: 2790014]
91. Karsten WE, Hwang CC, Cook PF. Biochemistry. 1999; 38:4398. [PubMed: 10194359]
92. Rickert KW, Klinman JP. Biochemistry. 1999; 38:12218. [PubMed: 10493789]
93. Kuznetsov AM, Ulstrup J. Can J Chem. 1999; 77:1085.

94. Kohen A, Klinman JP. Chem Biol. 1999; 6:R191. [PubMed: 10381408]
95. Scrutton NS, Basran J, Sutcliffe MJ. Eur J Biochem. 1999; 264:666. [PubMed: 10491112]
96. Rucker J, Klinman JP. J Am Chem Soc. 1999; 121:1997.
97. Alhambra C, Gao J, Corchado JC, Villa J, Truhlar DG. J Am Chem Soc. 1999; 121:2253.
98. Thomas A, Jourand D, Bret C, Amara P, Field MJ. J Am Chem Soc. 1999; 121:9693.
99. Kohen A, Cannio R, Bartolucci S, Klinman JP. Nature. 1999; 399:496. [PubMed: 10365965]
100. Frauenfelder, H. Protein Dynamics, Functions, and Design. Jardetzky, O.; Holbrock, RE.; Lefevre, JF., editors. Springer; New York: 1999. p. 95
101. Harris RJ, Meskys R, Sutcliffe MJ, Scrutton NS. Biochemistry. 2000; 39:1189. [PubMed: 10684595]
102. Chin JK, Klinman JP. Biochemistry. 2000; 39:1278. [PubMed: 10684607]
103. Chowdhury S, Banerjee R. J Am Chem Soc. 2000; 122:5417.
104. Alhambra C, Corchado J, Sanchez ML, Gao J, Truhlar DG. J Am Chem Soc. 2000; 122:8197.
105. Kohen A, Klinman JP. J Am Chem Soc. 2000; 122:10738.
106. Feierberg I, Luzhkov V, Åqvist J. J Biol Chem. 2000; 275:22657. [PubMed: 10801792]
107. Webb SP, Hammes-Schiffer S. J Chem Phys. 2000; 113:5214.
108. Lamb DC, Kriegl J, Kastens K, Nienhaus GU. J Phys Org Chem. 2000; 13:659.
109. Grishanin BA, Romanovskii YM, Chikishev AY, Shuvalova EV. Lect Notes Phys. 2000; 557:338.
110. Sutcliffe MJ, Scrutton NS. Trends Biochem Sci. 2000; 25:405. [PubMed: 10973049]
111. Tsai SC, Klinman JP. Biochemistry. 2001; 40:2303. [PubMed: 11329300]
112. Chih HW, Marsh EN. Biochemistry. 2001; 40:13060. [PubMed: 11669644]
113. Alhambra C, Sanchez ML, Corchado JC, Gao J, Truhlar DG. Chem Phys Lett. 2001; 347:512, 355, 388 (E).
114. Faulder PF, Tresadern G, Chohan KK, Scrutton NS, Sutcliffe MJ, Hillier IH, Burton NA. J Am Chem Soc. 2001; 123:8604. [PubMed: 11525672]
115. Billeter SR, Webb SP, Agarwal PK, Iordanov T, Hammes-Schiffer S. J Am Chem Soc. 2001; 123:11262. [PubMed: 11697969]
116. Basran J, Patel S, Sutcliffe MJ, Scrutton NS. J Biol Chem. 2001; 276:6234. [PubMed: 11087744]
117. Billeter SR, Webb SP, Iordanov T, Agarwal PK, Hammes-Schiffer S. J Chem Phys. 2001; 114:6925.
118. Dybala-Defratyka A, Paneth P. J Inorg Biochem. 2001; 86:681. [PubMed: 11583786]
119. Antoniou D, Schwartz SD. J Phys Chem B. 2001; 105:5553.
120. Schenter GK, Garrett BC, Truhlar DG. J Phys Chem B. 2001; 105:9672.
121. Alhambra C, Corchado J, Sanchez ML, Garcia-Viloca M, Gao J, Truhlar DG. J Phys Chem B. 2001; 105:11326.
122. Seymour SL, Klinman JP. Biochemistry. 2002; 41:8747. [PubMed: 12093294]
123. Tresadern G, McNamara JP, Mohr M, Wang H, Burton NA, Hillier IH. Chem Phys Lett. 2002; 358:489.
124. Sutcliffe MJ, Scrutton NS. Eur J Biochem. 2002; 269:3096. [PubMed: 12084049]
125. Antoniou D, Caratzoulas S, Kalyanaraman C, Mincer JS, Schwartz SD. Eur J Biochem. 2002; 269:3103. [PubMed: 12084050]
126. Knapp MJ, Klinman JP. Eur J Biochem. 2002; 269:3113. [PubMed: 12084051]
127. Garcia-Viloca M, Alhambra C, Truhlar DG, Gao J. J Am Chem Soc. 2002; 124:7268. [PubMed: 12071725]
128. Cui Q, Karplus M. J Am Chem Soc. 2002; 124:3093. [PubMed: 11902900]
129. Knapp MJ, Rickert K, Klinman JP. J Am Chem Soc. 2002; 124:3865. [PubMed: 11942823]
130. Cui Q, Elstner M, Karplus M. J Phys Chem B. 2002; 106:2721.
131. Agarwal PK, Billeter SR, Hammes-Schiffer S. J Phys Chem B. 2002; 106:3283.
132. Cui Q, Karplus M. J Phys Chem B. 2002; 106:7927.

133. Garcia-Viloca M, Truhlar DG, Gao J. Biochemistry. 2003; 42:13558. [PubMed: 14622003]
134. Doll KM, Finke RG. Inorg Chem. 2003; 42:4849. [PubMed: 12895106]
135. Smedarchina Z, Siebrand W, Fernadez-Ramos A, Cui Q. J Am Chem Soc. 2003; 125:243. [PubMed: 12515527]
136. Doll KM, Bender BR, Finke RG. J Am Chem Soc. 2003; 125:10877. [PubMed: 12952467]
137. Garcia-Viloca M, Alhambra C, Truhlar DG, Gao J. J Comput Chem. 2003; 24:177. [PubMed: 12497598]
138. Poulsen TD, Garcia-Viloca M, Gao J, Truhlar DG. J Phys Chem B. 2003; 107:9567.
139. Tresadern G, Wang H, Faulder PF, Burton NA, Hillier IH. Mol Phys. 2003; 101:2775.
140. Klinman JP. Pure Appl Chem. 2003; 75:601.
141. Tresadern G, Faulder PF, Gleeson MP, Tai Z, MacKenzie G, Burton NA, Hillier IH. Theor Chem Acc. 2003; 109:108.
142. Agrawal N, Hong B, Mihai C, Kohen A. Biochemistry. 2004; 43:1998. [PubMed: 14967040]
143. Romesberg FE, Schowen RL. Adv Phys Org Chem. 2004; 39:27.
144. Truhlar DG, Gao J, Garcia-Viloca M, Alhambra C, Corchado J, Sanchez ML, Poulsen TD. Int J Quantum Chem. 2004; 100:1136.
145. Olsson MHM, Siegbahn PEM, Warshel A. J Am Chem Soc. 2004; 126:2820. [PubMed: 14995199]
146. Sikorski RS, Wang L, Markham KA, Rajagopalan PTR, Benkovic SJ, Kohen A. J Am Chem Soc. 2004; 126:4778. [PubMed: 15080672]
147. Bertránd P. J Biol Inorg Chem. 2004; 9:2. [PubMed: 14661082]
148. Olsson MHM, Siegbahn W, Warshel A. J Biol Inorg Chem. 2004; 9:96. [PubMed: 14663649]
149. Siebrand W, Smedarchina Z. J Phys Chem B. 2004; 108:4185.
150. Kim HS, Damo SM, Lee SY, Wemmer D, Klinman JP. Biochemistry. 2005; 44:11428. [PubMed: 16114879]
151. Meyer MP, Klinman JP. Chem Phys. 2005; 319:283. [PubMed: 21132078]
152. Major DT, York DM, Gao J. J Am Chem Soc. 2005; 127:16374. [PubMed: 16305206]
153. Pu J, Ma S, Gao J, Truhlar DG. J Phys Chem B. 2005; 109:8551. [PubMed: 16852008]
154. Schwartz, SD. Isotope Effects in Chemistry and Biology. Kohen, A.; Limbach, H-H., editors. Taylor and Francis; Boca Raton, FL: 2006. p. 475
155. Hammes-Schiffer, S. Isotope Effects in Chemistry and Biology. Kohen, A.; Limbach, H-H., editors. Taylor and Francis; Boca Raton, FL: 2006. p. 499
156. Kiefer, PM.; Hynes, JT. Isotope Effects in Chemistry and Biology. Kohen, A.; Limbach, H-H., editors. Taylor and Francis; Boca Raton, FL: 2006. p. 549
157. Warshel, A.; Olsson, MHM.; Villa-Freixa. Isotope Effects in Chemistry and Biology. Kohen, A.; Limbach, H-H., editors. Taylor and Francis; Boca Raton, FL: 2006. p. 621
158. Basran, J.; Masgrau, L.; Sutcliffe, MJ.; Scrutton, NS. Isotope Effects in Chemistry and Biology. Kohen, A.; Limbach, H-H., editors. Taylor and Francis; Boca Raton, FL: 2006. p. 671
159. Kuznetsov, AM.; Ulstrup, J. Isotope Effects in Chemistry and Biology. Kohen, A.; Limbach, H-H., editors. Taylor and Francis; Boca Raton, FL: 2006. p. 691
160. Siebrand, W.; Smedarchina, Z. Isotope Effects in Chemistry and Biology. Kohen, A.; Limbach, H-H., editors. Taylor and Francis; Boca Raton, FL: 2006. p. 725
161. Watney JB, Soudackov A, Wong KF, Hammes-Schiffer S. Chem Phys Lett. 2006; 418:268.
162. Banerjee, R.; Truhlar, DG.; Dybala-Defratyka, A.; Paneth, P. Biological Aspects of Hydrogen Transfer. Schowen, RL.; Klinman, JP., editors. in press
163. Pang J, Pu J, Gao J, Truhlar DG, Allemann RK. J Am Chem Soc. 2006; 128:8015. [PubMed: 16771517]
164. Warshel A. Proc Natl Acad Sci, USA. 1984; 81:444. [PubMed: 6582500]
165. Hwang JK, King G, Creighton S, Warshel A. J Am Chem Soc. 1988; 110:5297.
166. Warshel A, Sussmann F, Hwang JK. J Mol Biol. 1988; 201:139. [PubMed: 3047396]
167. Verkhivker G, Elber R, Gibson QH. J Am Chem Soc. 1992; 114:7866.

168. Warshel, A.; Bentzien, J. Transition State Modeling for Catalysis. Truhlar, DG.; Morokuma, K., editors. American Chemical Society; Washington, DC: 1999. p. 489ACS Symposium Series 721
169. Nam K, Prat-Resina X, Garcia-Viloca M, Devi-Kesavan LS, Gao J. J Am Chem Soc. 2004; 126:1369. [PubMed: 14759194]
170. Wang M, Lu Z, Yang W. J Chem Phys. 2004; 121:101. [PubMed: 15260526]
171. Soriano A, Silla E, Tuñón I, Ruiz-Lopez MF. J Am Chem Soc. 2005; 127:1946. [PubMed: 15701029]
172. Roca M, Andres J, Moliner V, Tuñón I, Bertrán J. J Am Chem Soc. 2005; 127:10648. [PubMed: 16045352]
173. Roca M, Moliner V, Tuñón I, Hynes JT. J Am Chem Soc. 2006; 128:6186. [PubMed: 16669689]
174. Welch GR, Smogg B, Damjanovich S. Prog Biophys Mol Biol. 1982; 39:109. [PubMed: 7048419]
175. Sumi H, Ulstrup J. Biochim Biophys Acta. 1986; 955:26. [PubMed: 2838088]
176. Bahar I, Jernigan RL. Biochemistry. 1999; 38:3478. [PubMed: 10090734]
177. Radkiewicz JL, Brooks CL III. J Am Chem Soc. 2000; 122:225.
178. Rubach JK, Ramaswamy S, Plapp BV. Biochemistry. 2001; 40:12686. [PubMed: 11601993]
179. Hammes-Schiffer S. Biochemistry. 2002; 41:13335. [PubMed: 12416977]
180. Agarwal PK, Billeter SR, Rajagopalan PTR, Benkovic SJ, Hammes-Schiffer S. Proc Natl Acad Sci, USA. 2002; 99:2794. [PubMed: 11867722]
181. Watney JB, Agarwal PK, Hammes-Schiffer S. J Am Chem Soc. 2003; 125:3745. [PubMed: 12656604]
182. Swanwick RS, Shrimpton PJ, Allemann RK. Biochemistry. 2004; 43:4119. [PubMed: 15065854]
183. Agarwal PK, Geist A, Gorin A. Biochemistry. 2004; 43:10605. [PubMed: 15311922]
184. Tousignant A, Pelletier JN. Chem Biol. 2004; 11:1037. [PubMed: 15324804]
185. Liang ZX, Lee T, Resing KA, Ahn NG, Klinman JP. Proc Natl Acad Sci, USA. 2004; 101:9556. [PubMed: 15210941]
186. Thorpe IF, Brooks CL III. Proteins: Struct, Funct, Bioinf. 2004; 57:444.
187. Argarwal PK. J Am Chem Soc. 2005; 127:15248. [PubMed: 16248667]
188. Wong KF, Selzer T, Benkovic SJ, Hammes-Schiffer S. Proc Natl Acad Sci, USA. 2005; 102:6807. [PubMed: 15811945]
189. Dogonadze RR, Kuznetsov AM, Ulstrup J. J Theor Biol. 1977; 69:239. [PubMed: 592874]
190. Ma B, Kumar S, Tsai CJ, Hu Z, Nussinov R. J Theor Biol. 2000; 203:383. [PubMed: 10736215]
191. Pogocki D, Ghezzo-Schoneich E, Schoneich C. J Phys Chem B. 2001; 105:1250.
192. Hammes GG. Biochemistry. 2002; 41:8221. [PubMed: 12081470]
193. Piana S, Carloni P, Parrinello M. J Mol Biol. 2002; 319:567. [PubMed: 12051929]
194. Zhang Y, Kua J, McCammon JA. J Phys Chem B. 2003; 107:4459.
195. Thorpe IF, Brooks CL III. J Phys Chem B. 2003; 107:14042.
196. Venkitakrishnan RP, Zabarowski E, McIlheny D, Benkovic SJ, Dyson HJ, Wright PE. Biochemistry. 2004; 43:16046. [PubMed: 15609999]
197. Thorpe IF, Brooks CL III. J Am Chem Soc. 2005; 127:12997. [PubMed: 16159295]
198. Greenwald J, Le V, Butler SL, Bushman FD, Choe S. Biochemistry. 1999; 38:8892. [PubMed: 10413462]
199. Alper KO, Singla M, Stone JL, Bagdassarian CK. Protein Sci. 2001; 10:1319. [PubMed: 11420434]
200. Noonan RC, Carter CWJ, Bagdassarian CK. Protein Sci. 2002; 11:1424. [PubMed: 12021441]
201. Truhlar DG, Hase WL, Hynes JT. J Phys Chem. 1983; 87:2664.
202. Truhlar DG, Garrett BC, Klippenstein SJ. J Phys Chem. 1996; 100:12771.
203. Garrett, BC.; Truhlar, DG. Theory and Applications of Computational Chemistry: The First Forty Years. Dykstra, CE.; Frenking, G.; Kim, K.; Scuseria, GE., editors. Elsevier; Amsterdam: 2005. p. 67
204. Gibbs JW. Trans Conn Acad Arts Sci. 1876; 3:228.

205. Hill, TL. An Introduction to Statistical Thermodynamics. Addison-Wesley; Reading, MA: 1960. p. 313
206. Lewis, GN.; Randall, M.; Pitzer, KS.; Brewer, L. Thermodynamics. 2. McGraw-Hill; New York: 1961.
207. Denbigh, K. The Principles of Chemical Equilibrium. 3. Cambridge University Press; London: 1971.
208. Northrop, DB. Isotope Effects in Enzyme-Catalyzed Reactions. Cleland, WW.; O'Leary, MH.; Northrup, DB., editors. University Park Press; Baltimore, MD: 1977. p. 122
209. Kohen, A. Isotope Effects in Chemistry and Biology. Kohen, A.; Limbach, H-H., editors. Taylor and Francis; Boca Raton, FL: 2006. p. 743
210. Cleland, WW. Isotope Effects in Chemistry and Biology. Kohen, A.; Limbach, H-H., editors. Taylor and Francis; Boca Raton, FL: 2006. p. 915
211. Kuppermann A. J Phys Chem. 1979; 83:171.
212. Boyd RK. Chem Rev. 1977; 77:93.
213. Chandler D. J Chem Phys. 1978; 68:2959.
214. Lim C, Truhlar DG. J Chem Phys. 1983; 79:3296.
215. Truhlar DG, Garrett BC. J Am Chem Soc. 1989; 111:1232.
216. Wigner E. Z Phys Chem. 1932; B19:203.
217. Eyring H. Chem Rev. 1935; 17:65.
218. Truhlar DG, Wyatt RE. Annu Rev Phys Chem. 1976; 27:1.
219. Chatfield DC, Friedman RS, Schwenke DW, Truhlar DG. J Phys Chem. 1992; 96:2414.
220. Schrödinger E. Ann Phys. 1926; 79:734.
221. Dirac P. Proc R Soc London, Ser A. 1927; 113:621.
222. Feynman RP. Rev Mod Phys. 1948; 20:367.
223. Gottfield, K.; Yan, T-M. Quantum Mechanics: Fundamentals. 2. Springer; New York: 2003.
224. Smith FT. J Chem Phys. 1965; 42:2419.
225. Heller EJ. J Chem Phys. 1975; 62:1544.
226. Schatz, GC.; Ratner, MA. Quantum Mechanics in Chemistry. Prentice Hall; Englewood Cliffs, NJ: 1993. p. 169ff
227. Miller WH. Adv Chem Phys. 1974; 25:69.Miller WH. Theor Chem Acc. 2000; 103:236.
228. Wentzel G. Z Phys. 1926; 38:518.Kramers HA. Z Phys. 1926; 39:828.Brillouin L. Comptes Rendus. 1926; 24:183.
229. Kemble, EC. The Fundamental Principles of Quantum Mechanics with Elementary Applications. Dover; New York: 1937.
230. Garrett BC, Truhlar DG. J Phys Chem. 1979; 83:2921.
231. Melander, L.; Saunders, WH, Jr. Reaction Rates of Isotopic Molecules. Wiley; New York: 1980.
232. Schramm, VL. Transition State Modeling for Catalysis. Truhlar, DG.; Morokuma, K., editors. American Chemical Society; Washington, DC: 1999. p. 213ACS Symposium Series 721
233. Schramm VL, Shi W. Curr Opin Struct Biol. 2001; 11:657. [PubMed: 11751045]
234. Cleland WW. J Biol Chem. 2003; 278:51975. [PubMed: 14583616]
235. Cleland WW. Arch Biochem Biophys. 2005; 433:2. [PubMed: 15581561]
236. Truhlar, DG. Isotope Effects in Chemistry and Biology. Kohen, A.; Limbach, H-H., editors. Taylor and Francis; Boca Raton, FL: 2006. p. 579
237. Gao, J.; Thompson, M., editors. Combined Quantum Mechanical and Molecular Mechanical Methods. American Chemical Society; Washington, DC: 1998. ACS Symposium Series 712
238. Hall, MB.; Margl, P.; Naray-Szabo, G.; Schramm, VL.; Truhlar, DG.; van Santen, RA.; Warshel, A.; Witten, JL. Transition State Modeling for Catalysis. Truhlar, DG.; Morokuma, K., editors. American Chemical Society; Washington, DC: 1999. p. 2ACS Symposium Series 721
239. Northrop DB, Duggleby RG. Bioorg Chem. 1990; 18:435.
240. McIntire WS, Everhart ET, Craig JC, Kuusk V. J Am Chem Soc. 1999; 121:5865.

241. Saunders, WHJ. Investigation of Rates and Mechanisms of Reactions. 4. Bernasconi, CF., editor. Wiley; New York: 1986. p. 565Techniques of Chemistry Series 6
242. Westheimer FH. Chem Rev. 1961; 61:265.
243. Bell, RP. The Tunnel Effect in Chemistry. Chapman & Hall; London and New York: 1980.
244. Masgrau L, Roujeinikova A, Johannissen LO, Hothi P, Basran J, Ranaghan KE, Mulholland AJ, Sutcliffe MJ, Scrutton NS, Leys D. Science. 2006; 312:237. [PubMed: 16614214]
245. Swain CG, Stivers EC, Reuwer JF, Schaad LJ. J Am Chem Soc. 1958; 80:5885.
246. Kurz LC, Frieden C. J Am Chem Soc. 1980; 102:4198.
247. Cook PF, Oppenheimer NJ, Cleland WW. Biochemistry. 1981; 20:1817. [PubMed: 7013802]
248. Streitwieser A, Jagow RH, Fahey RC, Suzuki S. J Am Chem Soc. 1958; 80:2326.
249. Saunders WH Jr. J Am Chem Soc. 1985; 107:164.
250. Bigeleisen J. J Chem Phys. 1955; 23:2264.
251. Bigeleisen J, Mayer MG. J Chem Phys. 1947; 15:261.
252. Kohen A, Jensen JH. J Am Chem Soc. 2002; 124:3858. [PubMed: 11942822]
253. Tautermann CS, Loferer MJ, Voegele AF, Liedl KR. J Chem Phys. 2004; 120:11650. [PubMed: 15268199]
254. Hirschi J, Singleton DA. J Am Chem Soc. 2005; 127:3294. [PubMed: 15755143]
255. Smedarchina Z, Siebrand W. Chem Phys Lett. 2005; 410:370.
256. Marcus RA. J Chem Phys. 1964; 41:610.
257. Truhlar DG, Kuppermann A. J Am Chem Soc. 1971; 93:1840.
258. Marcus RA, Coltrin ME. J Chem Phys. 1977; 67:2609.
259. Skodje RT, Truhlar DG, Garrett BC. J Chem Phys. 1982; 77:5955.
260. Garrett BC, Truhlar DG, Wagner AF, Dunning TH Jr. J Chem Phys. 1983; 78:4400.
261. Kreevoy MM, Ostovic D, Truhlar DG, Garrett BC. J Phys Chem. 1986; 90:3766.
262. Kim Y, Kreevoy MM. J Am Chem Soc. 1992; 114:7116.
263. Schneider ME, Stern MJ. J Am Chem Soc. 1972; 94:1517.
264. Padmakumar R, Padmakumar R, Banerjee R. Biochemistry. 1997; 36:3713. [PubMed: 9132024]
265. Chowdhury S, Banerjee R. Biochemistry. 2000; 39:7998. [PubMed: 10891081]
266. Goldanskii VI, Frank-Kamenetskii MD, Barkalov IM. Science. 1973; 182:1344. [PubMed: 17733114]
267. Trakhtenberg LI, Klochikhin VL, Pshezhetsky SY. Chem Phys. 1981; 59:191.
268. Wonchoba SE, Hu WP, Truhlar DG. Phys Rev B. 1995; 51:9985.
269. Zuev P, Sheridan RS, Albu TV, Truhlar DG, Hrovat DA, Borden WT. Science. 2003; 299:867. [PubMed: 12574623]
270. Francisco WA, Knapp MJ, Blackburn NJ, Klinman JP. J Am Chem Soc. 2002; 124:8194. [PubMed: 12105892]
271. Fan F, Gadda G. J Am Chem Soc. 2005; 127:17954. [PubMed: 16351127]
272. Ruddat VC, Mogul R, Chorny I, Chen C, Perrin N, Whitman S, Kenyon V, Jacobson MP, Bernasconi CF, Holman TR. Biochemistry. 2004; 43:13063. [PubMed: 15476400]
273. Hwang CC, Grissom CB. J Am Chem Soc. 1994; 116:795.
274. Glickman MH, Klinman JP. Biochemistry. 1995; 34:14077. [PubMed: 7578005]
275. Wiseman JS. Biochemistry. 1989; 28:2106. [PubMed: 2497775]
276. Brooks HB, Jones LH, Davidson VL. Biochemistry. 1993; 32:2725. [PubMed: 8448129]
277. Hyun YL, Davidson VL. Biochim Biophys Acta. 1995; 1251:198. [PubMed: 7669810]
278. Marsh ENG, Ballou DP. Biochemistry. 1998; 37:11864. [PubMed: 9718309]
279. Abad JL, Camps F, Fabrias G. Angew Chem, Int Ed. 2000; 39:3279.
280. Valley MP, Fitzpatrick PF. J Am Chem Soc. 2004; 126:6244. [PubMed: 15149217]
281. Lewis ER, Johansen E, Holman TR. J Am Chem Soc. 1999; 121:1395.
282. Plapp, BV. Isotope Effects in Chemistry and Biology. Kohen, A.; Limbach, H-H., editors. Taylor and Francis; Boca Raton, FL: 2006. p. 811

283. Brazeau BJ, Wallar BJ, Lipscomb JD. J Am Chem Soc. 2001; 123:10421. [PubMed: 11604007]
284. Lipscomb, JD. Isotope Effects in Chemistry and Biology. Kohen, A.; Limbach, H-H., editors. Taylor and Francis; Boca Raton, FL: 2006. p. 93
285. Nesheim JC, Lipscomb JD. Biochemistry. 1996; 35:10240. [PubMed: 8756490]
286. Hothi P, Basran J, Sutcliffe MJ, Scrutton NS. Biochemistry. 2003; 42:3966. [PubMed: 12667088]
287. Jonsson T, Edmondson DE, Klinman JP. Biochemistry. 1994; 33:14871. [PubMed: 7993913]
288. Basran J, Harris RJ, Sutcliffe MJ, Scrutton NS. J Biol Chem. 2003; 278:43973. [PubMed: 12941965]
289. Maglia G, Allemann RK. J Am Chem Soc. 2003; 125:13372. [PubMed: 14583029]
290. Frantom PA, Pongdee R, Sulikowski GA, Fitzpatrick PF. J Am Chem Soc. 2004; 124:4202. [PubMed: 11960436]
291. Hanzlik RP, Ling KHJ. J Am Chem Soc. 1993; 115:9363.
292. Miller SM, Klinman JP. Biochemistry. 1983; 22:3091. [PubMed: 6882738]
293. Marcus RA. J Chem Phys. 1956; 24:966.
294. Levich VG, Dogonadze RR. Dokl Akad Nauk SSSR. 1959; 124:123.
295. Marcus RA. Discuss Faraday Soc. 1960; 29:21.
296. Dogonadze RR. Dokl Akad Nauk SSSR. 1960; 133:1368.
297. Dogonadze RR. Dokl Akad Nauk SSSR. 1961; 142:1108.
298. Hush NS. Trans Faraday Soc. 1961; 57:557.
299. Marcus RA. Annu Rev Phys Chem. 1964; 15:155.
300. Dogonadze RR, Kuznetsov AM, Levich VG. Elektrokhim (Sov Electrochem). 1967; 3:739.
301. Marcus RA. Electrochim Acta. 1968; 13:995.
302. Dogonadze RR, Kuznetsov AM, Levich VG. Electrochim Acta. 1968; 13:1025.
303. Marcus RA. Faraday Discuss Chem Soc. 1982; 74:7.
304. Marcus RA, Sutin N. Biochim Biophys Acta, Rev Bioenerg. 1985; 811:265.
305. Kuznetsov, AM. Charge Transfer in Physics, Chemistry and Biology. Gordon & Breach; Reading, U.K: 1995.
306. Barbara PF, Meyer TJ, Ratner MA. J Phys Chem. 1996; 100:13148.
307. Kuznetsov, AM.; Ulstrup, J. Electron Transfer in Chemistry and Biology. Wiley; Chichester, U.K: 1999.
308. Silverman DN. Biochim Biophys Acta. 2000; 1458:88. [PubMed: 10812026]
309. May, V.; Kohn, O. Charge and Energy Transfer in Molecular Systems. Wiley-VCH; Berlin: 2000.
310. Marcus, RA. Physical Chemistry. 2. Berry, RS.; Rice, SA.; Ross, J., editors. Oxford University Press; New York: 2000. p. 945ff
311. Kong YS, Warshel A. J Am Chem Soc. 1995; 117:6234.
312. Dogonadze RR, Kuznetsov AM, Levich VG. Electrochim Acta. 1968; 13:1025.
313. Cohen AO, Marcus RA. J Phys Chem. 1968; 72:4249.
314. Hine J. J Am Chem Soc. 1971; 93:3701.
315. Kreevoy MM, Oh S-w. J Am Chem Soc. 1973; 95:4805.
316. Kresge AJ. Acc Chem Res. 1975; 8:354.
317. Albery WJ, Kreevoy MM. Adv Phys Org Chem. 1978; 16:87.
318. Miller DJ, Sauders WHJ. J Org Chem. 1981; 46:4247.
319. Kreevoy MM, Lee ISH. J Am Chem Soc. 1984; 106:2550.
320. Kreevoy, MM.; Truhlar, DG. Investigation of Rates and Mechanisms of Reactions, Part I. Bernasconi, CF., editor. Wiley; New York: 1986. p. 13
321. Lee ISH, Ostovic D, Kreevoy MM. J Am Chem Soc. 1988; 110:3989.
322. Bernasconi CF. Adv Phys Org Chem. 1992; 27:119.
323. Gerlt JA, Gassman PG. J Am Chem Soc. 1993; 115:11552.
324. Krshtalik LI. Biochim Biophys Acta. 2000; 1458:6. [PubMed: 10812022]
325. Roth JP, Yoder JC, Won TJ, Mayer JM. Science. 2001; 294:2524. [PubMed: 11752572]

326. Kiefer PM, Hynes JT. J Phys Chem A. 2002; 106:1834.
327. Bertrán P. Radiat Phys Chem. 2005; 72:105.
328. Braun-Sand S, Olsson MHM, Warshel A. Adv Phys Org Chem. 2005; 40:201.
329. Warshel, A. Computer Modeling of Chemical Reactions in Enzymes and Solutions. Wiley; New York: 1991.
330. Kreevoy, MM.; Truhlar, DG. Investigation of Rates and Mechanisms of Reactions. In: Bernasconi, CF., editor. Technol Chem (N Y. 4. Vol. 6. Wiley; New York: 1986. p. 13
331. Warshel A, Hwang JK, Åqvist J. Faraday Discuss. 1992; 93:225. [PubMed: 1337846]
332. Silverman DN, Tu C, Chen X, Tanhauser SM, Kresge AJ, Laipis PJ. Biochemistry. 1993; 32:10757. [PubMed: 8399223]
333. Gerlt JA, Gassman PG. J Am Chem Soc. 1993; 115:11552.
334. Kresge AJ, Silverman DN. Methods Enzymol. 1999; 308:276. [PubMed: 10507009]
335. Earnhardt JN, Tu C, Silverman DN. Can J Chem. 1999; 77:726.
336. Schutz CN, Warshel A. J Phys Chem B. 2004; 108:2066.
337. Bearne SL, Spiteri RJ. J Theor Biol. 2005; 233:563. [PubMed: 15748916]
338. Atkins, P.; Friedman, R. Molecular Quantum Mechanics. 4. Oxford University Press; New York: 2005. p. 199-200.
339. German ED, Dogonadze RR, Kuznetsov AM, Levich VG, Kharkats YuI. Electrokhim (Sov Electrochem). 1970; 6:350.
340. German ED, Kuznetsov AM. J Chem Soc, Faraday Trans 2. 1981; 77:2203.
341. Dogonadze RR, Kuznetsov AM. Dokl Akad Nauk SSSR. 1971; 198:130.
342. Kuznetsov AM. Elektrokhim (Sov Electrochem). 1986; 22:291.
343. Kuznetsov, AM. Stochastic and dynamic views of chemical reaction kinetics in solutions. Presses Polytechniques et Universitaires Romandes; Lausanne: 1999.
344. Vrotyntsev MA, Dogonadze RR, Kuznetsov AM. Dokl Akad Nauk SSSR, Ser Fiz Khim. 1973; 209:1135.
345. Kuznetsov AM, Ulstrup J. Elektrokhim (Russ J Chem). 2003; 39:11.
346. Bondi DK, Connor JNL, Garrett BC, Truhlar DG. J Chem Phys. 1983; 78:5981.
347. Garrett BC, Abusalbi N, Kouri DJ, Truhlar DG. J Chem Phys. 1985; 83:2252.
348. Truhlar DG, Garrett BC. J Chim Phys. 1987; 84:365.
349. Truhlar DG, Gordon MS. Science. 1990; 249:491. [PubMed: 17735282]
350. Kim Y, Truhlar DG, Kreevoy MM. J Am Chem Soc. 1991; 113:7837.
351. Lu DH, Truong TN, Melissas VS, Lynch GC, Liu YP, Garrett BC, Steckler R, Isaacson AD, Rai SN, Hancock GC, Lauderdale JG, Joseph T, Truhlar DG. Comput Phys Commun. 1992; 71:235.
352. Liu YP, Lu DH, Gonzalez-Lafont A, Truhlar DG, Garrett BC. J Am Chem Soc. 1993; 115:7806.
353. Fernandez-Ramos A, Truhlar DG. J Chem Phys. 2001; 114:1491.
354. Fernandez-Ramos A, Ellingson BA, Garrett BC, Truhlar DG. Rev Comput Chem. in press.
355. Benderskii V, Makarov D, Wight C. Adv Chem Phys. 1994; 88:1.
356. Warshel A. Curr Opin Struct Biol. 1992; 2:230.
357. Morokuma, K.; Kato, S. Potential Energy Surfaces and Dynamics Calculations. Truhlar, DG., editor. Plenum; New York: 1981. p. 243
358. Marcus RA. J Chem Phys. 1968; 49:2617.
359. Wu SF, Marcus RA. J Chem Phys. 1970; 53:4026.
360. Bowman JM, Kuppermann A, Adams JT, Truhlar DG. Chem Phys Lett. 1973; 20:229.
361. Duff JW, Truhlar DG. Chem Phys Lett. 1973; 23:327.
362. Clary DC, Connor JNL. Chem Phys Lett. 1979; 66:493.
363. Garrett BC, Truhlar DG. J Chem Phys. 1980; 72:3460.
364. Schatz GC. J Chem Phys. 1983; 79:5386.
365. Skodje RT, Schwenke DW, Truhlar DG, Garrett BC. J Phys Chem. 1984; 88:628.
366. Caratzoulas S, Mincer JS, Schwartz SD. J Am Chem Soc. 2002; 124:3270. [PubMed: 11916410]

367. Kalyanaraman C, Schwartz SD. J Phys Chem B. 2002; 106:13111.
368. Schwartz SD. J Phys Chem B. 2003; 107:12372.
369. Mincer JS, Schwartz SD. J Phys Chem B. 2003; 107:366.
370. Mincer JS, Schwartz SD. J Proteome Res. 2003; 2:438.
371. Nunez S, Antoniou D, Schramm VL, Schartz SD. J Am Chem Soc. 2004; 126:15720. [PubMed: 15571394]
372. Mincer JS, Schwartz SD. J Chem Phys. 2004; 120:7755. [PubMed: 15267689]
373. Basner JE, Schwartz SD. J Phys Chem B. 2004; 108:444.
374. Basner JC, Schwartz SD. J Am Chem Soc. 2005; 127:13822. [PubMed: 16201803]
375. Liu Y-P, Lynch GC, Truong TN, Lu D-h, Truhlar DG, Garrett BC. J Am Chem Soc. 1993; 115:2408.
376. Garrett BC, Truhlar DG. J Chem Phys. 1983; 79:4931.
377. Miller WH, Handy NC, Adams JE. J Chem Phys. 1980; 72:99.
378. Borgis D, Hynes JT. J Chem Phys. 1991; 94:3619.
379. Soudackov A, Hammes-Schiffer S. J Chem Phys. 1999; 111:4672.
380. Soudackov A, Hammes-Schiffer S. J Chem Phys. 2000; 113:2385.
381. Hatcher E, Soudackov AV, Hammes-Schiffer S. J Am Chem Soc. 2004; 126:5763. [PubMed: 15125669]
382. Kiefer PM, Hynes JT. J Phys Chem A. 2002; 106:1850.
383. Kiefer PM, Hynes JT. J Phys Chem A. 2003; 107:9022.
384. Benderskii VA, Makarov DE, Wight CH. Adv Chem Phys. 1994; 88:1.
385. Smedarchina Z, Siebrand W, Zgierski MZ. J Chem Phys. 1995; 103:5326.
386. Smedarchina Z, Fernadez-Ramos A, Siebrand W. J Comput Chem. 2001; 22:787.
387. Torrie GM, Valleau JP. J Chem Phys. 1977; 66:1402.
388. Case DA, McCammon AJ. Ann N Y Acad Sci. 1986; 482:222. [PubMed: 3471106]
389. Kottalam J, Case DA. J Am Chem Soc. 1988; 110:7690.
390. Carter EA, Ciccotti G, Hynes JT, Kapral R. Chem Phys Lett. 1989; 156:472.
391. Fonseca T. NATO ASI Ser A. 1989; 178:331.
392. Avbelj F. Biochemistry. 1992; 31:6290. [PubMed: 1627567]
393. Gao J. J Am Chem Soc. 1993; 115:2930.
394. Truhlar DG, Liu YP, Schenter GK, Garrett BC. J Phys Chem. 1994; 98:8396.
395. Roux B. Comput Phys Commun. 1995; 91:275.
396. Neria E, Fischer S, Karplus M. J Chem Phys. 1996; 105:1902.
397. Hinsen K, Roux B. J Chem Phys. 1997; 106:3567.
398. Sprik M, Ciccotti G. J Chem Phys. 1998; 109:7737.
399. Pak Y, Voth GA. J Phys Chem A. 1999; 103:925.
400. Schenter GK, Garrett BC, Truhlar DG. J Chem Phys. 2003; 119:5828.
401. Watanabe YS, Kim JG, Fukunishi Y, Nakamura H. Chem Phys Lett. 2004; 400:258.
402. Patey GN, Valleau JP. Chem Phys Lett. 1973; 21:297.
403. Valleau, JP.; Torrie, GM. Statistical Mechanics, Part A. Berne, BJ., editor. Plenum Press; New York: 1977. p. 169
404. Ferrer S, Ruiz-Pernia J, Tuñón I, Moliner V, Garcia-Viloca M, Gonzalez-Lafont A, Lluch JM. J Chem Theory Comput. 2005; 1:750.
405. Wong KF, Watney JB, Hammes-Schiffer S. J Phys Chem B. 2004; 108:12231.
406. Warshel A. J Phys Chem. 1982; 86:2218.
407. Yadav A, Jackson RM, Holbrook J, Warshel A. J Am Chem Soc. 1991; 113:4800.
408. Pu J, Ma S, Garcia-Viloca M, Gao J, Truhlar DG, Kohen A. J Am Chem Soc. 2005; 127:14879. [PubMed: 16231943]
409. Proust-De Martin F, Dumas R, Field MJ. J Am Chem Soc. 2000; 122:7688.

410. Bennett, CH. Algorithms for Chemical Computations. Christofferson, RE., editor. American Chemical Society; Washington, DC: 1977. p. 63ACS Symposium Series 46
411. Garcia-Viloca M, Alhambra C, Truhlar DG, Gao J. J Chem Phys. 2001; 114:9953.
412. Roca M, Moliner V, Ruiz-Pernia JJ, Silla E, Tuñón I. J Phys Chem A. 2006; 110:503. [PubMed: 16405322]
413. Claeyssens F, Ranaghan KE, Manby FR, Harvey JN, Mulholland AJ. Chem Commun. 2005; 40:5068.
414. Allison, TC.; Truhlar, DG. Modern Methods for Multidimensional Dynamics Computations in Chemistry. Thompson, DL., editor. World Scientific; Singapore: 1998. p. 618
415. Albu TV, Corchado JC, Truhlar DG. J Phys Chem A. 2001; 105:8465.
416. Garrett BC, Truhlar DG, Grev RS, Magnuson AW. J Phys Chem. 1980; 84:1730, 1983, 87, 4554 (E).
417. Truhlar DG, Garrett BC. Acc Chem Res. 1980; 13:440.
418. Truong TN, Lu DH, Lynch GC, Liu YP, Melissas VS, Stewart JJP, Steckler R, Garrett BC, Isaacson AD, Gonzalez-Lafont A, Rai SN, Hancock GC, Joseph T, Truhlar DG. Comput Phys Commun. 1993; 75:143.
419. Marcus RA. Discuss Faraday Soc. 1967; 44:7.
420. Truong TN, McCammon AJ. J Am Chem Soc. 1991; 113:7504.
421. Storer JW, Houk KN. J Am Chem Soc. 1993; 115:10426.
422. Corchado JC, Espinosa-Garcia J. J Chem Phys. 1996; 105:3160.
423. Villa J, Gonzalez-Lafont A, Lluch JM. J Phys Chem. 1996; 100:19389.
424. Hynes, JT. Solvation Effects and Chemical Reactivity. Tapia, O.; Bertrán, J., editors. Kluwer; Dordrecht: 1996. p. 231Understanding Chemical Reactivity Series 17
425. Garrett BC, Truhlar DG. Proc Natl Acad Sci, USA. 1979; 76:4755. [PubMed: 16578754]
426. Garrett BC, Truhlar DG, Schatz GC. J Am Chem Soc. 1986; 108:2876.
427. Pu J, Corchado JC, Truhlar DG. J Chem Phys. 2001; 115:6266.
428. Pu J, Truhlar DG. J Chem Phys. 2002; 117:1479.
429. Warshel A, Levitt M. J Mol Biol. 1976; 103:227. [PubMed: 985660]
430. Singh UC, Kollman PA. J Comput Chem. 1986; 7:718.
431. Field MJ, Bash PA, Karplus MJ. J Comput Chem. 1990; 11:700.
432. Gao J, Xia XF. Science. 1992; 258:631. [PubMed: 1411573]
433. Garcia-Viloca M, Truhlar DG, Gao J. J Mol Biol. 2003; 327:549. [PubMed: 12628257]
434. Dewar MJS, Zoebisch EG, Healy EF, Stewart JJP. J Am Chem Soc. 1985; 107:3902.
435. Stewart JJP. J Comput Chem. 1989; 10:209.
436. Gonzalez-Lafont A, Truong TN, Truhlar DG. J Phys Chem. 1991; 95:4618.
437. Rossi I, Truhlar DG. Chem Phys Lett. 1995; 233:231.
438. Bash PA, Ho LL, MacKerell ADJ, Levine D, Hallstron P. Proc Natl Acad Sci, USA. 1996; 93:3698. [PubMed: 11607654]
439. Devi-Kesavan LS, Garcia-Viloca M, Gao J. Theor Chem Acc. 2003; 109:133.
440. Ruiz-Pernia JJ, Silla E, Tuñón I, Marti S, Moliner V. J Phys Chem B. 2004; 108:8427.
441. Marti S, Moliner V, Tuñón I, Williams IH. J Phys Chem B. 2005; 109:3707. [PubMed: 16851412]
442. Gao J, Amara P, Alhambra C, Field MJ. J Phys Chem A. 1998; 102:4714.
443. Amara P, Field MJ, Alhambra C, Gao J. Theor Chem Acc. 2000; 104:336.
444. Garcia-Viloca M, Gao J. Theor Chem Acc. 2004; 111:280.
445. Pu J, Gao J, Truhlar DG. J Phys Chem A. 2004; 108:632.
446. Pu J, Gao J, Truhlar DG. J Phys Chem A. 2004; 108:5454.
447. Pu J, Gao J, Truhlar DG. ChemPhysChem. 2005; 6:1853. [PubMed: 16086343]
448. Lin H, Truhlar DG. Theor Chem Acc. in press.
449. Dixon SL, Merz KM Jr. J Chem Phys. 1996; 104:6643.

450. Kohn W, Becke AD, Parr RG. J Phys Chem. 1996; 100:12974.
451. Garcia-Viloca, M.; Alhambra, C.; Corchado, JC.; Sanchez, ML.; Villa, J.; Gao, J.; Truhlar, DG. CHARMMRATE, version 2.0. University of Minnesota; Minneapolis, MN: 2002.
452. Brooks BR, Bruccoleri RE, Olafson BD, States DJ, Swaminathan S, Karplus M. J Comput Chem. 1983; 4:187.
453. Corchado, JC.; Chuang, Y-Y.; Fast, PL.; Hu, W-P.; Liu, Y-P.; Lynch, GC.; Nguyen, KA.; Jackels, CF.; Ramos, AF.; Ellingson, BA.; Lynch, BJ.; Melissas, VS.; Villa, J.; Rossi, I.; Costino, EL.; Pu, J.; Albu, TV.; Steckler, R.; Garrett, BC.; Isaacson, AD.; Truhlar, DG. POLYRATE 9.3.1. University of Minnesota; Minneapolis, MN: 2005.
454. Webb SP, Agarwal PK, Hammes-Schiffer S. J Phys Chem B. 2000; 104:8884.
455. Garrett BC, Truhlar DG, Bowman JM, Wagner AF, Robie D, Arepalli S, Presser N, Gordon RJ. J Am Chem Soc. 1986; 108:3515.
456. Warshel A, Hwang JK. J Chem Phys. 1986; 84:4938.
457. Yadav A, Jackson RM, Holbrook J, Warshel A. J Am Chem Soc. 1991; 113:4800.
458. Chu JW, Brooks BR, Trout BL. J Am Chem Soc. 2004; 126:16601. [PubMed: 15600366]
459. Feynman, RP.; Hibbs, AR. Quantum Mechanics and Path Integrals. McGraw-Hill; New York: 1965.
460. Feynman, RP. Statistic Mechanics. Benjamin; New York: 1972.
461. Pollock EL, Ceperley DM. Phys Rev B. 1984; 30:2555.
462. Gillan MJ. J Phys C: Solid State Phys. 1987; 20:3621.Gillan MJ. Phys Rev Lett. 1987; 58:563. [PubMed: 10034973]
463. Voth GA, Chandler D, Miller WH. J Chem Phys. 1989; 91:7749.
464. Topper RQ, Truhlar DG. J Chem Phys. 1992; 97:3647.
465. Voth GA. J Phys Chem. 1993; 97:8365.
466. Hwang JK, Warshel A. J Phys Chem. 1993; 97:10053.
467. Mielke SL, Truhlar DG. J Chem Phys. 2001; 114:621.
468. Mielke SL, Truhlar DG. J Chem Phys. 2001; 115:652.
469. Mielke SL, Truhlar DG. Chem Phys Lett. 2003; 378:317.
470. Major DT, Gao J. J Mol Graphics Modell. 2005; 24:121.
471. Feierberg I, Aqvist J. Theor Chem Acc. 2002; 108:71.
472. Keck JC. Adv Chem Phys. 1967; 13:85.
473. Anderson JB. J Chem Phys. 1973; 58:4684.
474. Neria E, Karplus M. Chem Phys Lett. 1997; 267:23.
475. Grote RF, Hynes JT. J Chem Phys. 1980; 73:2715.
476. Czerminski R, Elber R. J Chem Phys. 1990; 92:5580.
477. Becker OM, Karplus M. J Chem Phys. 1997; 106:1495.
478. Rosenberg RO, Berne BJ, Chandler D. Chem Phys Lett. 1980; 75:162.
479. Field, MJ. Computer Simulation of Biomolecular Systems. van Gunsteren, WF.; Weiner, PK.; Wilkinson, AJ., editors. Vol. 2. ESCOM; Leiden: 1993. p. 82
480. Gertner BJ, Wilson KR, Hynes JT. J Chem Phys. 1989; 90:3537.
481. Tucker, SC. New Trends in Kramers' Reaction Rate Theory. Talkner, P.; Hanggi, P., editors. Kluwer; Dordrecht: 1995. p. 5
482. Bergsma JP, Reimcrs JR, Wilson KR, Hynes JT. J Chem Phys. 1986; 85:5625.
483. Grote RF, van der Zwan G, Hynes JT. J Phys Chem. 1984; 88:4676.
484. Chuang YY, Truhlar DG. J Am Chem Soc. 1999; 121:10157.
485. Anderson SR, Anderson VE, Knowles JR. Biochemistry. 1994; 33:10545. [PubMed: 8068695]
486. Hwang JK, King G, Creighton S, Warshel A. J Am Chem Soc. 1998; 110:5297.
487. Warshel A, Sussman F, Hwang JK. J Mol Biol. 1988; 201:139. [PubMed: 3047396]
488. Truhlar DG, Kohen A. Proc Natl Acad Sci, USA. 2001; 98:848. [PubMed: 11158559]
489. Limbach HH, Lopez JM, Kohen A. Philos Trans R Soc B. in press.

490. Olsson MHM, Warshel A. J Am Chem Soc. 2004; 126:15167. [PubMed: 15548014]
491. Shurki A, Strajbl M, Villa J, Warshel A. J Am Chem Soc. 2002; 124:4097. [PubMed: 11942849]
492. Devi-Kesavan LS, Gao J. J Am Chem Soc. 2003; 125:1532. [PubMed: 12568613]
493. Blakley RL. Adv Enzymol. 1995; 70:23. [PubMed: 8638484]
494. Falzone CJ, Wright PE, Benkovic SJ. Biochemistry. 1994; 33:439. [PubMed: 8286374]
495. Sawaya MR, Kraut J. Biochemistry. 1997; 36:586. [PubMed: 9012674]
496. Castillo R, Andres J, Moliner V. J Am Chem Soc. 1999; 121:12140.
497. Dams T, Auerbach G, Bader G, Jacob U, Ploom T, Huber R, Jaenicke R. J Mol Biol. 2000; 297:659. [PubMed: 10731419]
498. Rajagopalan PTR, Lutz S, Benkovic SJ. Biochemistry. 2002; 41:12618. [PubMed: 12379104]
499. Ferrer S, Silla E, Tuñón I, Martí S, Moliner V. J Phys Chem B. 2003; 107:14036.
500. Hammond GS. J Am Chem Soc. 1955; 77:334.
501. Maglia G, Javed MH, Allemann RK. Biochem J. 2003; 374:529. [PubMed: 12765545]
502. Ridderström M, Cameron AD, Jones TA, Mannervik B. Biochem J. 1997; 328:231. [PubMed: 9359858]
503. Roca M, Martí S, Andres J, Moliner V, Tuñón I, Bertrán J, Williams IH. J Am Chem Soc. 2003; 125:7726. [PubMed: 12812514]
504. Lu HP, Xun L, Xie XS. Science. 1998; 282:1877. [PubMed: 9836635]
505. Xie S, Lu HP. J Biol Chem. 1999; 274:15967. [PubMed: 10347141]
506. Schenter GK, Lu HP, Xie XS. J Phys Chem A. 1999; 103:10477.
507. Cao J. Chem Phys Lett. 2000; 327:38.
508. Yang S, Cao J. J Chem Phys. 2002; 117:10996.
509. Witkoskie JB, Cao J. J Chem Phys. 2004; 121:6361. [PubMed: 15446933]
510. Min W, English BP, Luo G, Cherayil BJ, Kou SC, Xie XS. Acc Chem Res. 2005; 38:923. [PubMed: 16359164]
511. Kou SC, Cherayil BJ, Min W, English BP, Xie XS. J Phys Chem B. 2005; 109:19068. [PubMed: 16853459]
512. Mo Y, Gao J. J Comput Chem. 2000; 21:1458.
513. Mo Y, Gao J. J Phys Chem A. 2000; 104:3012.
514. Gao J, Garcia-Viloca M, Poulsen TD, Mo Y. Adv Phys Org Chem. 2003; 38:161.
515. Major DT, Garcia-Viloca M, Gao J. J Chem Theor Comput. 2006; 2:236.
516. Lewandowicz A, Rudzinski J, Tronstad L, Widersten M, Ryberg P, Matsson O, Paneth P. J Am Chem Soc. 2001; 123:4550. [PubMed: 11457241]
517. Truhlar DG, Garrett BC. Acc Chem Res. 1980; 13:440.

Biographies

Jingzhi Pu was born in Beijing, China, in 1976. He received a B.A. in Chemistry from Peking University in 1999 and a Ph.D. from the University of Minnesota in 2004 under the direction of Donald G. Truhlar. After finishing a short postdoc with Jiali Gao, he moved to Boston. He is currently a postdoctoral associate at Harvard with Martin Karplus. His recent

research interests include quantum effects in enzymatic reactions and protein dynamics. He has been married to Yan He since 2002.

Jiali Gao was born in China in 1962. He received a B.S. in Chemistry from Beijing University in 1982, which marked the first collegial graduation after a decade of political turmoil, called “the Cultural Revolution”, when millions of high school graduates were sent to the remote countryside for re-education. Subsequently, he came to Purdue University, under a Graduate Program arranged by William von E. Doering, and obtained a Ph.D. in 1987 under the guidance of William L. Jorgensen. After postdoctoral research with Martin Karplus at Harvard, he joined the faculty of the State University of New York at Buffalo in 1990 and was promoted to full Professor in 1997. Since 2000, he has been on the faculty of the University of Minnesota, where he is Professor of Chemistry. His research interests include computational studies of chemical and biological problems. He is a recipient of the 2000 Dirac Medal from the World Association for Theoretically Oriented Chemists.

Donald G. Truhlar was born in Chicago in 1944. He received a B.A. in Chemistry from St. Mary’s College of Minnesota in 1965 and a Ph.D. from Caltech in 1970 under the direction of Aron Kuppermannn. He has been on the faculty of the University of Minnesota since 1969, where he is currently Lloyd H. Reyerson Professor of Chemistry, Chemical Physics, Scientific Computation, and Nanoparticle Science and Engineering. His research interests are theoretical and computational chemical dynamics and molecular structure and energetics. He is the author of over 800 scientific publications, and he has received several awards for his research, including a Sloan Fellowship, Fellowships in the American Physical Society and the American Association for the Advancement of Science, an NSF Creativity Award, the ACS Award for Computers in Chemical and Pharmaceutical Research, the Minnesota Award, the National Academy of Sciences Award for Scientific Reviewing, the ACS Peter Debye Award for Physical Chemistry, and the Schrödinger Medal of The World Association of Theoretical and Computational Chemists. He has been married to Jane Truhlar since 1965, and he has two children, Sara Elizabeth Truhlar and Stephanie Marie Eaton Truhlar.

11. Appendix. Glossary

11.1. Enzymes

AADH	aromatic amine dehydrogenase
ADH	alcohol dehydrogenase
BSAO	bovine plasma amine oxidase
BsDHFR	thermophilic DHFR from *Bacillus stearothermophilus*
COMT	catechol *O*-methyltransferase
DHase	haloalkane dehalogenase
DHFR	dihydrofolate reductase
EcDHFR	*E. coli* dihydrofolate reductase
EcTS	*E. coli* thymidylate synthase
GO	glucose oxidase
htADH	thermophilic ADH
LADH	liver ADH
MADH	methylamine dehydrogenase
MMCM	methylmalonyl-CoA mutase
PHM	peptidylglycine α-hydroxylating monooxygenase
SBL	same as SLO
SCAD	short-chain acyl-CoA dehydrogenase
SLO	soybean lipoxygenase
SOX	sarcosine oxidase
TIM	triosephosphate isomerase

TmDHFR	hyperthermophilic DHFR from *Thermotoga maritima*
XyI	xylose isomerase
YADH	yeast ADH
YE	yeast enolase

11.2. Other Acronyms

AM1	Austin model 1, an electronic structure method
DRC	distinguished reaction coordinate—a reaction coordinate that has been selected on intuitive grounds rather than optimized. This term is usually only used with valence reaction coordinates, although collective reaction coordinates are also usually intuitive rather than optimized.
E	enzyme
EA^{-}VTST	ensemble-averaged VTST
EA^{-}VTST/MT	EA-VTST with multidimensional tunneling, that is, ensemble-averaged VTST/MT
EP	enzyme–product complex
ES	enzyme–substrate complex
EVB	empirical valence bond—in particular a special case of SEVB in which MM is used for the diagonal elements of a configuration interaction matrix, and the off-diagonal elements are represented by parameterized analytic functions or constants
GHO	generalized hybrid orbital
KIE	kinetic isotope effect
LCT	large-curvature tunneling, a special case of multidimensional tunneling that includes extreme corner cutting
MEP	minimum-energy path, which is the path of steepest descents in an isoinertial coordinate system. It is also called the intrinsic reaction path or (in a confusing but popular terminology) the intrinsic reaction coordinate.

	Experience has shown that the MEP is usually a reasonably well optimized reaction coordinate for VTST.[144,414,517]
MM	molecular mechanics—sometimes called the classical force field approximation. It refers to an approximation based on valence interactions described by stretching, bending, and torsional force constants, analytical approximations to van der Waals interactions, and explicit Coulomb and/or dipole forces based on electric moments of atoms or bonds.
MQCMD	mixed quantum-classical molecular dynamics—dynamics in which some degrees of freedom are treated classically and others are treated quantum mechanically. This is sometimes called a classical path method in the chemical physics literature.
μOMT	microcanonically optimized multidimensional tunneling
OMT	optimized multidimensional tunneling
P	product
PMF	potential of mean force
PM3	parametrized model 3, an electronic structure method
QCP	quantized classical path—an approximate path integral method for adding quantum effects to a classical simulation
QM	quantum mechanics
QM/MM	an approach to evaluating potential energy surfaces based on a combination of QM for the electronic structure of a subsystem and MM for the rest of the system
S	substrate
SCT	small-curvature tunneling, a special case of multidimensional tunneling that includes mild corner cutting
SEVB	semiempirical valence bond
SRP	specific reaction parameters
SVB	simple valence bond

TST	transition state theory or generalized TST, which includes VTST
VTST	variational TST
VTST/MT	VTST with multidimensional tunneling contributions
WKB	Wentzel–Kramers–Brillouin. This denotes an approximate form of quantum mechanics based on approximating quantum mechanical quantities based on classical-like concepts obtained by a stationary-phase approximation to the Schrödinger equation or to Feynman path integrals.[224–230] It is sometimes called BWK or by other permutations of these letters and sometimes called JWKB to include the contributions of H. Jeffries in 1923 (prior to the development of modern quantum mechanics).
ZCT	zero-curvature tunneling, a special case of multidimensional tunneling that does not include corner cutting—also called MEP tunneling

11.3. Terms with a Special Usage

diabatic	same as nonadiabatic (see text)
hydrogen	denotes hydron (proton, deuteron, or triton), hydride ion (protide, deuteride, or tritide), or hydrogen atom (protium, deuterium, or tritium). This is sometimes called a light atom in the chemical physics literature.
N	number of atoms in the system
nonadiabatic	same as diabatic (see text)
quasiclassical	an approximation in which the bound motion is quantized but the unbound motion is not
semiclassical	WKB-like—not to be confused with combined QM/MM potential energy surface methods, with mixed quantum-classical dynamics methods, or with quasiclassical dynamics. Note that workers in the field of KIEs often use “semiclassical” to mean what is here called “quasiclassical”. (The translation into English of the well-known quantum mechanics text by Landau and Lifshitz refers to the WKB approximation as “quasiclassical” whereas most other quantum mechanics texts and most of the current chemical physics literature use “semiclassical” to refer to the WKB approximation, as is done here.)

system	the atoms included in a TST calculation, excluding the surroundings

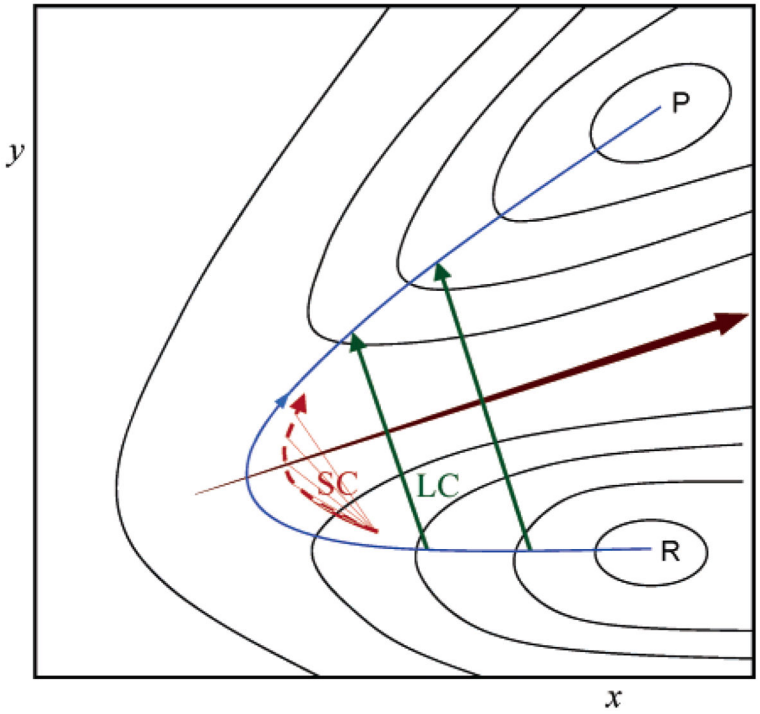

Figure 1.

Schematic tunneling paths (green and red) for an H transfer reaction as functions of two isoinertial rectilinear coordinates. (For example, for a triatomic reaction D – X + A → D + X –A, where D and A are donor and acceptor atoms, *x* would be the mass-scaled distance of A to DX, and *y* would be the mass-scaled distance of D to X.) The black curves are potential energy surface contours plotted in a mass-weighted coordinate. The figure shows a two-dimensional cut through the (3*N* − 1)-dimensional space. The minimum energy path (MEP) is depicted as a blue curve that connects the reactant (R) and product (P) regions. In a one-dimensional tunneling model, the reaction path curvature is ignored, and the tunneling path is the MEP. When the reaction path is moderately curved, the dominant tunneling path (depicted in red and called a small-curvature (SC) tunneling path) corner-cuts the MEP on its concave side. Although the tunneling path does not follow the MEP (and hence is not perfectly adiabatic), the effective potential along this kind of path is adiabatic. In the limit of reaction paths with large curvature, the optimal tunneling paths (depicted in green and called large-curvature (LC) tunneling paths) are straight lines connecting the reactant and product valleys; the effective potential for these tunneling paths is nonadiabatic. For a symmetric reaction, the distance between the donor and acceptor atoms is approximately constant along LC tunneling paths. A brown arrow is used to depict the direction of increasing the donor–acceptor distance.

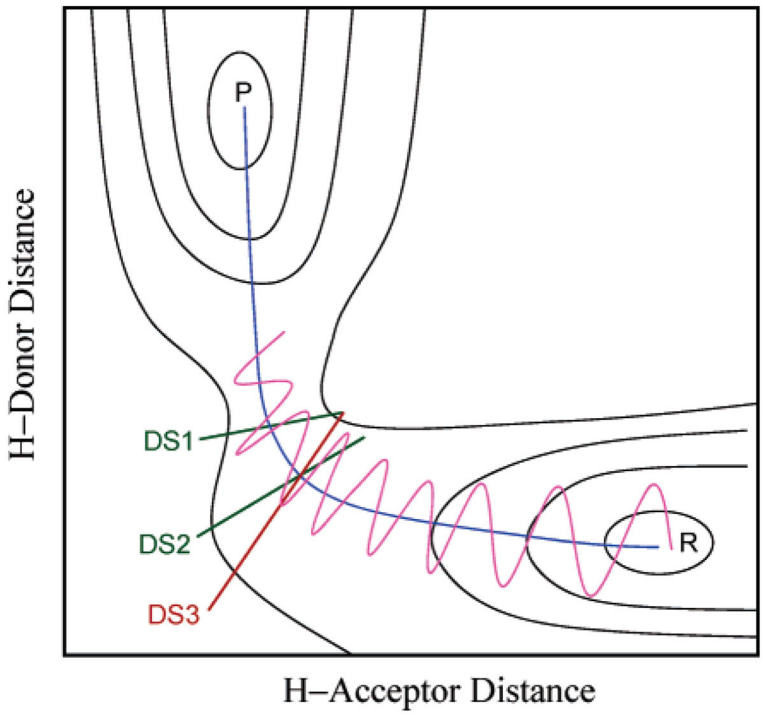

Figure 2.

Schematic trajectory for an H transfer reaction as a function of the H-to-donor and H-to-acceptor distances. The black curves are potential energy surface contours. Keep in mind that the figure shows a two-dimensional cut through the (3N − 1)-dimensional space. The minimum energy path (MEP) is depicted as a blue curve that connects the reactant (R) and product (P) regions. Three possible transition state dividing surfaces are shown. The magenta curve represents the projection of an example trajectory into this 2D cut; only the portion of the trajectory from the reactant to slightly past the dynamical bottleneck is shown, but we assume that the remainder of the trajectory proceeds to products without recrossing any of the three dividing surfaces. The conventional transition state dividing surface (DS1 in green) is orthogonal to the MEP at the saddle point, and it is crossed twice in the forward direction by the example trajectory; therefore, is has a transmission coefficient less than unity. Displacing the dividing surface to DS2 (also in green) also gives a dividing surface that is crossed twice in the forward direction. DS3 (in red) is a variationally improved transition state that is not recrossed, yielding a unity recrossing transmission. (The canonical variational transition state is defined to minimize recrossing for the canonical ensemble, not for a single trajectory, as used here for illustrative purposes only.) Note that DS3 is rotated as compared to DS2. Since the reaction coordinate is the degree of freedom normal to the dividing surface, rotating the dividing surface corresponds to rotating the reaction coordinate, that is, choosing a different reaction coordinate. Although the dividing surfaces are shown as hyperplanes in this diagram (in a 2D diagram, a hyperplane is a straight line; in a 3D world, a hyperplane is a 2D plane; in the 3N-dimensional coordinate space, a hyperplane has dimension 3N − 1), general dividing surfaces can be nonplanar, and general reaction coordinates can be curved. For example, a dividing surface defined by a linear transformation of Cartesian coordinates would be nonplanar (nonstraight in this picture)

because the axes are nonlinear functions of Cartesians, a dividing surface defined as a difference of bond stretches would curved in a Cartesian coordinate system, and an energy gap reaction coordinate would be curved in almost any coordinate system. Notice that the dividing surface defined by $z = 0$ where z is defined in eq 9 would be a straight line at an angle of 45° in this figure (and mass-weighting the two distances would change this angle); for comparison, we note that DS1, DS2, and DS3 are at angles of 11, 31, and 56°, respectively.

Table 1

Summary of Computed Recrossing Transmission Coefficients in Enzymes

enzyme	Γ^a	ref
Valence Reaction Coordinates[b]		
YE	0.76 (H)	97
	0.99 (D)	
TIM	0.43 ± 0.08	474
TIM	0.47	170
TIM	0.69	32
DHase	0.53	169
DHase	0.77	171
EcDHFR	0.75 ± 0.26 (H, 298 K)	133
	0.82 ± 0.21 (D, 298 K)	
EcDHFR	0.79 ± 0.27 (H, 278 K)	153
	0.78 ± 0.25 (D, 278 K)	
	0.85 ± 0.21 (H, 318 K)	
	0.86 ± 0.17 (D, 318 K)	
TmDHFR	0.66(0.29) (H, 278 K)	163
	0.63(0.28) (D, 278 K)	
	0.66(0.28) (H, 298 K)	
	0.64(0.28) (D, 298 K)	
	0.79(0.21) (H, 338 K)	
	0.71(0.26) (D, 338 K)	
XyI	0.95 ± 0.04 (H)	137
	0.95 ± 0.02 (D)	
LADH	0.983 (HH)	121
	0.977 (HT)	
	0.976 (DD)	
	0.977 (DT)	
	0.977 (TH)	
	0.981 (TD)	
SCAD	0.36 ± 0.3 (HH, stage-2)	138
	0.40 ± 0.3 (DD, stage-2)	
	0.86 ± 0.04 (HH, stage-3)	
	0.82 ± 0.10 (DD, stage-3)	
MADH	0.76 (CH3)	113
	0.81 (CD3)	
COMT	0.83 ± 0.03	172
Collective Energy Gap Reaction Coordinates[c]		
EcDHFR (300 K)	0.80 ± 0.03 (H)	131
	0.85 ± 0.01 (D)	
LADH	0.947 ± 0.011 (H)	115

enzyme	Γ^a	ref
	0.983 ± 0.017 (D)	

[a] Room temperature except where specified otherwise.

[b] Also called geometric reaction coordinates.

[c] See ref 120 for a general discussion of energy gap reaction coordinates.

Table 2

Individual *k* Factors for MADH-Catalyzed Reaction at 300 K[a]

	CH_3		CD_3	
conf no.	k_{ZCT}	k_{SCT}	k_{ZCT}	k_{SCT}
1	15.3	22.8	9.3	14.8
2	22.0	38.1	10.6	18.0
3	31.2	66.7	12.5	22.7
4	61.2	153.5	17.7	34.4
5	25.0	46.7	11.4	19.9
6	52.6	173.5	16.3	37.7
avg	34.6	83.6	13.0	24.6
SD[b]	18.3	63.8	3.3	9.3

[a] From unpublished details of the results reported in ref 113. Averaged over 6 reaction coordinates.

[b] SD denotes standard deviation.

Table 3

Averaged Transmission Coefficients of LADH-Catalyzed Reaction[a]

		k		γ	
isotope	**Γ**	**ZCT**	**μOMT**	**ZCT**	**μOMT**
HH	0.983	1.68	2.495	1.64	2.42
HT	0.977	1.55	2.14	1.51	2.06
DD	0.976	1.74	2.352	1.69	2.27
DT	0.977	1.70	2.29	1.66	2.21
TH	0.977	1.71	2.40	1.67	2.34
TD	0.981	1.66	2.29	1.63	2.24

[a]Reference 121. Averaged over 18 reaction coordinates.

Table 4

Averaged Transmission Coefficients for the EcDHFR-Catalyzed Reaction at 25 °C[a]

	HH			DH			HD		
	κ	Γ	γ	κ	Γ	γ	κ	Γ	γ
avg	3.13	0.75	2.54	2.88	0.82	2.46	2.84	0.73	2.25
SD	1.29	0.26	1.61	0.82	0.21	1.09	1.10	0.27	1.45

[a]Reference 133. Averaged over 13 reaction coordinates. XY in the column headings denotes that X is the hydride or deuteride transferred, and Y is the hydrogen or deuterium vicinal to the transferred atom.

Table 5

Averaged Calculated Transmission Coefficients and Their Standard Deviations for EcDHFR-Catalyzed Reactions at 5 and 45 °C[a]

	278 K (5 °C)		318 K (45 °C)	
level	**H**	**D**	**H**	**D**
recrossing (Γ)	0.79 [0.27]	0.78 [0.25]	0.85 [0.21]	0.86 [0.17]
tunneling (κ, μOMT)[b]	3.77 [1.94]	3.48 [1.24]	2.84 [0.73]	2.69 [0.58]
tunneling (κ, μOMT(0))[c]	3.77 [1.94]	3.48 [1.24]	2.84 [0.73]	2.66 [0.49]
overall (γ)[b]	3.12 [1.89]	2.74 [1.16]	2.48 [0.95]	2.32 [0.62]

[a] Reference 153. Averaged over 20 reaction coordinates; standard deviations are given in the brackets.

[b] μOMT based on SCT and LCT, where tunneling contributions to all allowed excited states are included.

[c] μOMT based on SCT and LCT(0). This agrees well with μOMT based on SCT and LCT mainly because SCT dominates in this case, although the LCT κ exceeds the LCT(0) one, as it should.

Table 6

Individual Tunneling Transmission Coefficients for EcDHFR-Catalyzed Reactions[a]

	T = 278 K, H				*T* = 318 K, H			
conf no.[b]	SCT	LCT	LCT(0)	μOMT[c]	SCT	LCT	LCT(0)	μOMT[c]
1	5.60	3.54	3.16	5.60	2.80	1.93	1.93	2.80
2	8.56	5.13	4.54	8.56	3.48	2.29	2.28	3.50
3	4.10	2.82	2.82	4.13	2.88	2.00	2.00	2.88
4	3.57	2.26	2.26	3.57	1.95	1.57	1.45	1.95
5	5.46	3.52	3.17	5.46	3.75	2.64	2.44	3.75
6	3.07	2.38	2.03	3.07	2.64	1.87	1.87	2.64
7	7.98	4.39	4.28	8.02	3.16	2.29	2.14	3.16
8	2.45	2.03	1.77	2.45	4.20	2.70	2.69	4.23
9	2.90	2.10	1.97	2.90	2.07	1.63	1.62	2.05
10	2.54	1.89	1.88	2.54	1.87	1.67	1.51	1.87
11	3.40	3.03	3.03	3.40	3.71	2.47	2.45	3.73
12	2.38	2.20	2.14	2.38	2.83	2.83	1.99	2.83
13	5.60	3.20	3.20	5.60	3.00	2.00	2.08	3.00
14	1.66	1.36	1.36	1.66	2.13	1.68	1.68	2.13
15	1.69	1.55	1.37	1.75	4.22	2.82	2.64	4.23
16	2.46	1.82	1.82	2.46	1.97	1.58	1.58	1.97
17	2.47	1.83	1.82	2.47	2.28	2.28	1.78	2.28
18	3.80	2.41	2.41	3.80	2.43	1.73	1.73	2.43
19	3.21	2.28	2.14	3.21	2.63	1.88	1.88	2.63
20	2.34	1.78	1.77	2.34	2.72	1.92	1.84	2.72

[a] Reference 153. Averaged over 20 reaction coordinates.

[b] Note that the configurations at two temperatures are unrelated.

[c] μOMT based on SCT and LCT, where tunneling contributions to all allowed excited states are included.

Table 7

Calculated Transmission Coefficients and Their Standard Deviations for TmDHFR[a]

	278 K (5 °C)		298 K (25 °C)		338 K (65 °C)	
level	**H**	**D**	**H**	**D**	**H**	**D**
recrossing (Γ)	0.66 [0.29]	0.63 [0.28]	0.66 [0.28]	0.64 [0.28]	0.79 [0.21]	0.71 [0.26]
tunneling (κ)	5.25 [1.38]	4.92 [0.89]	4.13 [0.99]	3.81 [0.54]	2.00 [0.38]	1.97 [0.52]
overall (γ)	3.38 [1.74]	3.09 [1.55]	2.72 [1.31]	2.44 [1.12]	1.64 [0.66]	1.51 [0.86]

[a]Reference 163. Averaged over 14 configurations.

Table 8

Individual Transmission Coefficients for the Xylose Isomerase-Catalyzed Reaction[a]

	H			D		
conf no.	κ	Γ	γ	κ	Γ	γ
4	7.10	0.90	6.37	3.36	0.94	3.17
16	6.94	0.97	6.71	3.32	0.96	3.19
8	7.15	0.95	6.79	3.34	0.95	3.16
20	6.52	0.95	6.17	3.24	0.94	3.04
01	6.83	1.00	6.83	3.34	0.98	3.26
avg	6.91	0.95	6.57	3.32	0.95	3.16
SD	0.25	0.04	0.29	0.05	0.02	0.08

[a]Unpublished details from the work described in ref 137. Averaged over 5 reaction coordinates.

Table 9

Static-Secondary-Zone (SSZ) Transmission Coefficients and Their Standard Deviations for SCAD Catalyzed Reaction[a]

isotope	Γ	κ	γ
HH	0.36 [0.3]	3.5 [2]	1.9 [2]
DD	0.40 [0.3]	3.0 [1]	1.6 [2]

[a]Reference 138. Averaged over 15 reaction coordinates.